Title

THE INFLUENCE OF SURFACE TURBULENCE AND SURFACTANTS ON GAS TRANSPORT THROUGH LIQUID INTERFACES

Authors

Springer, Thomas G.
Pigford, Robert L.

Publication Date

1969-11-01

UCRL-18995

c.2

THE INFLUENCE OF SURFACE TURBULENCE AND SURFACTANTS ON GAS TRANSPORT THROUGH LIQUID INTERFACES

Thomas G. Springer* and Robert L. Pigford

November 1969

AEC Contract No. W-7405-eng-48

*Filed as a Ph. D. Thesis

LAWRENCE RADIATION LABORATORY
UNIVERSITY of CALIFORNIA BERKELEY

UCRL-18995

DISCLAIMER

CONTENTS

Abstract vi

List of Figures viii

List of Tables (Chapter II) xii

Introduction 1

Chapter I. An Interface Impedance Bridge 1

Abstract 1

Introduction 2

The Interface Impedance Bridge Apparatus 4

Quantitative Development of the Method 8

The Frequency-Dependent Mass Transfer Ceofficient for a Stagnant, Clean Surface 10

The Mass-Transfer Coefficient for a Randomly Turbulent Surface 11

Construction of the Apparatus 11

Typical Experimental Results 16

Conclusions 20

Chapter II. Results from the Interface Bridge 21

Abstract 21

Introduction 22

Quantitative Development 23

1. Statistical Characteristics of Turbulent Interfaces 23

2. Frequency Response of Interface Models 29

a. The Randomly Turbulent Interface 29

b. Film-Covered Liquid Surfaces 31

Materials 33

Experimental Results 36

1. Clean Turbulent Surfaces 37

2. Effect of soluble Surfactants 40

Contents (Continued)

3. Effect of Insoluble Surfactants 49

Discussion of Results 54

Conclusions 60

Nomenclature 62

References 64

Appendix A. Experimental Apparatus 67

General Design Criteria 67

Chamber Construction 67

Chamber Lid 70

The Balloons 72

The Drive System 72

Electrical Equipment 76

Stirrer System 82

Materials 84

Appendix B. Experimental Procedures 88

Surface Cleaning 88

Addition of Surfactant 88

Phase Measurement 90

Amplitude Measurement 93

Bridge Operation 95

Experimental Errors and Difficulties 101

Reproducibility of Data 103

Appendix C. Tabulation of Individual Runs 104

Appendix D. Numerical Evaluation of a Fourier Integral . . 128

Contents (Continued)

Appendix E. Data Reduction 134

Calculation of Q^* 134

Calculation of the True Pressure Signal from the Measured Response 134

Interchange of the Standard Reference of Measured Responses 136

Least Squares Analysis 137

Appendix F. Surface Concentration of the Soluble Surfactant . 138

Appendix G. Power Input 139

Acknowledgments 140

THE INFLUENCE OF SURFACE TURBULENCE AND SURFACTANTS ON GAS TRANSPORT THROUGH LIQUID INTERFACES

Thomas G. Springer and Robert L. Pigford

Department of Chemical Engineering
and Lawrence Radiation Laboratory
University of California
Berkeley, California 94720

ABSTRACT

An apparatus called an interface impedance bridge is described for the observation of the resistance to passage of a soluble gas through a gas-liquid interface under dynamic conditions. The apparatus resembles an electrical a.c. bridge circuit and permits measurements to be made over a range of frequencies.

The interface impedance bridge is used to measure passage of a soluble gas through a gas-liquid interface under varying conditions. Measurements over a range of frequencies of gas pressure oscillations allowed one to test interface mass transfer mechanisms, including the effects of soluble and insoluble surfactants on both stagnant and turbulent liquid surfaces.

Analysis of the turbulent interface of a clean liquid shows that a Danckwerts type distribution function of surface ages may be used to describe the statistical characteristics of the interface under the conditions of these experiments.

Addition of a soluble surfactant to the liquid produced no measurable change in the mass transfer rate through a stagnant gas-liquid interface, but reduced the intensity of turbulence at the

interface when the liquid was stirred from beneath. It was found that the statistical nature of the interface could still be described reasonably well with the Danckwerts random distribution function.

Placement of an insoluble surfactant on the surface of a clean stagnant surface reduced the mass transfer rate of soluble gas through it. The film resistance was found to be a function of the surface concentration. The film resistance was found to be a function of the surfactant's surface concentration. An insoluble surfactant had no effect on the mass transfer rate when the liquid was stirred from beneath.

The nature of surface films and their stability in the presence of interfacial turbulence is discussed.

LIST OF FIGURES

Chapter I.

Fig. 1. Diagram of an interface impedance bridge 5

Fig. 2. Analogous a.c. impedance bridge. (Capacitors are varied together sinusoidally; voltage difference, $\Delta E = \hat{\Delta E} \exp(i\omega t)$) 7

Fig. 3. Photograph of interface impedance bridge . . . 12

Fig. 4. Photograph of reciprocating drive mechanism . . . 14

Fig. 5. Bridge comparison of a stationary water interface with an impermeable surface. (The straight line is computed from Eq. (9) using accepted values of SO_2 and diffusion coefficient 17

Fig. 6. Bridge comparison of a turbulent water interface with an impermeable surface. (Data for SO_2 passing into surface of a stirred pool of water. The apparent value of s is about 2.96 sec^{-1} 19

Chapter II.

Fig. 1. Surface tension of sodium lauryl sulfonate solutions versus bulk liquid concentration 34

Fig. 2. Surface tension of 1-hexadecanol films versus equivalent surface concentration in monolayers 35

Fig. 3. Bridge comparison of a clean, turbulent water interface with an impermeable surface. (○-liquid stirred at a rate of 230 rpm; □-liquid stirred at a rate of 150 rpm.) . . 38

Fig. 4. Surface age distribution function versus surface element age for a liquid stirred at a rate of 230 rpm. Data points obtained with Eq. (15) 41

List of Figures (Continued)

Chapter II (Continued).

Fig. 5. Surface age distribution function versus surface element age for a liquid stirred at a rate of 150 rpm. Data points obtained with Eq. (15) 42

Fig. 6. Bridge comparison of turbulent sodium lauryl sulfonate solutions (stirring rate of 230 rpm) with an impermeable surface. (○ -clean liquid; Δ -0.0001635-M solution; □ -0.000327-M solution 44

Fig. 7. Photograph of 0.00106-M sodium lauryl sulfonate solution at time of maximum bubble concentration. (Stirring rate of 230 rpm.) 47

Fig. 8. Photograph of 0.00106-M sodium lauryl sulfonate solution at time of minimum bubble concentration. (Stirring rate of 150 rpm.) 48

Fig. 9. Bridge comparison of a stagnant liquid surface, covered by a 1-hexadecanol film, with a clean stagnant liquid surface. (○ -1/2 monolayer equivalent surface concentration; Δ -1 monolayer; □ -2 monolayers.) . . . 50

Fig. 10. Bridge comparison of a turbulent interface (stirring speed, 150 rpm), 1-hexadecanol surface film added, with an impermeable surface. (○ -1/2 monolayer equivalent surface concentration; Δ -1 monolayer, □ -2 monolayers.) . . . 52

Appendix A.

Fig. A-1. Photograph of Pyrex chamber and baffles . . . 69

List of Figures (Continued)

Appendix A (Continued).

Fig. A-2. Drawing of center inlet to chamber lid, showing movable cups and gas line concentrations 71

Fig. A-3. Photograph of insides of sheet metal boxes . . . 73

Fig. A-4. Photograph of Neoprene balloons before and after modification 74

Fig. A-5. Typical generated pressure waves at 0.5 cycles/sec. The upper waves represent a balance signal at two different filter settings (note second harmonic content), attenuation ×20. Lower waves represent input signal to a single chamber, attenuation ×2000 77

Fig. A-6. Block diagram of the quadrature demodulator and the equivalent analog circuits 80

Fig. A-7. Block diagram and circuit diagram of the harmonic analyzer 81

Fig. A-8. Photograph of stirrer and shaft 83

Fig. A-9. Photograph of a clean turbulent water interface stirred at a rate of 150 rpm 85

Fig. A-10. Photograph of a clean turbulent water interface stirred at a rate of 230 rpm 86

Appendix B.

Fig. B-1. The phase response characteristics of the demodulator as a function of signal frequency. (Test signals supplied by analog computer.) 92

List of Figures (Continued)

Appendix B (Continued).

Fig. B-2. Attenuation characteristics of the band-pass filter as a function of frequency where Y = the amplitude ratio when the filter frequency is set at 1/2 the signal frequency and Z = the amplitude ratio when the filter frequency is set at twice the signal frequency. X, the amplitude ratio when the filter frequency and signal frequency are identical, is a constant 1.89. (Test signals supplied by analog computer.) 94

LIST OF TABLES

Chapter II.

Table I. Results of lease squares analysis of data for a clean, turbulent interface 39

Table II. Results of least squares analysis on data for water solutions of sodium lauryl sulfonate 45

Table III. Calculated film coefficients from least squares analysis of data for stagnant surfaces covered with 1-hexadecanol 51

Table IV. Results of least squares analysis on turbulent data for 1-hexadecanol 53

Table V. The surface resistance of a 1-hexadecanol film compared with the results of previous investigations 55

INTRODUCTION

The effect of surface films on mass transfer through stagnant interfaces has been studied in recent years, particularly with reference to retardation of the evaporation of water. The investigation of surfactant behavior at turbulent interfaces, produced by violent mixing some distance from the surface with fluid elements continually bombarding the interface, has received little attention.

The purpose of this thesis is characterization of the statistical nature of turbulent interfaces and examination of surfactant behavior at turbulent gas-liquid interfaces. The resistance of a surface film, placed on a stagnant surface, is measured in order to allow separation of hydrodynamic and film resistance effects.

The format of this thesis has been chosen to meet two goals. First, Chapters I and II are written so that they would be suitable for publication without major revision. Second, the thesis is written so that anyone who is interested in only the main features and conclusions of this work may read from the beginning through Chapter II. For the person who is interested in all details of apparatus, procedures, and calculations, this material is supplied as appendices.

Chapter I deals with introduction of a new experimental technique and explanation of its possible uses. Chapter II presents results obtained when the new technique was used not only to measure surfactant effects on stagnant and turbulent interfaces but also to characterize the statistical nature of clean and surfactant-covered turbulent interfaces.

CHAPTER I

AN INTERFACE IMPEDANCE BRIDGE*

ABSTRACT

An apparatus is described for the observation of the resistance to passage of a soluble gas through a gas-liquid interface under dynamic conditions. The apparatus resembles an electrical a.c. bridge circuit and permits measurements to be made over a range of frequencies. From the data one can test various interface mass transfer mechanisms, including the effects of surfactants on both stagnant and turbulent interfaces.

*This Chapter will be published as a research paper by William B. Lamb, Thomas G. Springer, and Robert L. Pigford in Fundamentals Quarterly, Industrial and Engineering Chemistry, November, 1969.

INTRODUCTION

Throughout most of the large body of work that has been done to determine mass transfer resistances of gas-liquid interfaces the experiments have been carried out at steady state, the rate of transfer being determined from chemical analysis of streams entering and leaving or from measurements of the volume of gas taken up by the liquid at a constant rate. The difficulties of determining the resistance of one of the phases from such measurements when both phases offer resistance are well known. And the fact that wholly different assumptions about the fluid mechanical structure or other characteristics of interfaces lead to nearly the same predictions of steady state mass transfer coefficients has led to question whether the traditional measurements will ever reveal the details of interface structure. After all, each theory has quantities in it which are not known a priori for real equipment and which can be chosen arbitrarily to make the theories fit empirical data. It is only by using highly idealized gas absorbers, such as wetted-wall columns or liquid jet devices, that physically important quantities like times of exposure of the surfact to the gas (Higbie, 1935) can be determined uniquely by the design of the apparatus. Moreover, no way has been found heretofore to expose a turbulent liquid interface to a gas under conditions where the frequency of random replacement of elements of the liquid surface is known accurately or even where such interface statistical phenomena can be controlled precisely.

In fields such as electrical engineering, however, the use of frequency response experimental methods for the exploration of rate phenomena is well established. Indeed the art of electrical measurements involving a.c. bridges and linear circuits has not been exploited very often in chemical engineering laboratory research, although the use of such procedures for the design of control systems is familiar. Particularly in the field of mass transfer mechanisms, the use of transient methods of observation would appear to be promising (cf. Whitaker and Pigford, 1966).

THE INTERFACE IMPEDANCE BRIDGE APPARATUS

Consider an apparatus consisting of two identical chambers, each containing a deep pool of liquid with a pure gas phase above, as shown in Fig. 1. The liquid is saturated with dissolved gas at the time-average gas pressure, but through the use of duplicate gas cylinders driven from the same rotating shaft the volumes of the two gas spaces vary sinusoidally in an identical manner. If the gas were insoluble in each chamber there would be no pressure difference between the chambers although the pressure in each chamber would oscillate. On the other hand, if there is even a small difference in the rates of solution of the gas in the chambers a pressure-difference signal will be detected on an electrical transducer. After filtering of noise through a band-pass filter circuit this signal can be recorded on a chart beside a second signal representing the pressure variations on one side; the phase difference and the ratio of the amplitudes can be observed over a range of frequencies. From such a frequency response and, on the

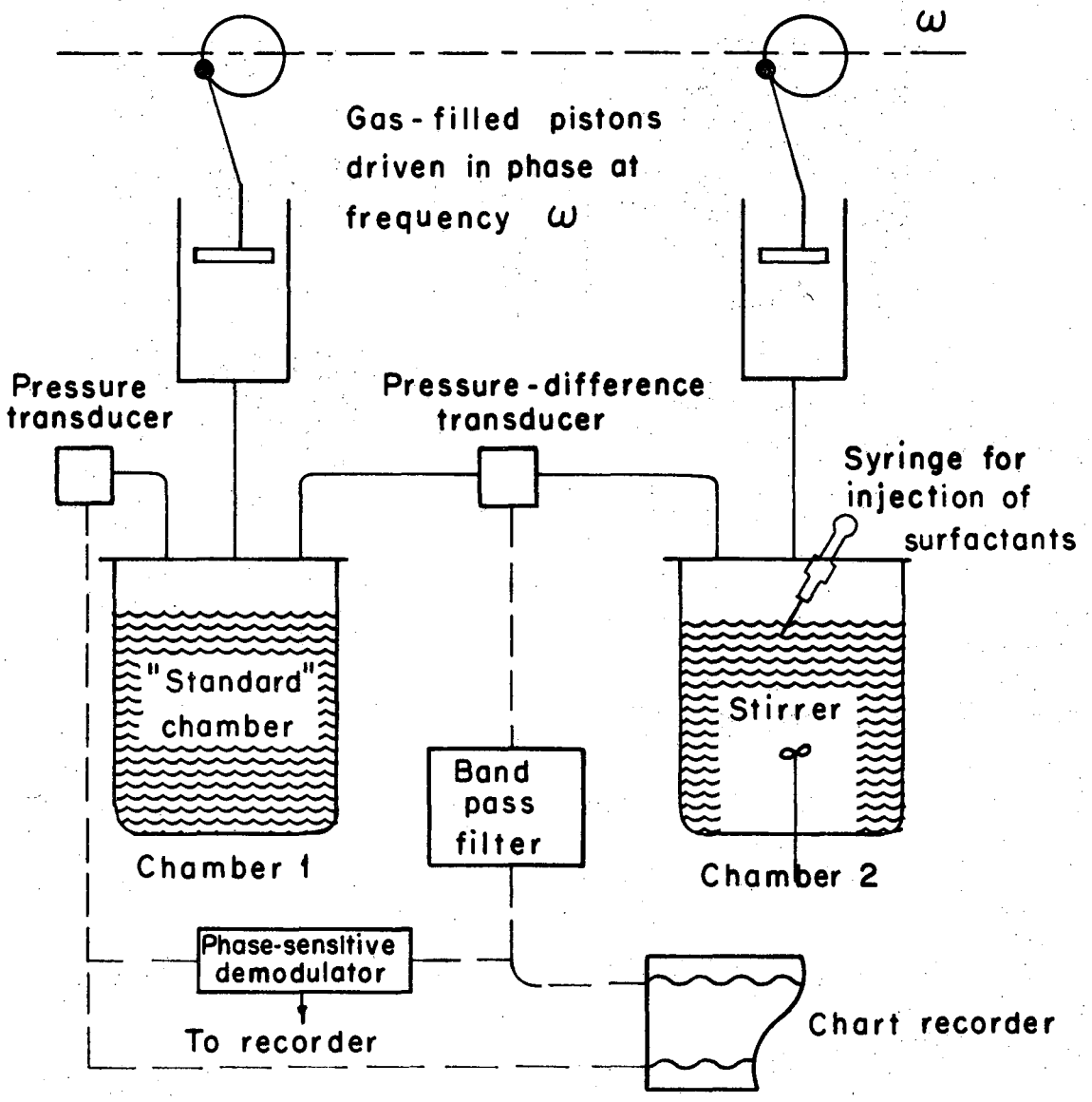

Fig. 1. Diagram of an interface impedance bridge.

assumption that all the distrubances are small enough to be governed by the linearized approximations to the necessary rate equations, constants in such rate expressions can be found. Distinctions can be made between alternative assumptions about the rate processes themselves and detailed information can be developed about the statistical characteristics of turbulent interfaces, as will be shown.

Such an apparatus can be called an "interface impedance bridge" because it is wholly analogous to a bridge-type electrical circuit, as indicated in Fig. 2. The electrical circuit consists of two parallel paths from a constant-voltage current source to ground. Each is through a series combination of a condenser and a resistor, the capacitance of the condenser being changed sinusoidally by moving the plates toward and away from each other. The a.c. voltage appearing across the bridge depends on the difference in the two resistances if the condensers are duplicates. If one of the resistors has known a.c. impedance, the frequency response data will determine the other impedance.

In the mass transfer version of the bridge the resistors correspond to the interfaces and the underlying diffusional resistance of the phases. When the frequency is increased the waves of concentration present in the liquid will be confined to thinner and thinner layers of liquid and the resistance of the interface itself will be emphasized.

One version of the interface bridge consists, therefore, in having a stagnant, clean, liquid surface on one side for use as a standard interface of calculable impedance. On the other side one can have, for example, a similar interface covered with a layer of a

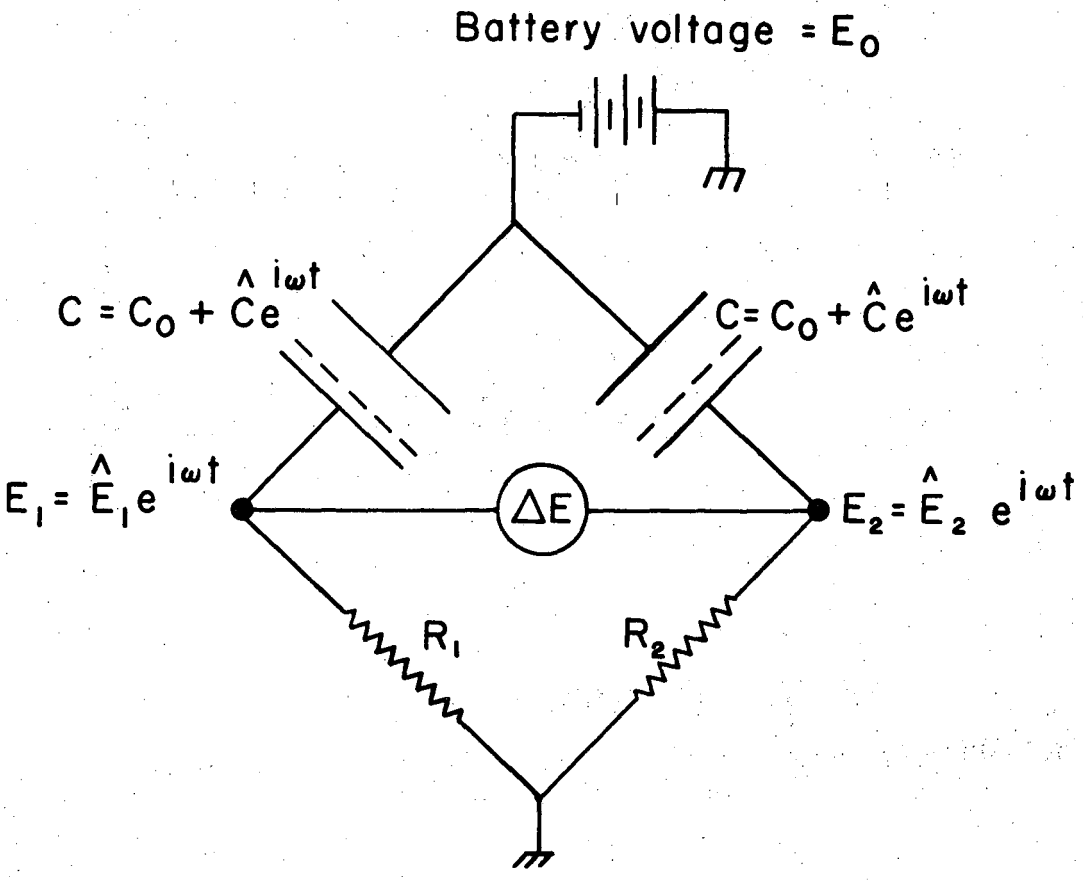

$$\frac{\hat{\Delta E}}{\hat{E}_2} = \frac{(1/C_0)\left(\frac{1}{r_2} - \frac{1}{r_1}\right)}{i\omega + \frac{1}{C_0 r_1}}$$

XBL695 - 2746

Fig. 2. Analogous a.c. impedance bridge. (Capacitors are varied together sinusoidally; voltage difference, $\Delta E = \hat{\Delta E} \exp(i\omega t)$).

surfactant whose impedance we wish to measure. Likewise, opposite the stagnant interface we might place a turbulent interface, obtained by stirring the pool of liquid below. The frequency response information would yield in this case the whole statistical distribution of fluid particle residence times in the interface as well as the average surface element replacement frequency. Obviously, studies can be conducted to find the ways in which surfactants inhibit fluid motion at interfaces.

QUANTITATIVE DEVELOPMENT OF THE METHOD

Consider first the calculation of pressure changes that occur inside a single chamber containing a constant volume of liquid as the volume of the gas space is varied sinusoidally according to

$$V(t) = V_o + \hat{V} \exp(i\omega t) \quad . \tag{1}$$

Assume that the gas follows $pV = nRT$ and that heat transfer between the gas and the solid or liquid surfaces which surround it can be represented by the usual rate expression with an overall coefficient U and an area S. Then the energy balance for the gas is

$$n C_v \dot{T} = US(T_o - T) - p \dot{V} \tag{2}$$

where the dots above mean differentiation with respect to time and where T_o is the constant temperature of the surroundings.

The material balance includes rate expression, $Hk_L(\omega)\ (p - p_o)$, where H is the Henry's Law coefficient, $k_L(\omega)$ is the possibly frequency-dependent mass transfer coefficient of the liquid surface,

and p_o is the time-average pressure of the gas. It is assumed that the liquid mass is so large and the frequencies so high that the bulk of the liquid does not change its concentration as the gas pressure p varies. The balance is

$$\dot{n} = - Hk_L A(p - p_o) \tag{3}$$

where A is the known area of the interface.

By assuming that the linearly correct solution is of the form

$$p = p_o + \hat{p} \exp(i\omega t)$$

$$T = T_o + \hat{T} \exp(i\omega t)$$

$$n = n_o + \hat{n} \exp(i\omega t)$$

one can easily find the result,

$$\frac{\hat{p}}{p_o} = - \frac{1 + \dfrac{\gamma - 1}{1 + (\gamma - 1)(UST_o/p_oV_o)(i/i\omega)}}{1 + (HART_o/V_o)(k_L(\omega)i\omega)} \quad \frac{\hat{V}}{V_o} \quad . \tag{4}$$

Obviously, the volume changes produce pressure oscillations which depend on the frequency for two reasons. One is that the changes in gas temperature may be nearly adiabatic and reversible (at high frequencies) or nearly isothermal (at low frequencies); the other is that the mass transfer into the liquid causes dissolved gas to be stored there temporarily and that the mass transfer coefficient, k_L, may itself depend on the frequency.

Suppose that Eq. (4) is applied to each side of the bridge and that the mass transfer coefficients are k_{L1} and k_{L2} on the two sides, respectively. The difference in pressure can be represented by the formula $\Delta p = \hat{\Delta p} \exp(i\omega t)$ and an equation for the frequency dependence of $\hat{\Delta p}$ can be obtained by applying Eq. (4) to each side. It is convenient, however, to divide the result by the pressure coefficient for one side because thereby the factor representing the effects of temperature changes in the two chambers drops out. The result is

$$\frac{\hat{\Delta p}}{\hat{p}_2} = \frac{(HART_o/V_o)[\tilde{k}_{L2}(\omega) - k_{L1}(\omega)]}{i\omega + (HART_o/V_o)\, k_{L1}(\omega)} \qquad (5)$$

which suggests a comparison of the amplitudes and the phase of the signals, Δp and $p_2 - p_o$.

THE FREQUENCY-DEPENDENT MASS TRANSFER COEFFICIENT FOR A STAGNANT, CLEAN SURFACE

A convenient surface to use as a reference on the side of the bridge having a known impedance is formed by a pool of clean liquid at rest. If there is no resistance at the interface itself to the passage of soluble gas molecules the mass transfer coefficient is determined entirely by the molecular diffusional resistance of the liquid substrate. Since the pool is very deep there are negligible changes in composition at any large depth in the liquid and the solution of Fick's second law is simply

$$C(x,t) = H\,\hat{p}\,\exp\left(i\omega t - \sqrt{\frac{i\omega}{\mathcal{D}}}\,x\right) + Hp_o \qquad (6)$$

where x represents distance from the interface. The mass transfer coefficient is easily calculated from the interface concentration gradient as

$$k_L = (i\omega\mathcal{D})^{1/2} \quad . \qquad (7)$$

THE MASS-TRANSFER COEFFICIENT FOR A RANDOMLY TURBULENT SURFACE

Following the suggestion of Danckwerts (1951), a liquid interface which is continually exchanging liquid particles with the substrate can be thought of as being composed of a mosaic of small liquid patches, each having arrived randomly in time and, upon arrival in a fresh condition, having displaced another particle which was then completely submerged. Whether such a conception of the structure of an interface is correct can be investigated by comparing an observed frequency response with the one which is expected,

$$k_L = \sqrt{\mathcal{D}(s + i\omega)} \qquad (8)$$

where s^{-1} is the average lifetime of a surface element.

CONSTRUCTION OF THE APPARATUS

An early apparatus built along the lines described here was used by Lamb (1965). Some of these preliminary data will be presented below. Figure 3 shows a more recent, improved version of the same equipment as described in complete detail in Appendix A.

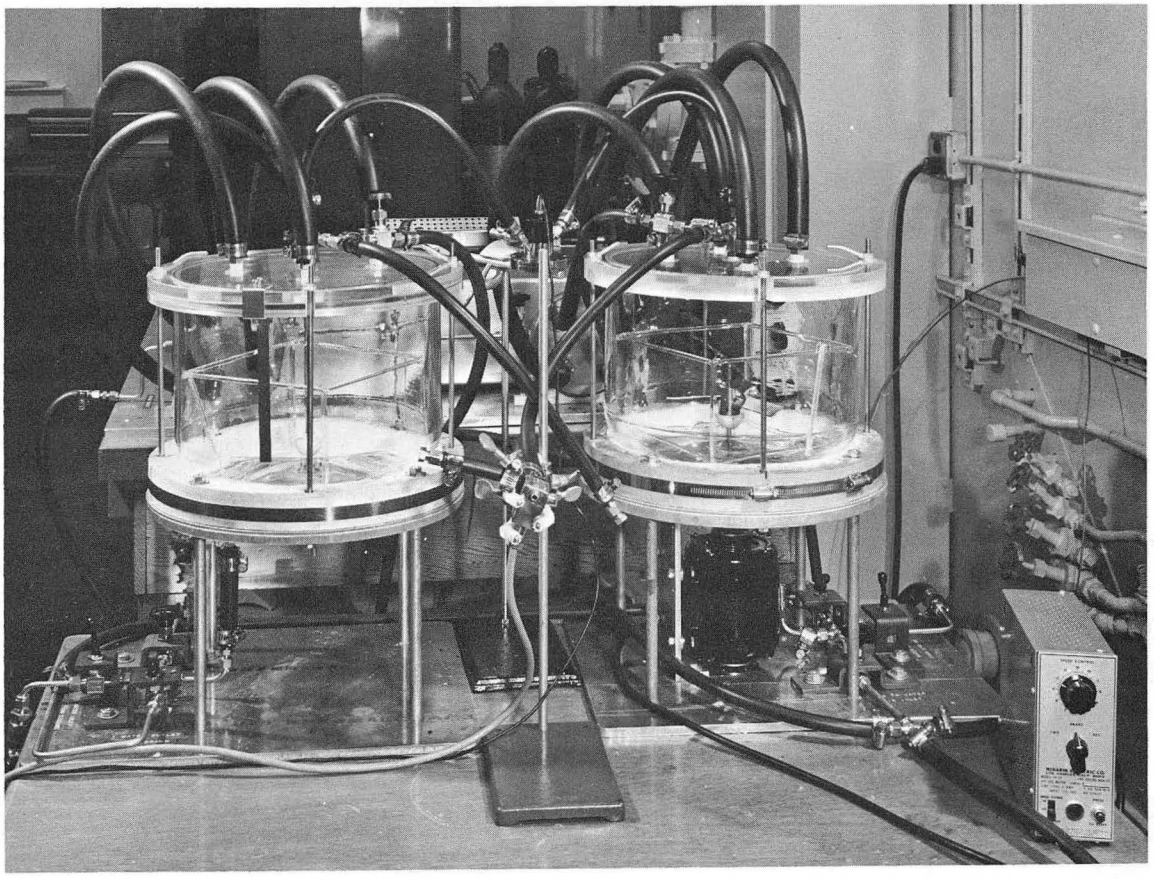

XBB 693-1581

Fig. 3. Photograph of interface impedance bridge

Two "Pyrex" containers, each holding 10 liters of water, are placed side by side on a sturdy table. The water level in each container is about an inch below a carefully machined "Lucite" cover, which is held tightly against the smooth upper rim of the glass vessel and a "Neoprene" O-ring. Each vessel rests in a base which has been filled with Plaster of Paris to fit the glass. Such measures are needed to avoid unwanted volume changes owing to the pressure excursions in the confined gas, which is pure sulfur dioxide.

Behind the glass jars is an electrically driven piston rod as shown in Fig. 4. This device simultaneously moves the hinged covers of two sheet metal boxes in which are "Neoprene" balloons. The balloons are hospital rebreathing bags. The insides of the metal boxes are shaped to the elliptical contour of the balloons by insertion of hollowed pieces of hardwood thereby forming a cavity about the same size as the balloons in their average positions. The balloons are connected by several parallel lengths of large-bore butyl rubber vacuum tubing to their respective glass chambers. When the piston moves the balloons compress or expand and the gas pressure inside the two chambers changes very nearly sinusoidally.

The gas pressure in one chamber and the smaller difference in the pressures were measured with Statham strain gauge transducers. The pressure difference instrument was capable of readings as small as 0.001 in. of water, an amount which would correspond to a volume change on one side of the bridge of only 0.2 cc. The transducers were connected to a Sanborn Transducer Amplifier-Indicator and then to a Sanborn

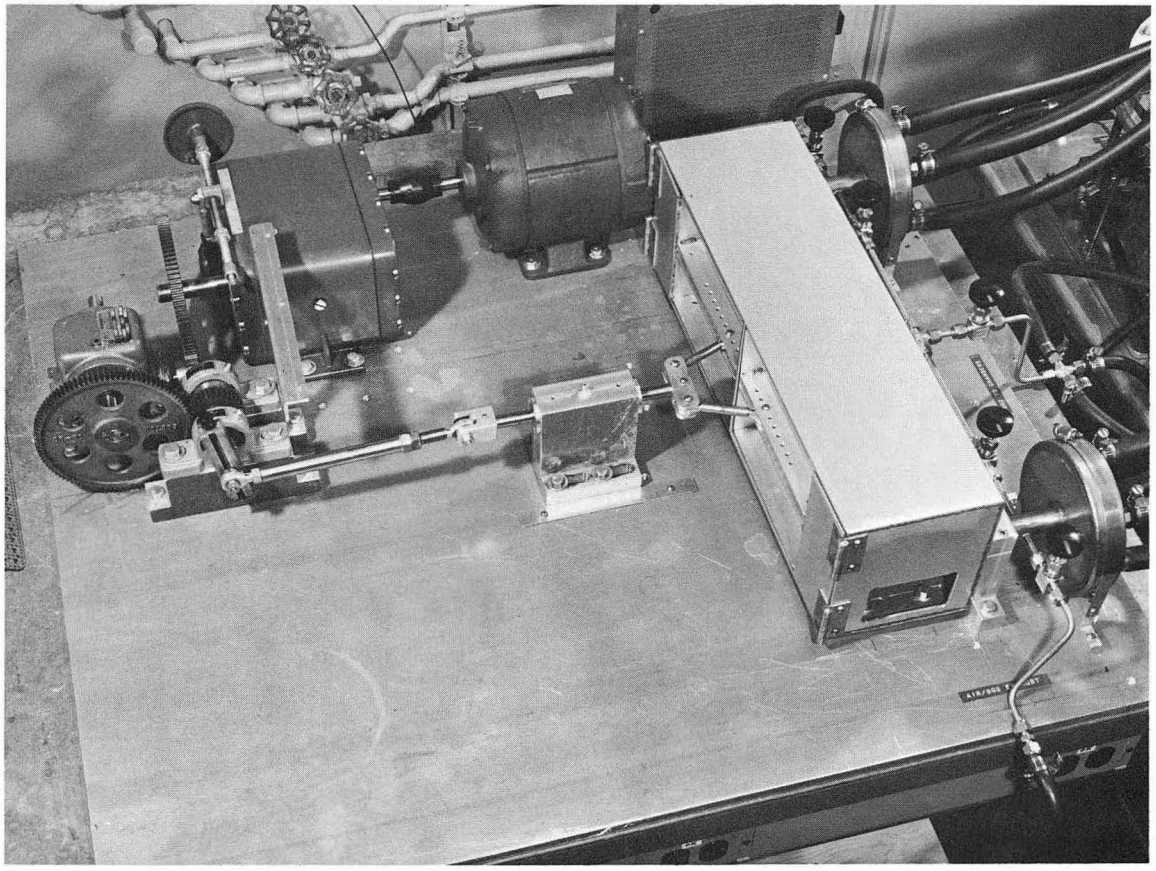

XBB 693-1582

Fig. 4. Photograph of reciprocating drive mechanism.

two-channel inking recorder. The ratio of amplitudes could be found from the ink records. The phase difference between the signals could be read from the charts but more accurate measurements were possible with the aid of a phase-sensitive demodulator.

A critical step in the use of the apparatus was the initial adjustments of the two liquid volumes to give a zero output from the bridge. For example, if it is desired to compare a still and a stirred liquid surface, operation was begun with both sides still. The pressure difference signal was not zero initially but the amplitude could be reduced to about 0.0125 in. water by carefully adding or removing gas-saturated water. The amplitude of the input pressure signal was about 16.6 in. water; during an experiment comparing a turbulent water interface with a stationary interface a pressure difference signal on the order of 0.25 in. water was obtained. Adjustment of the gas pressures to make them equal on both sides was essential and time had to be allowed for the whole mass of liquid in each chamber to come to equilibrium at the average gas pressure. Watching changes in the phase difference was very helpful in making these adjustments.

In our earliest work the reference chamber was a dry container having the same volume as the wet chamber. In order to obtain the initial zero adjustment the liquid surface in the wet chamber was covered with a thin film of polyvinyl fluoride to make it impermeable to the passage of sulfur dioxide. After the volumes of the chambers had been adjusted the film was pushed under the water surface and the measurements of the surface impedance began.

A flat paddle with inclined blades was provided in one of the chambers, entering through a "Teflon" seal in the bottom, in order to stir the liquid. Connections were provided at the top of the chamber for introducing small quantities of surfactants through a hypodermic needle or small movable cups attached to the chamber lid. Details are given in Appendix A.

TYPICAL EXPERIMENTAL RESULTS

Figure 5 shows some of the results of Springer (1969) obtained by comparing a clean stagnant liquid surface with a stagnant surface covered with a thin impermeable film. For the impermeable surface, $k_{L1} = 0$, and Eq. (5) is simplified. When the expression in Eq. (7) is introduced for k_{L2}, corresponding to a stagnant but active surface on side two of the bridge, the simple result is

$$\frac{\hat{\Delta p}}{\hat{p}_2} = (HART_o/V_o)(\mathcal{D}/i\omega)^{1/2} \quad . \tag{9}$$

As the figure shows, the amplitude does fall off as the inverse square root of the frequency, as expected. But, even more significantly, the values of the amplitude ratio agreed very well with those expected from Eq. (9) and from the established values of the Henry's Law coefficient for sulfur dioxide and its diffusion coefficient in water. This indicates that the liquid was very nearly stagnant, at least as far as its response to concentration pulses arriving no more slowly than about one per 30 sec. are concerned, and that such a surface should be a good standard of comparison for others in which there is greater practical interest.

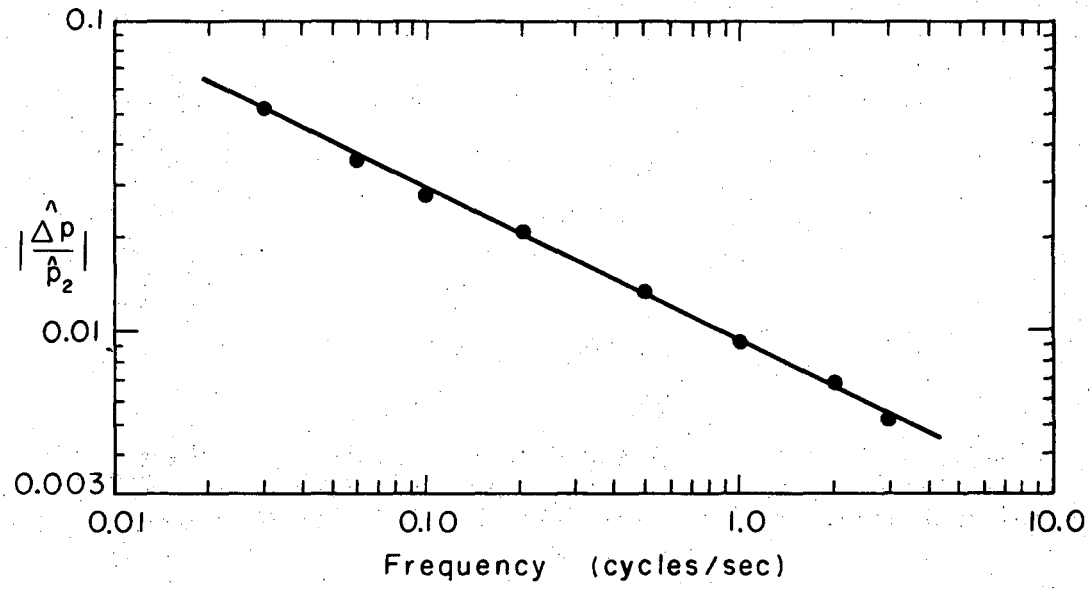

XBL698-3539

Fig. 5. Bridge comparison of a stationary water interface with an impermeable surface. (The straight line is computed from Eq. (9) using accepted values of SO_2 solubility and diffusion coefficient.)

The phase relationship was also measured as a function of frequency and compared to the theoretical response of $-45°$ (Eq. (9)). The measured phase gave an average value of $-46.6°$ and a range of $-43.9°$ to $-50°$ showing quite good agreement with the predicted result.

Figure 6 shows some of Lamb's (1965) results when one side of the bridge was stirred with a paddle having flat, inclined blades, each 1 in. wide by 1.7 in. long. The stirrer was located 3.5 in. above the bottom of the 10-in. deep pool of clean water and four 1-in. wide baffles were located around the inside of the 12 in. I.D. tank. The stirrer speed was 300 r.p.m. It is clear that the frequency response was affected by the interfacial turbulence, especially at low frequencies of the concentration signals. At high frequencies, however, the stirred interface and the stagnant one gave nearly the same responses.

These observations are qualitatively in agreement with the expectations based on the Danckwerts function, Eq. (8). It shows that, depending on the value of s, there will be a transition from a condition at low frequencies, where amplitude is proportional to ω^{-1}, to high frequencies, where it will be proportional to $\omega^{-1/2}$. In qualitative terms the cause of this change is as follows. At low frequencies of the pressure changes the average interfacial fluid element is exposed to only a small fraction of a single concentration cycle before it is submerged. During its life the originally fresh element of surface is able to absorb or desorb dissolved gas freely as needed to respond to the portion of the pressure signal which it feels. At high frequencies, on the other hand, an average fluid particle is buffeted

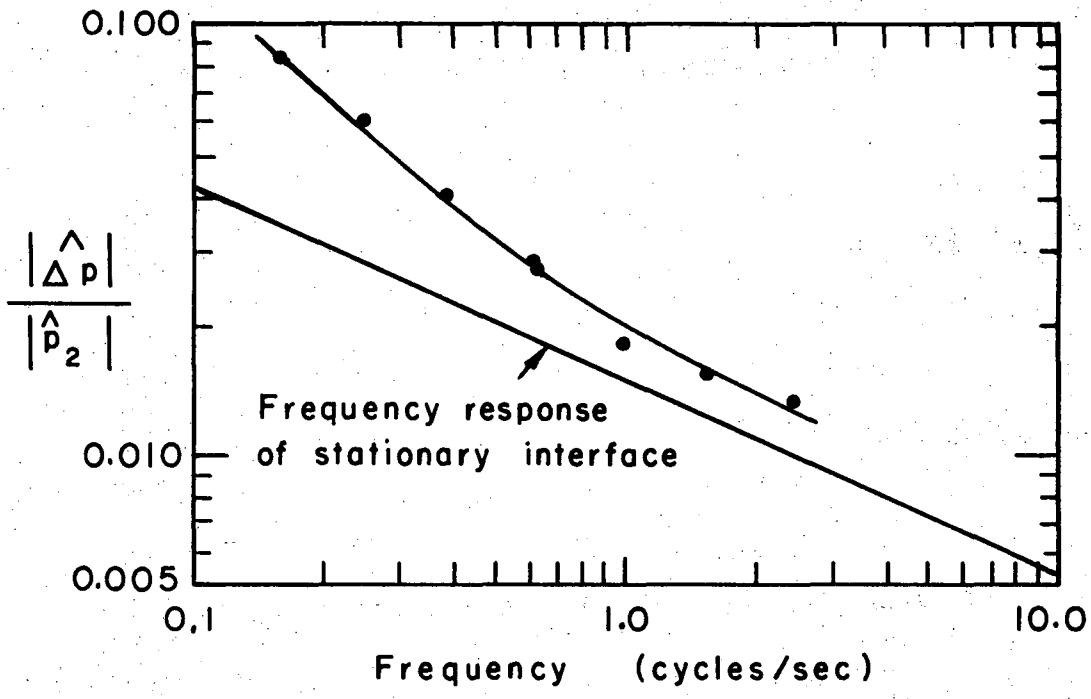

XBL695-2744

Fig. 6. Bridge comparison of a turbulent water interface with an impermeable surface. (Data for SO_2 passing into surface of a stirred pool of water. The apparent value of s is about 2.96 sec^{-1}.)

by several changes in surface concentration. Although it may experience some transient response during the first cycle or so, subsequent cycles find it behaving just as if it has been in the interface for a long time before. Thus, by changing the frequency one can pick out different parts of the surface age spectrum, including all the particles at low frequencies and smaller fractions of the total surface age spectrum as the frequency grows higher. In fact, as we intend to show in a later publication, it is possible to extract the residence time distribution function itself from the observed frequency response.

CONCLUSIONS

The interface impedance bridge is not an easy apparatus to use. Nevertheless, it yields a wealth of detailed information about the kinetic phenomena which affect interfacial mass transfer. The method is in use in our laboratories for the investigation of the role of soluble and insoluble surfactants when SO_2 gas molecules dissolve in water, including not only the ways in which surfactants inhibit the passage of dissolving molecules into a stationary surface but also the ways in which surfactants decrease the mobility of otherwise free particles of water at the interface. Results are reported in Chapter II.

CHAPTER II

RESULTS FROM THE INTERFACE BRIDGE*

ABSTRACT

A new experimental technique is used to measure the effects of surface turbulence and surfactants on mass transfer rates at gas-liquid interfaces. Results indicate that at high turbulence rates the statistical nature of interfaces, with and without surfactants present, may be described by a Danckwerts-type distribution function of surface ages. Measurements of surface film mass transfer resistances show that soluble surfactants offer no measurable resistance while insoluble films show definite resistance to passage of gas molecules. The nature of surface films and their stability in the presence of interfacial turbulence is discussed.

---

*This paper will be submitted for publication as a research paper by Thomas G. Springer and Robert L. Pigford in Fundamentals Quarterly, Industrial and Engineering Chemistry, November, 1969.

INTRODUCTION

There has been a large amount of work in recent years studying the interfacial mass transfer resistance of surfactant films, but the more important problem of characterization of the fluid motion at turbulent interfaces with and without surface films present has not received attention. Bussey (1966) showed the presence of soluble surfactants adds no measurable resistance to mass transfer through water interfaces. It is also known that insoluble materials such as 1-hexadecanol when spread as a monolayer on water can add an additional resistance to mass transfer through the interface (Plevan and Quinn, 1965), (Sada and Himmelblau, 1967), but the effects of surface films on interfacial mobility during turbulent mixing of the liquid are not known. It has been postulated (Davies, 1964) that possible hydrodynamic effects of surface films cause damping of eddies as they approach the interface and reduce mass transfer rates.

An experimental technique has been described (Lamb et al., 1969) for the observation of the resistance to passage of a soluble gas through a gas-liquid interface under dynamic conditions using frequency response analysis. From the data of the experiment one may test various interface mass transfer mechanisms.

The experimental apparatus, called an interface impedance bridge, is comprised of two chambers, each consisting of a variable-volume gas space with a deep pool of liquid below. One chamber has provisions for varying the surface conditions of the liquid; the second chamber is used as a reference chamber of calculable impedance. The gas pressure may

be varied in the two chambers simultaneously in a sinusoidal manner. From the measured frequency response of the bridge-type apparatus one can calculate the impedance of the test chamber and relate the impedance to resistances to mass transfer at the gas-liquid interface.

Characterization of the mass transfer coefficient for a randomly turbulent surface, following the suggestion of Danckwerts (1951) for example, may be examined since the frequency response information yields the whole statistical distribution of fluid particle residence times in the interface as well as the average surface element age and replacement frequency.

One may also examine the effect of surface films, both soluble and insoluble, on mass transfer through a stagnant interface as well as a turbulent interface. These measurements allow one to separate the surface resistance and hydrodynamic effects of films to determine their independent effects.

QUANTITATIVE DEVELOPMENT

1. Statistical Characteristics of Turbulent Interfaces

Comparison of pressure oscillations, occuring in two chambers each containing a soluble gas above deep pools of liquid, caused by sinusoidal volume changes yields (Lamb et al., 1969)

$$\frac{\hat{p}_1 - \hat{p}_2}{\hat{p}_2} = \frac{\hat{\Delta p}}{\hat{p}_2} = \frac{Q_2 k_{L2}(\omega) - Q_1 k_{L1}(\omega)}{i\omega + Q_1 k_{L1}(\omega)} \qquad (1)$$

with $Q = HART_o/V_o$, where H is the Henry's Law coefficient, A is the

known area of the interface, $k_L(\omega)$ is the possibly frequency-dependent mass transfer coefficient of the liquid surface, T_o is the time-average surrounding temperature and V_o is the average gas volume of the chambers. $\hat{p}$ is the amplitude of the pressure oscillations and $\hat{\Delta p}$ is that of the pressure difference signal.

Experimentally one may use either an impermeable surface or a stagnant, clean liquid surface for a standard interface of calculable impedance. Indeed, in our experimental work both types of reference chambers have been used. However, it is slightly more convenient mathematically to use an impermeable surface as the standard reference. Since it has been shown (Lamb et al., 1969) that the behavior of a clean, stagnant interface can be calculated reliably, it is a simple matter to convert from one standard reference to the other. For the sake of brevity the quantitative analysis presented here will deal with an impermeable surface as a reference.

Assume that in chamber two a turbulent interface exists, obtained by stirring a pool of clean liquid, and that an impermeable interface exists in the reference chamber. Equation (1) then becomes

$$\frac{\hat{\Delta p}}{\hat{p}_t} = \frac{Q_t k_{Lt}(\omega)}{i\omega} \quad . \tag{2}$$

Measurement of the indicated pressure and pressure-difference signals enables one to calculate the frequency-dependent mass transfer coefficient, $k_{Lt}(\omega)$.

To find the flux through a turbulent interface one must make some assumptions concerning the nature of the interfacial fluid motion. As a first approximation a randomly turbulent surface may be assumed, following the suggestion of Danckwerts (1951). He assumed that a turbulent interface consists of a mosaic of elements of varying ages, which are randomly replaced by fresh elements from the bulk of the liquid. Following this assumption, let

$f(\theta)$ = surface age distribution function

$f(\theta)d\theta$ = fraction of the interface which is occupied by particles which have been exposed there for a time, θ, within time increment, $d\theta$.

By definition

$$\int_0^\infty f(\theta)d\theta = 1 \quad .$$

If one assumes that the scale of turbulence is much greater than the depth of penetration of the solute diffusing from the surface, one may apply the transient diffusion equation to each surface element independently.

Let α = time when an element was first exposed at the surface. Then $\theta = t - \alpha$ = the age of the surface element and

$$\mathcal{D}\left(\frac{\partial^2 c}{\partial x^2}\right) = \frac{\partial c}{\partial t} \quad \text{for} \quad t \geqslant \alpha,\ x \geqslant 0 \quad . \tag{3}$$

The boundary conditions on $c(x,\theta)$ are,

$$c(0,\theta) = H\,\hat{p}\,\exp(i\omega t) = H\,\hat{p}\,\exp(i\omega\alpha)\,\exp(i\omega\theta)$$

$$c(\infty,0) = c(x,0) = 0 \quad .$$

Laplace transforms may be used to solve Eq. (3) subject to the listed boundary conditions. The solution is

$$\bar{c}(x,m) = H\,\hat{p}\,\left(\frac{1}{m-i\omega}\right)\,\exp\left(i\omega\alpha - \left(\frac{m}{\mathcal{D}}\right)^{1/2}x\right) \qquad (4)$$

where m represents the Laplace transform variable and x is the distance from the interface. The Laplace transform of the flux at the interface may be found from Eq. (4).

$$\bar{L}(\dot{n}) = AH\,\hat{p}\,\mathcal{D}^{1/2}\,\left(\frac{m^{1/2}}{m-i\omega}\right)\,\exp(i\omega\alpha) \qquad (5)$$

where n represents the instantaneous number of moles of gas above the liquid and the dot above represents differentiation with respect to time. The inverse transform (Erdelyi, 1954) of Eq. (5) is

$$\dot{n}(\theta,t) = AH\,\hat{p}\,\exp(i\omega t)(\mathcal{D}/\pi\theta)^{1/2}[\exp(i\omega\theta) + (i\omega\mathcal{D})^{1/2}\mathrm{erf}(i\omega\theta)^{1/2}] \quad . \qquad (6)$$

The average, steady state rate of absorption into the turbulent interface of age distribution $f(\theta)$ may be found by summation over all surface elements

$$\dot{n}(t) = \int_0^\infty \dot{n}(t,\theta)\, f(\theta)\, d\theta \quad . \tag{7}$$

This gives

$$\dot{n}(t) = HA\, \hat{p}\, \exp(i\omega t)\, G(\omega) \tag{8}$$

where

$$G(\omega) = (\mathscr{D}/\pi)^{1/2} \int_0^\infty \left[f(\theta) + i\omega \int_\theta^\infty f(x)dx \right] \theta^{-1/2} \exp(-i\omega\theta) d\theta \quad . \tag{9}$$

A mass balance at the liquid interface yields

$$\dot{n}(t) = -Hk_{Lt}(\omega)\, A(p-p_o) = -\mathscr{D} A \left(\frac{\partial c}{\partial x} \right) \Bigg|_{x=0} \tag{10}$$

where $p = p_o + \hat{p}\, \exp(i\omega t)$.

Using Eqs. (8) and (10), one can see that

$$k_{Lt}(\omega) = G(\omega) \quad . \tag{11}$$

It is obvious that knowledge of $f(\theta)$ allows calculation of the mass transfer coefficient for a turbulent interface. Conversely, since one can determine $k_{Lt}(\omega)$ experimentally, $f(\theta)$ can be found from measured values of $k_{Lt}(\omega)$ or $G(\omega)$ if Eq. (9) can be solved as an integral equation for the unknown function, $f(\theta)$.

Consider the integral Eq. (9) and note that we are free to define $f(\theta) = 0$ for $\theta < 0$. Thus

$$\int_{\theta}^{\infty} f(x)\, dx = 1 \quad \text{for} \quad \theta \leqslant 0 \quad .$$

The integral over the full range of θ is

$$G^*(\omega) = \left(\frac{\mathfrak{Q}}{\pi}\right)^{1/2} \int_{-\infty}^{\infty} \left[f(\theta) + i\omega \int_{\theta}^{\infty} f(x)dx \right] \theta^{-1/2} \exp(-i\omega\theta)d\theta$$

$$G^*(\omega) = \left(\frac{\mathfrak{Q}}{\pi}\right)^{1/2} \int_{-\infty}^{0} i\omega\theta^{-1/2} \exp(-i\omega\theta)d\theta + G(\omega) \quad . \tag{12}$$

Evaluation of the first integral gives

$$G^*(\omega) = (i\omega\mathfrak{Q})^{1/2} + G(\omega) \quad .$$

Consider now solving Eq. (12) to find $f(\theta)$. The second part of the integral in Eq. (12) can be integrated by parts. Combining the result with Eqs. (11) and (12) gives

$$G^*(\omega) = -\frac{1}{2} \left(\frac{\mathfrak{Q}}{\pi}\right)^{1/2} \int_{-\infty}^{\infty} \theta^{-3/2} \int_{\theta}^{\infty} f(x)dx \exp(-i\omega\theta)d\theta \quad . \tag{13}$$

This is in the form of a Fourier integral, and, subject to certain continuity conditions, it follows that

$$\int_{\theta}^{\infty} f(x)dx = -\left(\frac{\theta^3}{\mathcal{D}\pi}\right)^{1/2} \int_{-\infty}^{\infty} \exp(i\omega\theta)[G(\omega) + (i\omega\mathcal{D})^{1/2}]d\omega \quad . \tag{14}$$

Differentiation gives

$$f(\theta) = (1/2)(\pi\mathcal{D})^{-1/2} \int_{-\infty}^{\infty} (3\theta^{1/2} + 2i\omega\theta^{3/2})[G(\omega) + (i\omega\mathcal{D})^{1/2}] \tag{15}$$

$$\exp(i\omega\theta)d\omega \quad .$$

Equation (15) requires the observation of $G(\omega)$ over both positive and negative frequencies. The negative range is obviously impossible to observe experimentally. Fortunately, however, the fact that the distribution function $f(\theta)$ is real makes it possible to show that the real part, $R(\omega)$, of the observed frequency response is an even function of ω while the imaginary part, $I(\omega)$, is odd. After some algebra, Eq. (15) can be shown to be equivalent to

$$f(\theta) = (\theta/\pi\mathcal{D})^{1/2} \int_{0}^{\infty} [(3R - 2\omega\theta I)\cos(\omega\theta) - (3I + 2\omega\theta R)\sin(\omega\theta)]d\omega \tag{16}$$

which is the form most suitable for numerical evaluation. For details on how to do this, see Springer (1969).

2. Frequency Response of Interface Models

a. The Randomly Turbulent Interface

Using the previous analysis one may test models concerning the structure of a turbulent interface by comparison of an observed frequency

response with one which has been predicted. Many surface renewal models have been postulated, but one of the earliest and simplest of these theories was proposed by Danckwerts (1951). He assumed that the motion of a stirred liquid will continually replace with fresh fluid those elements which have been exposed for a finite length of time. Danckwerts also assumed that the chance of an element of surface being replaced within a given time is independent of its age; hence, the fractional rate of replacement of the elements belonging to every age group is equal to a constant s. According to these assumptions,

$$f(\theta) = s \exp(-s\theta) \quad . \tag{17}$$

Calculation of the frequency response behavior of such a surface by using Eqs. (2), (9), (11) and (17) yields

$$\frac{\hat{\Delta p}}{\hat{p}_t} = Q\mathcal{D}^{1/2}[(s^2 + \omega^2)^{1/4}/\omega]\angle \tan^{-1}\left[\frac{(s^2 + \omega^2)^{1/2} + s}{(s^2 + \omega^2)^{1/2} - s}\right]^{1/2} \quad . \tag{18}$$

From preliminary results by Lamb (1965) it appeared that frequency response results would be similar to those predicted by the Danckwerts model. For this reason, it was decided that this model would be used as a trial basis for evaluating new data. The phase and amplitude data may be analyzed separately, according to Eq. (18), to determine best-fit values for the constants Q and s. For convenience let $|\hat{\Delta p}/\hat{p}_t| = A(\omega)$ and represent the phase angle by $\phi(\omega)$. Using the amplitude results in the following form

$$(\omega A)^4 = Q\mathcal{D}^{1/2} s^2 + Q\mathcal{D}^{1/2} \omega^2 \qquad (19)$$

and the phase in the form

$$2 \tan \phi/(\tan^2\phi - 1) = \omega/s \qquad (20)$$

one may apply a linear least squares analysis to collected data as shown in Eqs. (19) and (20) to find Q and s. One can then graphically compare the observed frequency response, according to Eq. (2), with that from Eq. (18).

b. Film-Covered Liquid Surfaces

Consider next a stagnant liquid covered with a thin surface film. Transport of gas through the interface is described by the following equation and boundary conditions

$$\mathcal{D} \frac{\partial^2 c}{\partial x^2} = \frac{\partial c}{\partial t}$$

$$c(\infty,t) = c_o = Hp_o$$

$$N(t) = - \mathcal{D} \frac{\partial c(0,t)}{\partial x} = K_f[H\, p(t) - c(0,t)] \quad .$$

Assume a solution of the form

$$c(x,t) = \hat{c}(x) \exp(i\omega t) + H\, p_o$$

and remember that

$$p(t) = p_o + \hat{p} \exp(i\omega t) \quad .$$

Let $N = \hat{N} \exp(i\omega t)$, then

$$\hat{N} = \frac{K_f (i\omega \mathcal{D})^{1/2}}{K_f + (i\omega \mathcal{D})^{1/2}} H \hat{p} \quad .$$

Consider an interface impedance bridge where in the test chamber there is a stagnant liquid covered with a surface film and where the standard reference chamber is an impermeable surface. The pressure-difference signal from such a bridge may be found knowing the flux across the interface, N_o.

$$\frac{\hat{p}_I - \hat{p}_f}{\hat{p}_f} = Q_f \frac{K_f (i\omega \mathcal{D})^{1/2}}{i\omega (K_f + (i\omega \mathcal{D})^{1/2}} \quad . \tag{21}$$

The subscript f indicates that a film-covered surface is present in that chamber; I denotes a chamber containing an impermeable surface.

One may rearrange the above equation so that a linear least squares analysis may be applied to observed pressure signals to obtain the surface film coefficient K_f. One may recognize that K_f must be a real number to be physically realizable and therefore use only the real part of Eq. (21).

Thus it is clear that, using the frequency response data, one can obtain both statistical distributions and physical constants for specific models.

MATERIALS

In this work the gas-liquid system used was sulfur dioxide-water. An anhydrous grade (99.90% purity by weight) sulfur dioxide was obtained from the Matheson Company. The water used in the experiments was distilled water, from a laboratory supply, that had been degassed and stored under a sulfur dioxide atmosphere.

Two surfactants were used. They were 1-hexadecanol (cetyl alcohol) and sodium lauryl sulfonate. The insoluble surfactant, 1-hexadecanol, was obtained from Eastman Chemicals Company and was reported to be a reagent grade. The soluble surfactant, sodium lauryl sulfonate, was obtained from two sources, Procter and Gamble and E. I. du Pont de Nemours Company. The sample from Du Pont was of questionable purity, but the sample from Procter and Gamble was reported to be 99^{+}% pure.

No attempt was made to purify samples further, but as criteria for performance surface tension-versus-concentration curves were measured. A cenco Du Nouy (ring-type) Tensiometer was used to measure surface tension; the results are shown in Figs. 1 and 2. Note that, despite the unknown purity for the sample obtained from Du Pont, its curve in Fig. 1 agrees very well with the curve obtained with the carefully purified sample from Procter and Gamble, indicating that surface-active impurities must have been negligible. Note also that the concentration of 1-hexadecanol is given in monolayers present on the surface. They were calculated assuming that a single molecule occupies 20 sq Ångstroms of the surface.

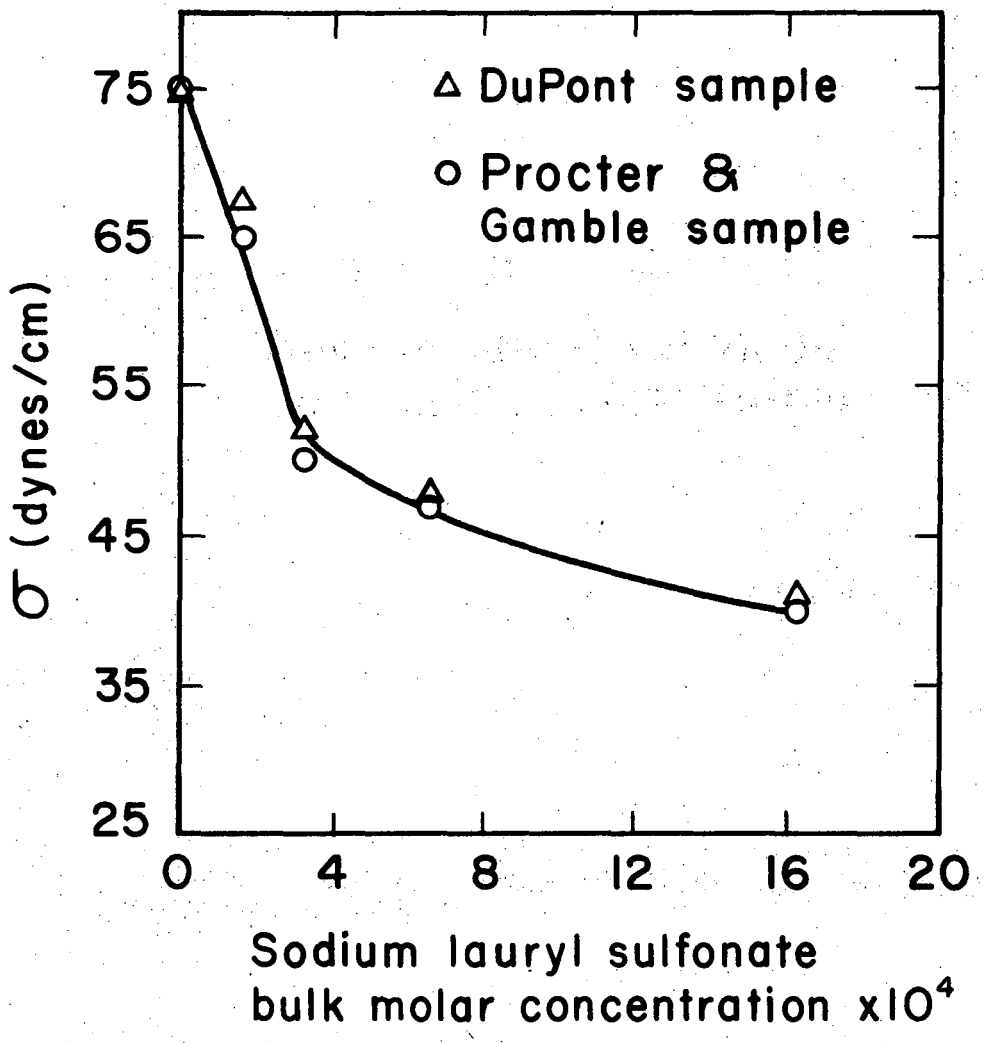

XBL6910-3915

Fig. 1. Surface tension of sodium lauryl sulfonate solutions versus bulk liquid concentration.

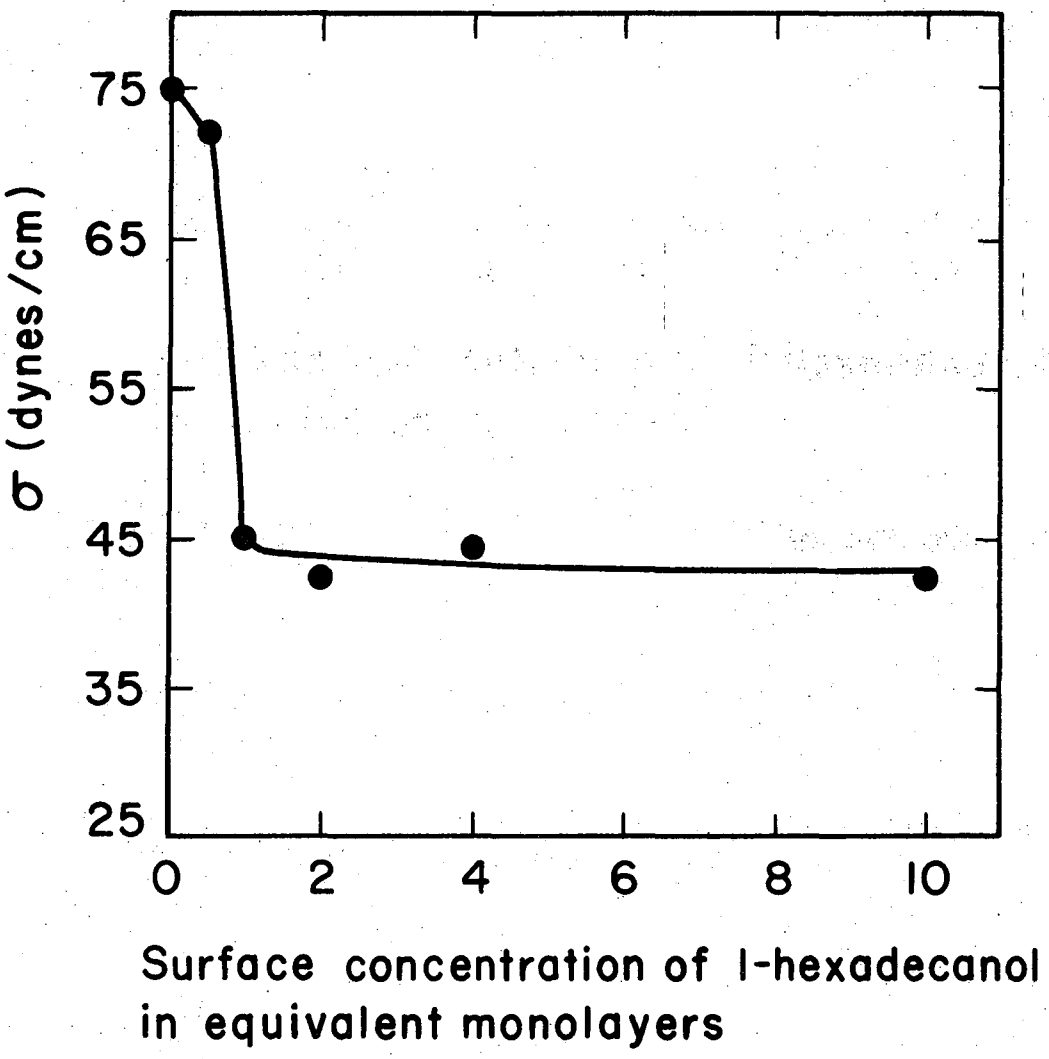

XBL6910-3916

Fig. 2. Surface tension of 1-hexadecanol films versus equivalent surface concentration in monolayers.

The liquid surfaces in all tests were initially cleaned by placing a clean absorbent filter paper on the surface to remove dust particles and any insoluble contaminants that might have collected there.

It was found that the insoluble surfactant was best spread by pipetting an ether solution onto a liquid surface contained in a small movable cup. The solvent was allowed to evaporate and the cup was attached to the inside of the test chamber lid. The surfactant was added to the surface by immersing the cup under the water in the closed chamber. The soluble surfactant was added by use of the cup also, but no solvent or liquid was added to the cup. For complete details of the cleaning procedure and the method of surfactant addition see Springer (1969).

EXPERIMENTAL RESULTS

Before results are given, the procedure for presentation of data needs to be explained. As noted earlier, it is possible for frequency response to be measured relative to either an impermeable surface or a stagnant liquid surface as standards in the reference chamber. Data were taken in both ways, but were presented relative to an impermeable surface in results shown here. To distinguish between methods of measurements, all data points taken relative to an impermeable surface are shown as darkened symbols; those taken relative to a stagnant liquid interface are shown as open symbols on the graphs.

It has also been shown earlier that data may be analyzed by treating the amplitude and phase data results separately. The data

shown for clean, turbulent interfaces includes plots of both amplitude and phase relationships. These plots are typical of other results, so to conserve space only the amplitude results will be plotted for other data. The tables containing results of analysis of data will contain results for both amplitude and phase data. Complete tables of all pertinent data have been deposited as Document No. 0000 with the ADI Auxiliary Publications Project, Photoduplication Service, Library of Congress, Washington, D. C. 20540, where copies may be secured.

1. Clean Turbulent Surfaces

Consider a turbulent, clean interface, obtained by stirring the pool of liquid below at a rate of 230 rpm. By comparing this interface with an impermeable one in a standard reference chamber using the interface impedance bridge, the frequency response shown in Fig. 3 was obtained. The solid curved line represents the response predicted by Eq. (18) using the values of s and $Q^* = Q\mathcal{D}^{1/2}$ given in Table I; the straight line is the theoretical response of a clean, stagnant surface compared to an impermeable surface. Note that as frequency becomes large the response of a turbulent interface should approach that of a stagnant interface. Introduction of turbulence to a stagnant interface causes an increase in the surface area for mass transfer because of ripples produced in the otherwise smooth surface and also because of wetting of the chamber wall directly above the normal liquid level due to the irregular motion of the surface. The apparent increase is shown by the values of Q^* listed in Table I. The dashed lines in Fig. 3 represent the theoretical response of a stagnant surface of surface area

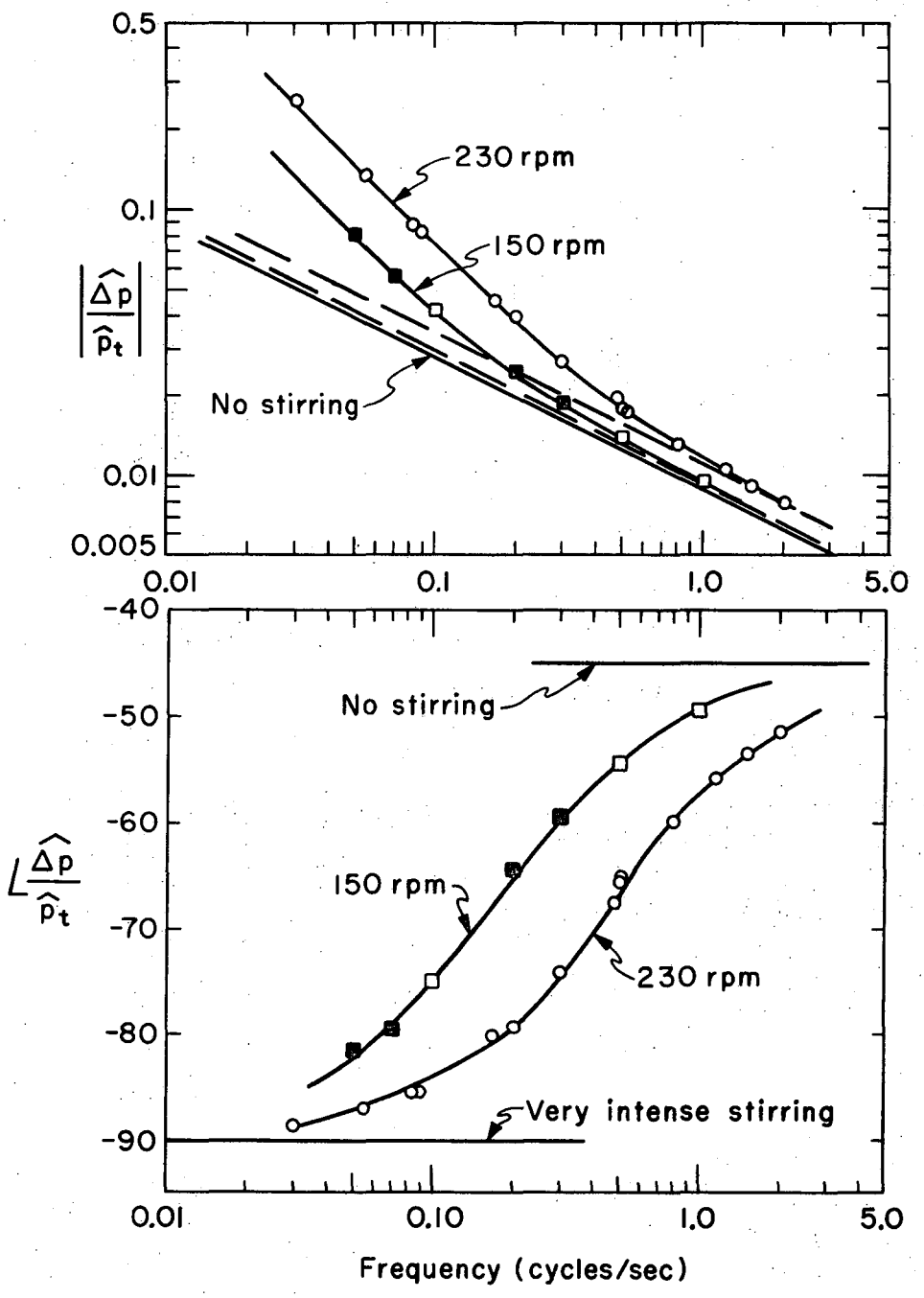

XBL6910-3913

Fig. 3. Bridge comparison of a clean, turbulent water interface with an impermeable surface. (○ -liquid stirred at a rate of 230 rpm; □ -liquid stirred at a rate of 150 rpm.)

Table I. Results of lease squares analysis of data for a clean, turbulent interface.

Stirring Speed rpm	Phase Data s, sec^{-1}	Amplitude Data s, sec^{-1}	Amplitude Data Q^*, cm^{-1}
0	0	0	0
150	1.04±0.07[a]	1.09±0.08	0.0233±0.00007
230	2.88±0.09	2.87±0.16	0.0272±0.00011

[a]Standard error computed on the basis of 95% confidence level, i.e. approximately two standard deviations.

equivalent to the turbulent interface. Based on the surface area of the stagnant pool of liquid (625 cc), a gas-space average volume of 4500 cc, a Henry's Law coefficient of 0.02368 g-moles/(cc)(atm), and a diffusivity in water of 0.0000146 sq cm/sec for dissolved sulfur dioxide, Q^* = 0.0225 cm^{-1} is expected.

Application of Eq. (16) allows one to calculate the age distribution function of the interface; the result is shown in Fig. 4. The solid line in this figure represents the response predicted by a Danckwerts age distribution function based on values of s and Q^* from Table I.

A similar analysis of a turbulent, clean interface, obtained by stirring the liquid at a rate of 150 rpm is shown in Figs. 3 and 5. Table I shows the results of the least squares analysis as described by Eqs. (19) and (20).

Examination of these results indicates that under the conditions of these experiments the age distribution proposed by Danckwerts is a good approximation to that obtained experimentally. This means that under these conditions of turbulence the Danckwerts approximation may be used to predict mass transfer through the interface.

2. Effect of soluble Surfactants

A stagnant liquid of a specified concentration of the soluble surfactant sodium lauryl sulfonate was compared to an impermeable reference chamber. The frequency response revealed that no measurable change in mass transfer through the interface could be detected at all concentrations tested. The concentrations were 0.0001635-M,

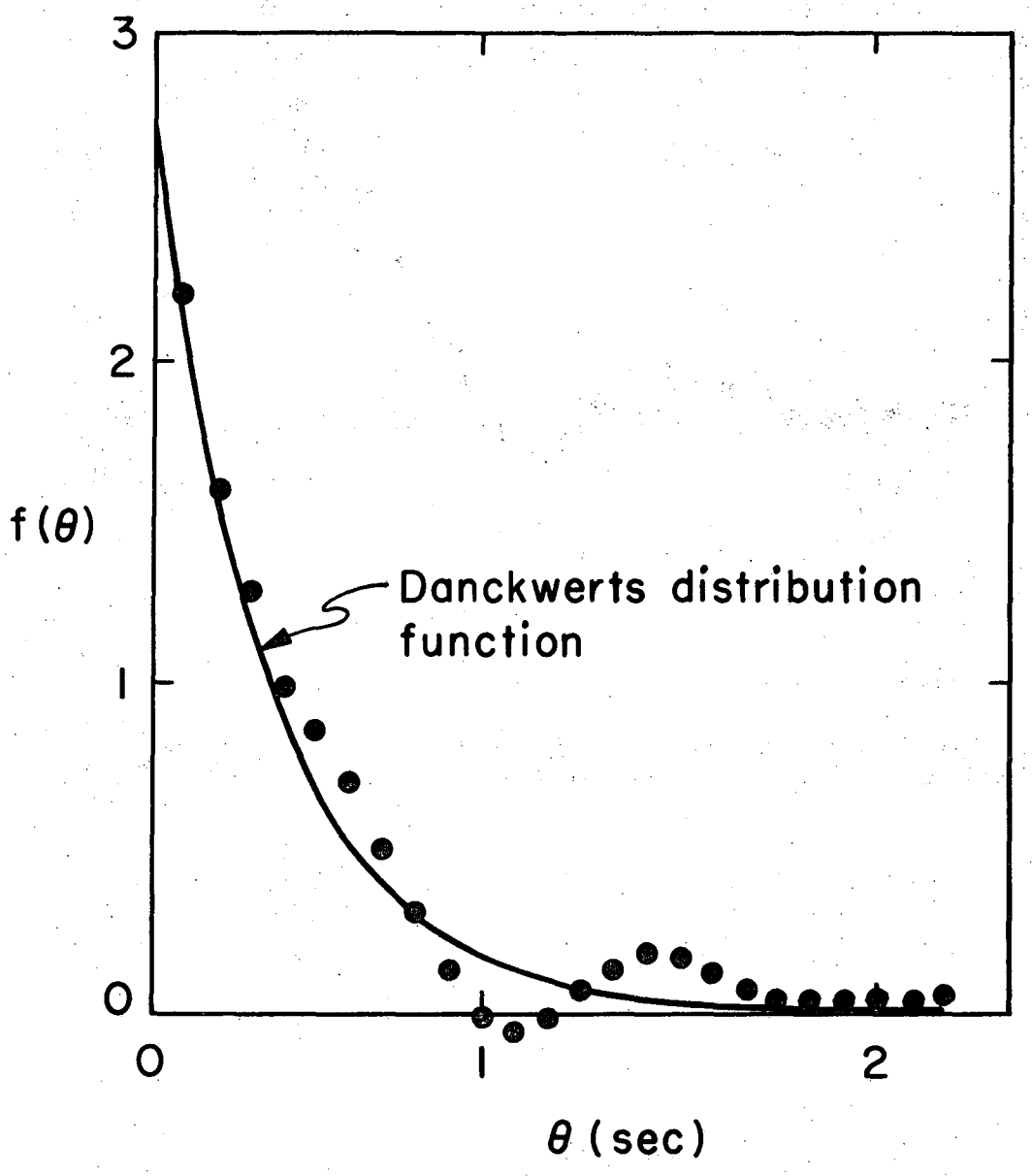

XBL6910-3911

Fig. 4. Surface age distribution function versus surface element age for a liquid stirred at a rate of 230 rpm. Data points obtained with Eq. (15).

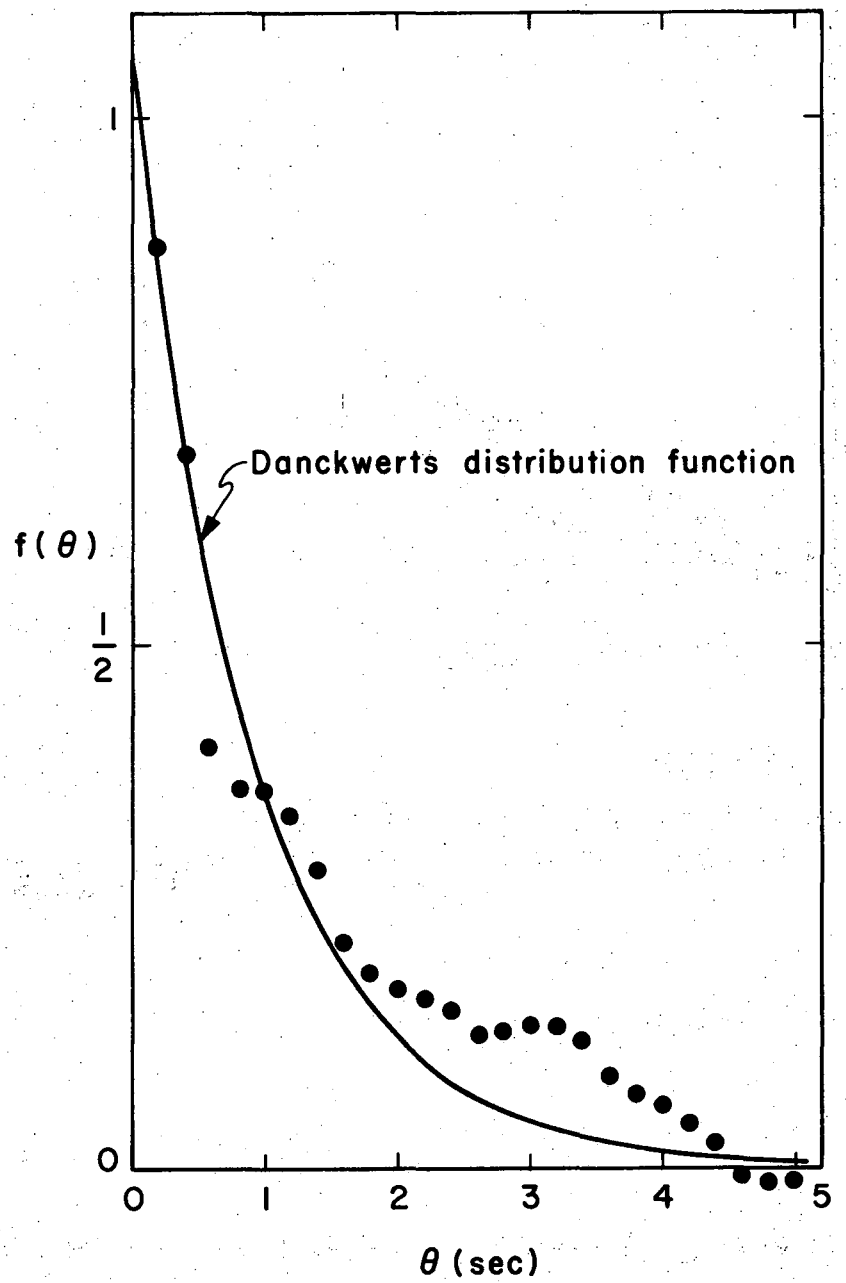

Fig. 5. Surface age distribution function versus surface element age for a liquid stirred at a rate of 150 rpm. Data points obtained with Eq. (15).

0.000327-M, and 0.00106-M. According to the Gibbs adsorption equation these concentrations correspond to surface excess concentrations approximately equivalent to 1/2, 1 and 3.1 monolayers, respectively, if one assumes that a surface concentration of approximately 10^{14} molecules/cm^2 is equivalent to a monolayer.

The effect of the soluble surfactant on transfer through a turbulent liquid interface was next examined. A turbulent interface, obtained by stirring the liquid at a rate of 230 rpm was compared with an impermeable surface. The frequency response results are shown in Fig. 6 for a clean, turbulent interface and for a turbulent liquid at the two lower concentrations of surfactant. The solid lines in the figure represent theoretical responses as explained earlier.

Tests were also carried out at a lower turbulence level, obtained by stirring the liquid at a rate of 150 rpm. The frequency response results were similar to those at the higher turbulence meaning that all concentrations tested showed the typical behavior shown in Fig. 6.

The turbulent data in the presence of sodium lauryl sulfonate were analyzed in the same manner as the clean interfaces. Calculation of the surface age distribution functions indicated that the surfactant did reduce the intensity of the turbulence at the given stirring speeds but did not affect the apparently random statistical nature of the surfaces. Thus, the assumptions of Danckwerts concerning random replacement of surface fluid elements are still very nearly true. The amplitude and phase data were treated separately according to Eqs. (19) and (20). The results are shown in Table II.

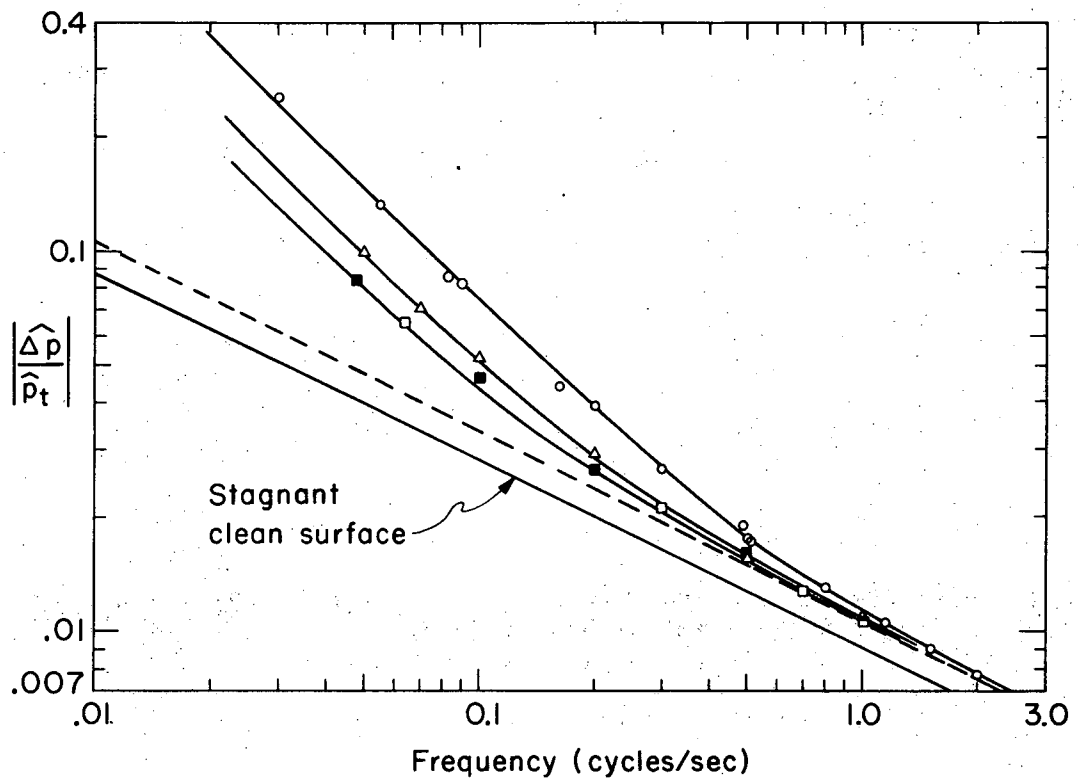

Fig. 6. Bridge comparison of turbulent sodium lauryl sulfonate solutions (stirring rate of 230 rpm) with an impermeable surface. (○ -clean liquid; Δ -0.0001635-M solution; □ -0.000327-M solution).

Table II. Results of least squares analysis on data for water solutions of sodium lauryl sulfonate.

Stirring Speed rpm	Bulk Concentration moles/liter	Phase Data s, sec^{-1}	Amplitude Data s, sec^{-1}	Amplitude Data Q^*, cm^{-1}
150	0.0001635	0.864±0.192[a]	0.853±0.106	0.0230±0.00006
150	0.000327	0.688±0.116	0.612±0.097	0.0235±0.00015
150	0.00106[b]	0.578±0.180	0.507±0.034	0.0231±0.00004
230	0.0001635	1.29 ±0.07	1.22 ±0.250	0.0272±0.00024
230	0.000327	0.828±0.076	0.782±1.17	0.0274±0.00061
230	0.00106	0.699±0.060	2.42 ±0.66	0.026 ±0.001

[a]Standard error computed on the basis of 95% confidence level, i.e. approximately two standard deviations.

[b]Sodium lauryl sulfonate sample obtained from du Pont was used in this run only.

For the 0.00106-M liquid concentration of sodium lauryl sulfonate an unusual phenomena was observed at a stirring speed of 230 rpm. During pressure oscillations in the gas phase there occured oscillating bubble nucleation and growth in the liquid phase. The nucleation and growth began as the gas pressure decreased and became a maximum when the gas pressure was smallest. As the gas pressure increased, the bubbles began to disappear and the bubble concentration was nearly zero at the maximum gas pressure. Figures 7 and 8 show the bubble concentrations at maximum and minimum values, respectively. These pictures were taken when the frequency of oscillation of the gas pressure was 0.1 cycles/sec. The formation and growth of bubbles was found nearly to disappear as the frequency increased to 0.7 cycles/sec.

Treatment of the frequency response results according to the Danckwerts model showed a considerable difference between s values calculated from the amplitude and the phase data, as shown in Table II. Obviously, a Danckwerts distribution cannot reasonably describe these results. The oscillating bubble concentration caused the apparent liquid volume and the gas-liquid surface area to vary with time and also with frequency of oscillation. No reasonable conclusions could be drawn from these data.

The phenomenon apparently occurs because reduction of the gas pressure during oscillation produces a liquid solution that is slightly oversaturated. The reduction in surface tension owing to the surfactant's presence allows bubbles to form and grow more easily. At lower concentrations of surfactant very few bubbles were observed at any stirring

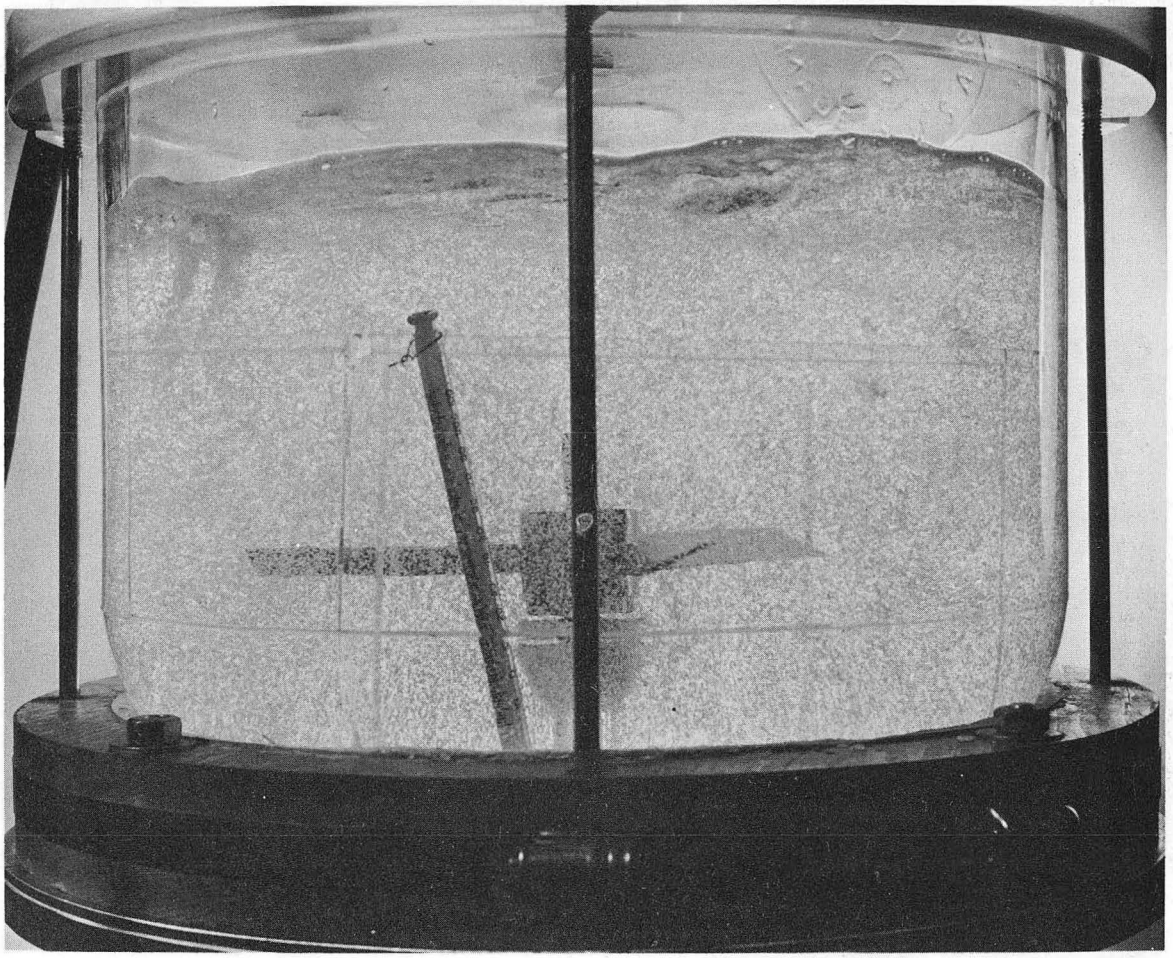

XBB 694-4064

Fig. 7. Photograph of 0.00106-M sodium lauryl sulfonate solution at time of maximum bubble concentration. (stirring rate of 230 rpm.)

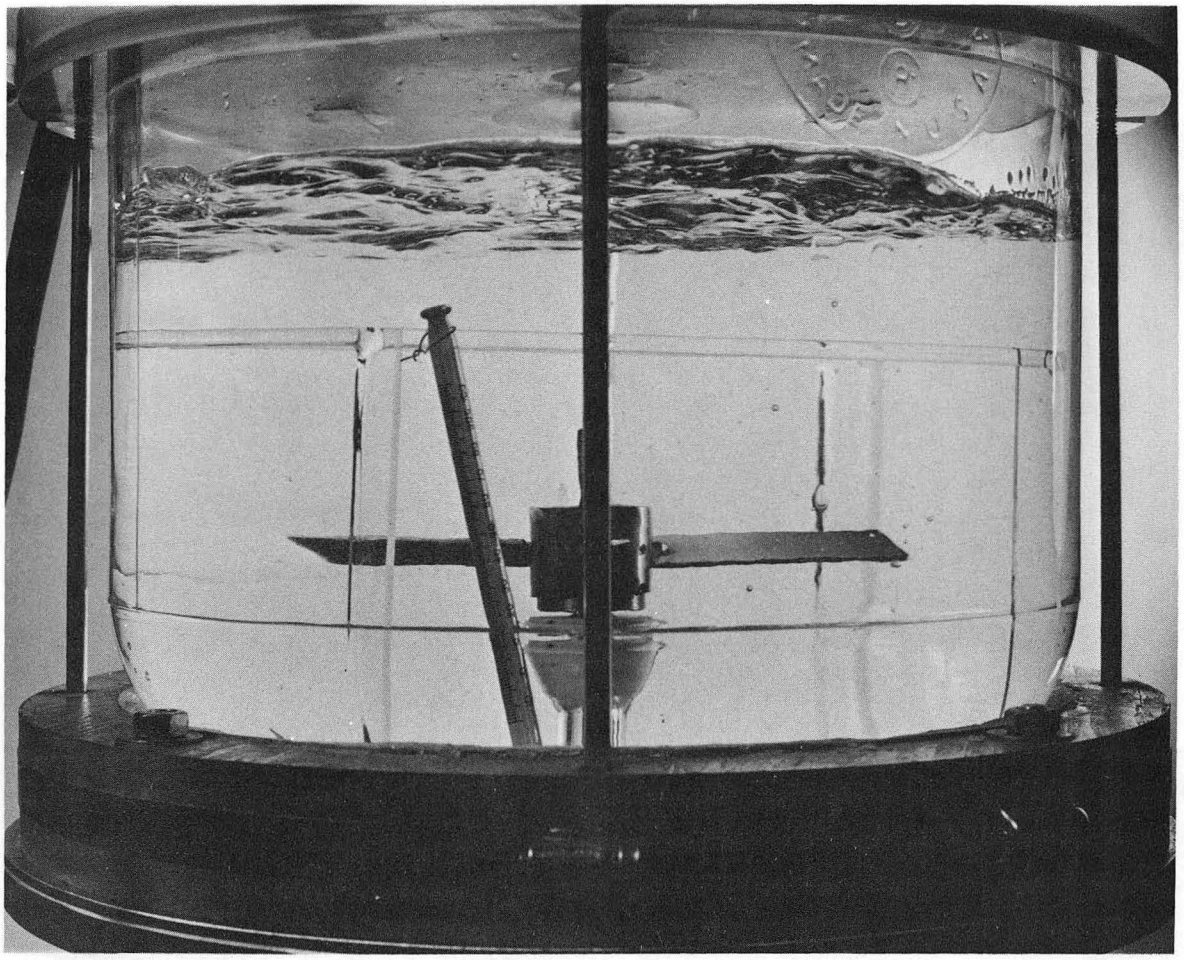

XBB 694-4063

Fig. 8. Photograph of 0.00106-M sodium lauryl sulfonate solution at time of minimum bubble concentration. (stirring rate of 150 rpm.)

speed. Because of the intensity of stirring, a few entrained bubbles could be seen even in a pure liquid.

3. Effect of Insoluble Surfactants

Insoluble films of 1-hexadecanol were placed on the surface of a stationary liquid and compared to a clean stagnant liquid surface as a standard reference chamber. Concentrations equivalent to 1/2, 1 and 2 monolayers were tested. Unlike the results for a soluble film, a definite film resistance to gas transport was observed. Figure 9 shows the frequency response results for the three concentrations tested. The solid lines represent solutions to Eq. (21), using in each case the value of K_f which produced the best fit of the data (Table III).

The effect of the insoluble film on transfer through turbulent interfaces was next analyzed. Consider a turbulent surface covered with a film of 1-hexadecanol with the liquid stirred at a rate of 150 rpm. When this surface was compared to an impermeable surface as a standard reference, the results shown in Fig. 10 were obtained. The theoretical solid line in this figure corresponds to the results obtained for a clean turbulent interface. Concentrations equivalent to 1/2, 1 and 2 monolayers were used.

When the stirring rate was increased to 230 rpm similar results were obtained, indicating that insoluble films at these turbulence levels do not reduce mass transfer rates.

Results of the least squares analysis on the previous data according to a Danckwerts model are shown in Table IV.

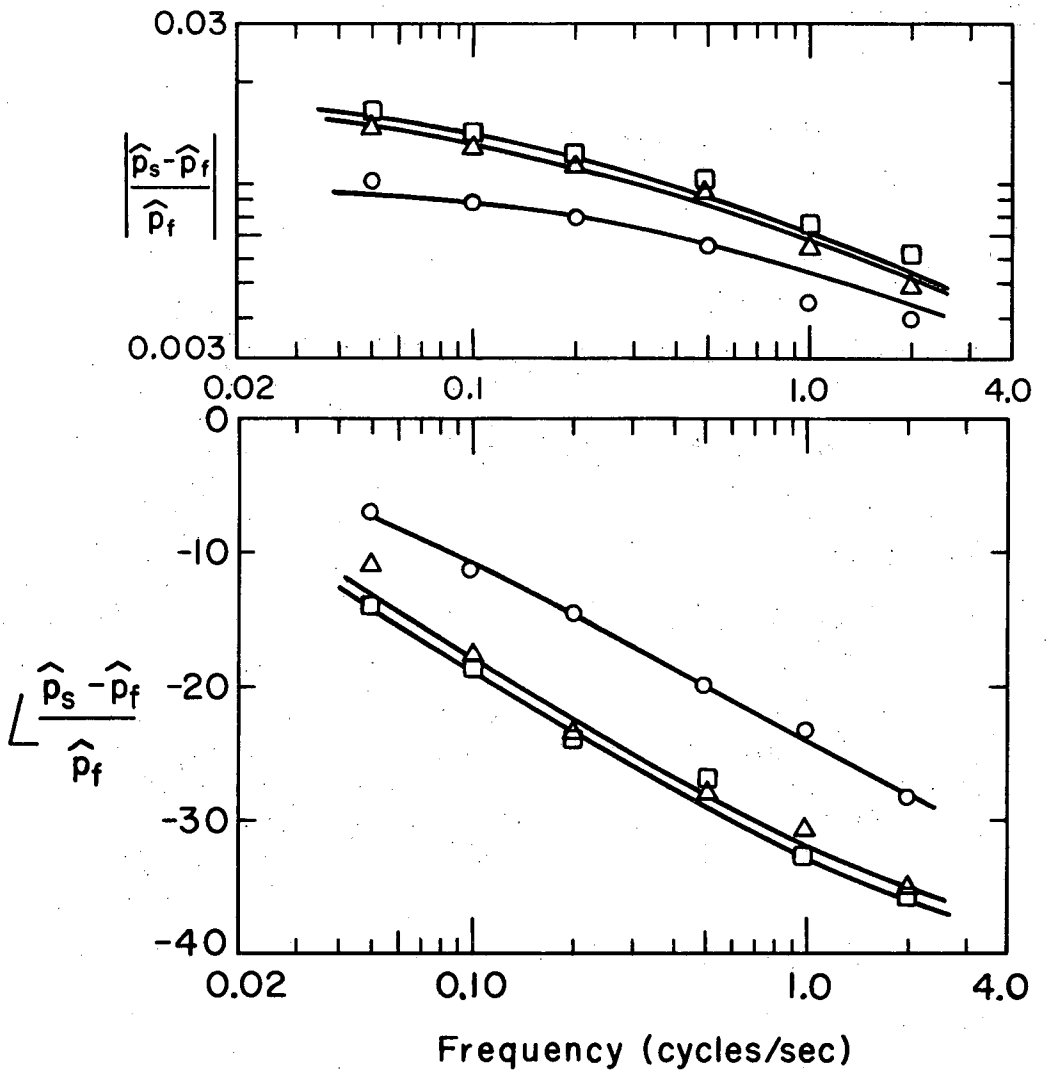

Fig. 9. Bridge comparison of a stagnant liquid surface, covered by a 1-hexadecanol film, with a clean stagnant liquid surface. (○ -1/2 monolayer equivalent surface concentration; △ -1 monolayer; □ -2 monolayers.)

Table III. Calculated film coefficients from least squares analysis of data for stagnant surfaces covered with 1-hexadecanol.

Surface Concentration in Equivalent Monolayers	Film Coefficient cm/sec
1/2	0.00754±0.00112
1	0.00385±0.00070
1[a]	0.00446±0.00048
2	0.00364±0.00056

[a]These data were taken in a separate series of experiments by comparing a film-covered surface with an impermeable surface in the reference chamber.

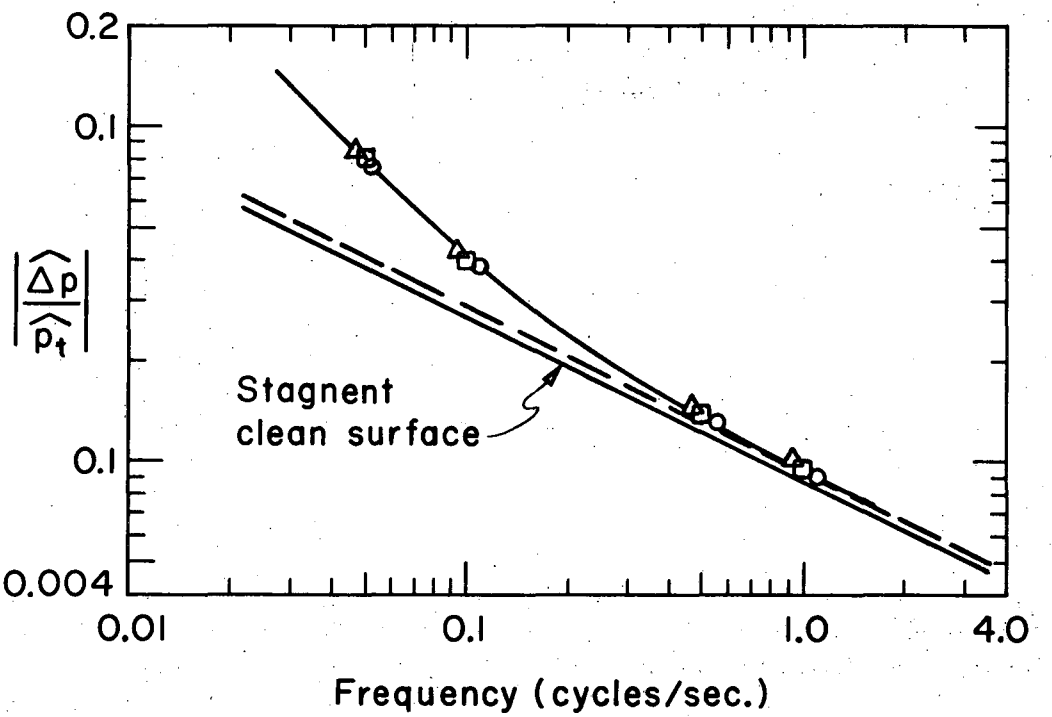

Fig. 10. Bridge comparison of a turbulent interface (stirring speed, 150 rpm), 1-hexadecanol surface film added, with an impermeable surface. (○ -1/2 monolayer equivalent surface concentration; △ -1 monolayer; □ -2 monolayers.)

Table IV. Results of least squares analysis on turbulent data for 1-hexadecanol.

Stirring Speed rpm	Surface Concentration in Equivalent Monolayers	Phase Data s, sec^{-1}	Amplitude Data s, sec^{-1}	Amplitude Data Q^*, cm^{-1}
150	1/2	1.16 ±0.47[a]	0.974±0.175	0.0234±0.00009
150	1	0.875±0.226	1.01 ±0.20	0.0231±0.00011
150	2	0.914±0.219	1.01 ±0.21	0.0232±0.00012
230	1/2	3.04 ±0.31	2.29 ±1.11	0.0280±0.00149
230	1	3.16 ±0.86	1.68 ±1.53	0.0309±0.00180
230	2	3.14 ±1.51	1.51 ±1.99	0.0311±0.00214

[a]Standard error computed on the basis of 95% confidence level, i.e. approximately two standard deviations.

DISCUSSION OF RESULTS

The results indicating that the soluble surfactant sodium lauryl sulfonate exhibits no measurable surface resistance is in accord with results of other researchers who investigated expanded-type surface layers (Bussey, 1966). Apparently the molecules in the surface are loosely bound and form an open lattice through which the gas molecules may easily pass. The measured resistance of a 1-hexadecanol film in the compressed state (i.e. at least 1 monolayer present) is compared with results of other researchers in Table V. Our measurements are in agreement with Plevan and Quinn (1966), who also used the sulfur dioxide-water system experimentally. An order of magnitude agreement is obtained between our work and others when the resistance of 1-hexadecanol films to passage of SO_2 molecules is compared with transport of CO_2 molecules. 1-hexadecanol molecules are believed to be closely packed together on the surface of water forming a rigid lattice through which gas molecules pass with some difficulty. By estimating the thickness of a monolayer film of 1-hexadecanol (approximately 25 Ångstroms) one may calculate the apparent diffusion coefficient of the gas molecules through the condensed monolayer. The result is on the order of 10^{-9} sq cm/sec. It seems that the surface film behaves more like a solid than a liquid.

The results of surfactant behavior at turbulent interfaces are more significant and qualitative explanation more difficult. In the presence of turbulence, several film properties come into play. A film must be able to withstand bombardment of the interface by eddies

Table V. The surface resistance of a 1-hexadecanol film compared with the results of previous investigations.

Source	Gas-Liquid System	Surface Resistance sec/cm
Blank et al. (1960)	CO_2-buffer	90[a]
Sada et al. (1967)	CO_2-water	105
Plevan et al. (1966)	SO_2-water	170-215
This work	SO_2-water	224-275

[a]All resistances reported are for films with at least 1 monolayer equivalent surface concentration.

generated far from the surface. The elastic and flow properties of a film become important as the surface distorts owing to turbulence. If the scale of turbulence is large enough to cause the liquid surface to be broken, recovery of the film after collapse becomes important. The recovery speed may depend upon the adsorption rate at the interface, the surfactant's diffusion rate in the liquid, and perhaps even its diffusion rate across the surface. To attempt a reasonable explanation of the results obtained here, one needs to be able to estimate time constants for the above film phenomena. Let us briefly examine some of the properties of films reported in the literature.

A discussion of diffusion limited mass transfer rates of surfactants is given in Davies and Rideal (1961). They considered a system in which only a thin stagnant layer of liquid separated the surface film from the stirred bulk solution. The adsorption rate of surfactants was found from experiment to be strongly dependent on the surfactant's bulk concentration and was predicted well by an indicated theory. Application of this theory showed that for lauryl sulfate ions, after a sudden 10% change in surface concentration, the rate of adsorption was such that the surface was 60% restored to equilibrium after 6.4 milliseconds. The bulk concentration was 10^{-3}M. By contrast, consider lauryl alcohol at a surface concentration equivalent to approximately 1/2 monolayer. After a sudden 10% change in surface concentration, the rate of adsorption was such that the surface was 60% restored to equilibrium after 60 seconds. For derivatives with longer chains the rates become correspondingly smaller, and the times correspondingly longer.

Results of work by Hanson (1961) showed that adsorption was not solely diffusion limited. He stated, if it is assumed that spreading pressures depend on amounts of solute adsorbed and on subsurface concentration in the same manner in dynamic and equilibrium systems and if amounts of solute adsorbed and subsurface concentrations are inferred from observation of spreading pressure-time data on this basis, then adsorption limited solely by diffusion fails to explain the slow initial variation of spreading pressure with time. Except for this initial behavior, diffusion must play an important role in limiting the adsorption rate. The adsorption appears to be diffusion-controlled except for an initial time lag; times required to reach any particular spreading pressure are always longer than would be expected if diffusion alone were the limiting factor.

McArthur and Durham (1957) studied spreading rates of fatty alcohols that form condensed or rigid films. The time to spread a distance of 76 cm in a test chamber 91 × 14 × 10 cm was measured. Spreading from 2 mm diameter particles of 85% cetyl alcohol required 15-18 minutes to reach a surface pressure of 20 dynes/cm. The equilibrium spreading pressure, or surface tension reduction, of cetyl alcohol is 44 dynes/cm. Recovery of spread films was assessed by compressing them until they collapsed and then observing the rate of increase of surface pressure. After spreading 95% cetyl alcohol, recovery to 20 dynes/cm requires 5 minutes.

Healy and La Mer (1964) studied damping of capillary waves by condensed monolayers and their effect on retardation of the evaporation

of water. Their experiments involved oscillation of a horizontal bar in a liquid surface at a given amplitude and frequency. They found that under dynamic conditions the surface pressure was reduced more than could be accounted for by the increase in surface area due to turbulence. They observed a maximum plateau for surface pressure under dynamic conditions much lower than the equilibrium spreading pressure, indicating that dynamic conditions may place a restriction on attainable surface pressure. They postulated that the reduction in surface pressure was due to submergence of monolayer molecules and concluded that the submergence should be highest at the bar. Nevertheless, no film breakage could be observed. They also found that recovery of the static surface pressure when the disturbance was removed was initially rapid but the final approach to equilibrium was slow.

Sakata and Berg (1969) measured the surface diffusivity of myristic acid, which forms an expanded surface layer. They found a surface diffusivity of 3×10^{-4} cm^2/sec indicating that expanded monolayers behave much like a liquid. Blank and Britten (1965) predicted that the surface diffusivity of condensed layers, like 1-hexadecanol, should be on the order of 10^{-8} cm^2/sec indicating a very rigid structure of the surface layer.

Application of the above information to interpretation of measured frequency responses at turbulent interfaces with surfactants present can be qualitative only. With the aid of this information, the following conclusions concerning surfactant behavior at turbulent interfaces seem reasonable.

The measured response of turbulent interfaces initially covered with 1-hexadecanol films indicates that the degree of turbulence was high enough that the rigid film must have been completely broken up and submerged in the bulk liquid. If one were to assume that the film was broken up into hydrocarbon particles on the order of 0.1 mm in diameter, Stokes Law would indicate that the time required to rise the average height of the bulk liquid (liquid depth is 8 inches) would be approximately 1.7 minutes. Since the spreading rate and the adsorption rate of 1-hexadecanol is very small compared to the average rate of submergance of any surface fluid element, it is unlikely that appreciable surfactant would be present on the stirred surface. The surfactant entering the surface through turbulent mixing will be immersed in a fluid element whose concentration will be equal to the very low bulk concentration of surfactant. Since only enough material was added to form a monolayer, mixing with the 10 liters of bulk liquid made the surfactant's concentration extremely small. Thus, only a small fraction of the surfactant originally added to the surface would exist there after the film is broken up. If one could reduce the turbulence low enough, there would be some level at which the monolayer would become stable. Under these conditions one could investigate possible damping of interfacial turbulence by condensed films. Unfortunately, in the experiments carried out here, the turbulence level could not be reduced much further without making the measured pressure-difference signal prohibitively small.

By comparing time for adsorption for the soluble surfactant with fluid element half lives, one can see that even if the film were broken some recovery should be obtained. As soon as a portion of the interface

is swept clean of surfactant, material immediately beneath can diffuse to the surface and adsorb. One can envision islands of surfactant on the turbulent surface. Fluid eddies which strike these areas from below may be slightly damped, as postulated by Davies (1964).

It must be reported that in all turbulent runs made that no visual change in the surface turbulence could be seen. Nevertheless, the measured average age of the surfaces ranged from approximately 0.3 - 2.0 seconds in experiments with and without surfactants.

These results indicate that owing to the nature of the surface films formed, a liquid type surface film can affect hydrodynamics at a turbulent interface even in the presence of vigorous turbulence, owing to the film's liquid mobility and fast rate of recovery. On the other hand, a condensed, insoluble film is very rigid and slow to recover after rupture. Its presence may only be important at low turbulence rates. The results reported by many researchers on the retardation of the rate of water evaporation help to strengthen this conclusion. They have found that even a slight wave action caused by wind or boating on water reservoirs considerably reduces the effectiveness of 1-hexadecanol films.

CONCLUSIONS

Although the interface impedance bridge is not simple to operate, it has yielded considerable information concerning interfacial turbulence. The apparatus is quite useful in measuring surface film resistances. It eliminates many problems encountered with previous techniques. Measurements can be carried out at small contact times, which were not possible previously, and density-driven convection currents have

negligible effect. The frequency response data allow one to examine the statistical nature of fluid interface as well as their time-average behavior.

The important problem of surfactant behavior at turbulent interfaces has been investigated. It was found that soluble films can dampen turbulence at the interface and reduce mass transfer rates, while insoluble films tend to break up and to have no measurable effect on mass transfer rates.

The results of this paper were drawn from data taken at high turbulence rates where the scale of turbulence was much greater than the depth of penetration of the dissolving gas. This type of turbulence is described well by the assumptions of Danckwerts (1951), as experimental results verify. As turbulence is reduced, these assumptions will no longer be valid and the relative motion of liquid at different levels close beneath the surface may not be disregarded. Solution of models of this type are much more difficult as can be seen in work by Scriven (1968) in which irrotational stagnation flow near interfaces is considered.

Another important problem not resolved here occurs when turbulence is not great enough to cause collapse of the condensed films. Surface resistance to gas transport plus possible hydrodynamic effects like those mentioned in the preceeding paragraph may be present.

NOMENCLATURE

A = area of liquid surface, sq cm

c = concentration of gas in liquid, g-moles/liter

C = capacitance of condenser in analgous electrical bridge

C_V = molar heat capacity of gas at constant volume

$\mathcal{D}$ = diffusion coefficient of dissolved gas in liquid, sq cm/sec

H = Henry's Law coefficient for gas in liquid, g-moles/(cc)(atm)

k_L = liquid phase mass transfer coefficient, cm/sec

K = surface film mass transfer coefficient, cm/sec

n = number of moles of gas in chamber

p = gas pressure, atm

$\hat{p}$ = amplitude of gas pressure oscillations, atm

Q = $HART_o/V_o$

Q^* = $Q\mathcal{D}^{1/2}$

r = impedance of resistance element in analogous electrical bridge

R = gas constant, 82.06 (cc)(atm)/(g-mole)°K)

s = replacement frequency of fluid elements in liquid surface, sec^{-1}

S = inside surface area of chamber, sq cm

t = time, sec

T = temperature of surroundings, °K

U = heat transfer coefficient between gas and walls of chamber

V = volume of gas space in chamber, cc

$\hat{V}$ = amplitude of gas volume oscillations, cc

x = distance from interface into liquid, cm

γ = ratio of heat capacities for gas

ω = frequency of oscillations, radians/sec

o = time-average value

1 = chamber number, reference chamber

2 = chamber number, test chamber

f = film-covered surface

s = stagnant surface

t = turbulent surface

REFERENCES

Alexander, A. E., in Third International Confress of Surface Activity, (1960), Vol. 2, p. 60.

Blank, M. and I. S. Britten, J. Colloid Sci., 20, 789 (1965).

Bussey, B. W., Ph.D. Thesis in Chemical Engineering, University of Delaware, (1966).

Danckwerts, P. V., Ind. Eng. Chem., 43, 1460 (1951).

Danckwerts, P. V. and A. M. Kennedy, Trans. Inst. Chem. Engrs., 32, S49 (1954).

Davies, J. T., "The Effects of Surface Films in Damping Eddies at a Free Surface of a Turbulent Liquid," paper presented at Boston meeting of the A. I. Ch. E. in December, 1964.

Davies, J. T., A. A. Kilner, and G. A. Ratcliff, Chem. Eng. Sci., 19, 583 (1964).

Davies, J. T. and E. K. Rideal, Interfacial Phenomena (Academic Press, New York, 1961).

Erdelyi, A., Ed., Table of Integral Transforms (McGraw-Hill, New York, 1954), Vol. 1.

Filon, L. G. N., Proc. Roy. Soc. Edinburgh, 49, 38 (1928-1929).

Gaines, G. L., Insoluble Monolayers at Liquid-Gas Interfaces (Inter-Science Publishers, New York, 1966).

Hanson, R. S., J. Colloid Sci., 16, 549 (1961).

Hanson, R. S. and J. Lucassen, J. Colloid Interface Sci., 22, 32 (1966).

Harriot, P., Chem. Eng. Sci., 17, 149 (1962).

Healy, T. W. and V. K. La Mer., J. Phys. Chem., 68, 3535 (1964).

Higbie, R., Trans. Am. Inst. Chem. Engrs., 31, 365 (1935).

La Mer, V. K., in Proceedings of the Second International Congress of Surface Activity, (Academic Press, New York, 1957), Vol. 1, p. 259.

La Mer, V. K., Ed., Retardation of Evaporation by Monolayers, (Academic Press, New York, 1962).

Lamb, W. B., Ph.D. Thesis in Chemical Engineering, University of Delaware, (1965).

Lamb, W. B., T. G. Springer, and R. L. Pigford, Ind. Eng. Chem. Fundamentals, in press.

Luyben, W. L., C. J. Messa, and G. W. Poehlein, Ind. Eng. Chem. Fundamentals, in press.

Lynn, S., J. R. Straatmeier, and H. Kramers, Chem. Eng. Sci., 4, 49, 48, 63 (1955).

Marchello, J. M. and H. L. Toor, Ind. Eng. Chem. Fundamentals, 2, 8 (1963).

Marchello, J. M. and H. L. Toor, A. I. Ch. E. J., 4, 97 (1958).

McArthur, I. K. H. and K. Durham, in Proceedings of the Second International Congress of Surface Activity, (Academic Press, New York, 1957), Vol. 1, p. 262.

Plevan, R. E. and J. A. Quinn, A. I. Ch. E. J., 12, 894 (1964).

Perlmutter, D. D., Chem. Eng. Sci., 14, 287 (1961).

Perry, R. H., C. Chilton, and S. D. Kirkpatrick, Ed., Chemical Engineers' Handbook, (McGraw-Hill, New York, 1963).

Posner, A. M. and A. E. Alexander, Trans. Faraday Soc., 45, 651 (1949)

Ries, H. E. and W. A. Kimball, in Proceedings of the Second International Congress of Surface Activity, (Academic Press, New York, 1957), Vol. 1, p. 75.

Sada, E. and D. M. Himmelblau, A. I. Ch. E. J., 13, 680 (1967).

Sakata, E. K. and J. C. Berg, Ind. Eng. Chem. Fundamentals, 8, 570 (1969).

Scriven, L. E., Chem. Eng. Education, 2, 145 (1968).

Springer, T. G., Ph.D. Thesis in Chemical Engineering, University of California, Berkeley (1969).

Wang, J. C. and D. M. Himmelblau, A. I. Ch. E. J., 10, 574 (1964).

Washburn, E. W., Ed., International Critical Tables of Numerical Data, Physics, Chemistry, and Technology, (McGraw-Hill, New York, 1928).

Whitaker, S. L. and R. L. Pigford, A. I. Ch. E. J., 12, 741 (1966).

APPENDIX A

EXPERIMENTAL APPARATUS

GENERAL DESIGN CRITERIA

An apparatus, called an interface impedance bridge, was briefly described in Chapter 1. Design and construction of the apparatus will be given in detail in this section.

The experimental apparatus and technique must meet the following conditions.

(1) construction of two chambers as nearly identical as possible

(2) a mechanical system capable of producing gas pressure oscillations over a suitable range of frequency

(3) an instrument system capable of measuring the pressure signals

(4) a gas-liquid system which will yield a sufficiently large pressure-difference signal.

A schematic of the system and photographs of the chambers and the mechanical system are shown in Chapter 1.

CHAMBER CONSTRUCTION

In construction of the test chambers, the following factors had to be kept in mind. One needs a large ratio of interfacial area to gas volume to ensure a measurable absorption signal, but at the same time the gas space must be deep enough to allow turbulent stirring of the liquid surface without splashing onto the lid. A large volume is needed to ensure no appreciable changes in bulk composition during absorption-desorption, and more importantly, to allow placement of a stirring system

within the liquid to produce interfacial turbulence. No breakage of the liquid surface by a stirring system can be tolerated. Therefore, one must allow for stirring from below. A transparent chamber and top is desirable to allow visual observation of the liquid and surface during operation.

For the above reasons a five gallon Pyrex solution jar was selected for chamber construction. Two identical chambers were made in the following manner. The tapered top of the solution jar was cut off and the surface ground smooth to produce a container 11.1 inch i.d. and approximately 8.5 inch in height. A stopcock was fused into the bottom of the jar for introduction of the liquid solutions. A valve arrangement permitted one to bubble gas into the liquid through the stopcock in order to saturate the liquid solutions with the pure gas. A 28/12 Pyrex ball joint was also fused into the bottom of the chamber to hold the stirring system, to be described in more detail later.

It was discovered that the chamber needed to be baffled in order to minimize vortex formation and to produce random turbulence at the interface. A system of four baffles was placed in the chamber. Each baffle was one inch wide and came to within 1.5 inches of the liquid surface. Since no easy way to attach the baffles to the walls of the chamber could be seen, they were constructed of Pyrex glass with a framework that rested on the chamber bottom. A glass rod, attached to the bottom of the framework, protruded into the stopcock neck at the bottom of the tank and kept the baffle framework from moving. One of the chambers and the baffles are shown in Fig. A-1. In order to measure the liquid temperature during experimental runs, a small thermometer was attached to the baffle framework in each chamber.

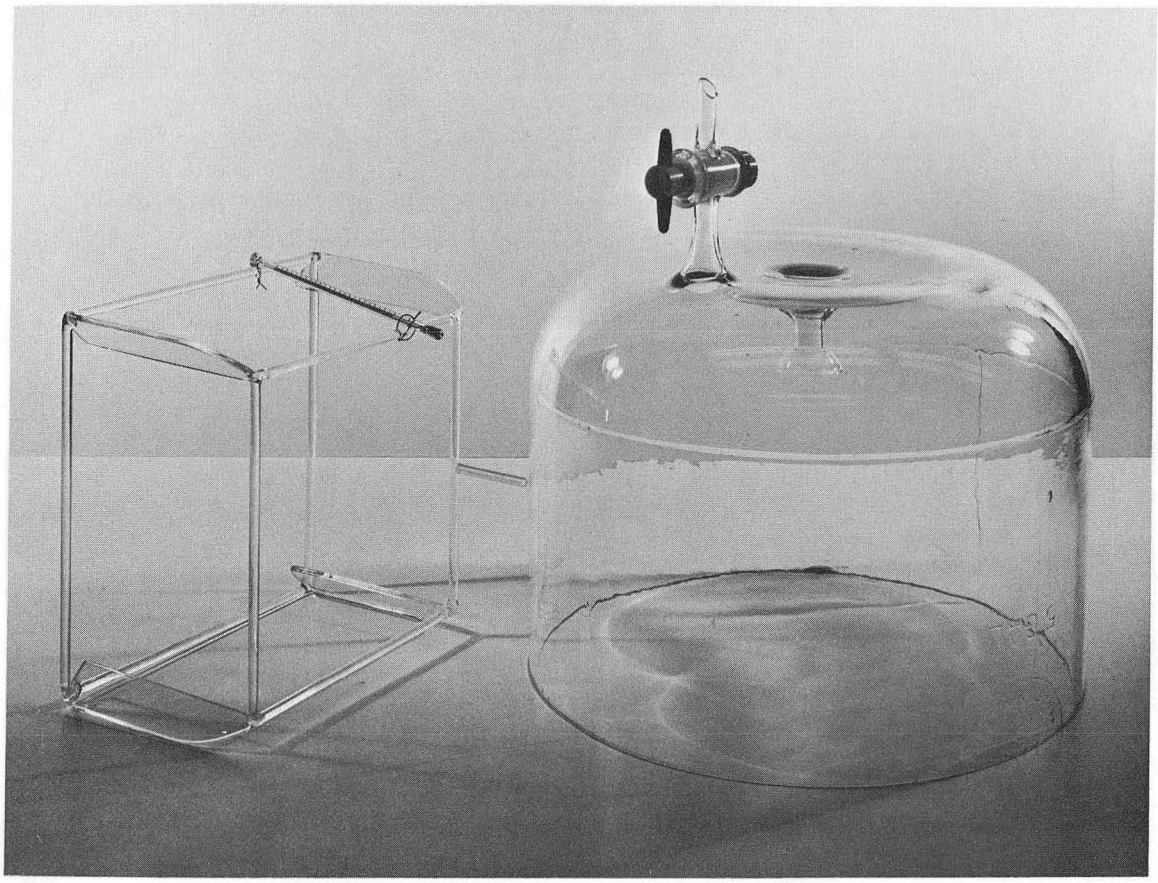

XBB 693-1584

Fig. A-1. Photograph of Pyrex chamber and baffles.

CHAMBER LID

The chamber lids were constructed of one inch thick Lucite to allow visual observation of the liquid surface during operation. Four 1/2 inch gas inlets were mounted in the lid to allow connection of the chamber to a Neoprene balloon, actually, a hospital rebreathing bag, used to vary the gas volume sinsuoidally. The gas inlets were baffled to ensure that incoming gas during oscillation did not disturb the liquid surface, which was approximately one inch below the lid. An inlet was provided in the center of the lid for connection of pressure transducers and a gas purge line. Provisions were also made for introduction of small amounts of surfactant.

Surfactant could be added to one of the chambers either by hypodermic syringe through a rubber seal or by small movable cups attached to the inside of the lid. Three cups were attached to tiny rods which protruded through a rubber seal in the lid. A drawing of the center inlet and cups is shown in Fig. A-2. The lid seal to the glass chamber was provided by a butyl rubber O-ring resting in a machined groove.

Each chamber rested in a wooden base filled with Plaster of Paris to fit the contour of the chamber bottom. The lid was held tightly in place by four metal rods attached to the base and secured to the lid with wing nuts.

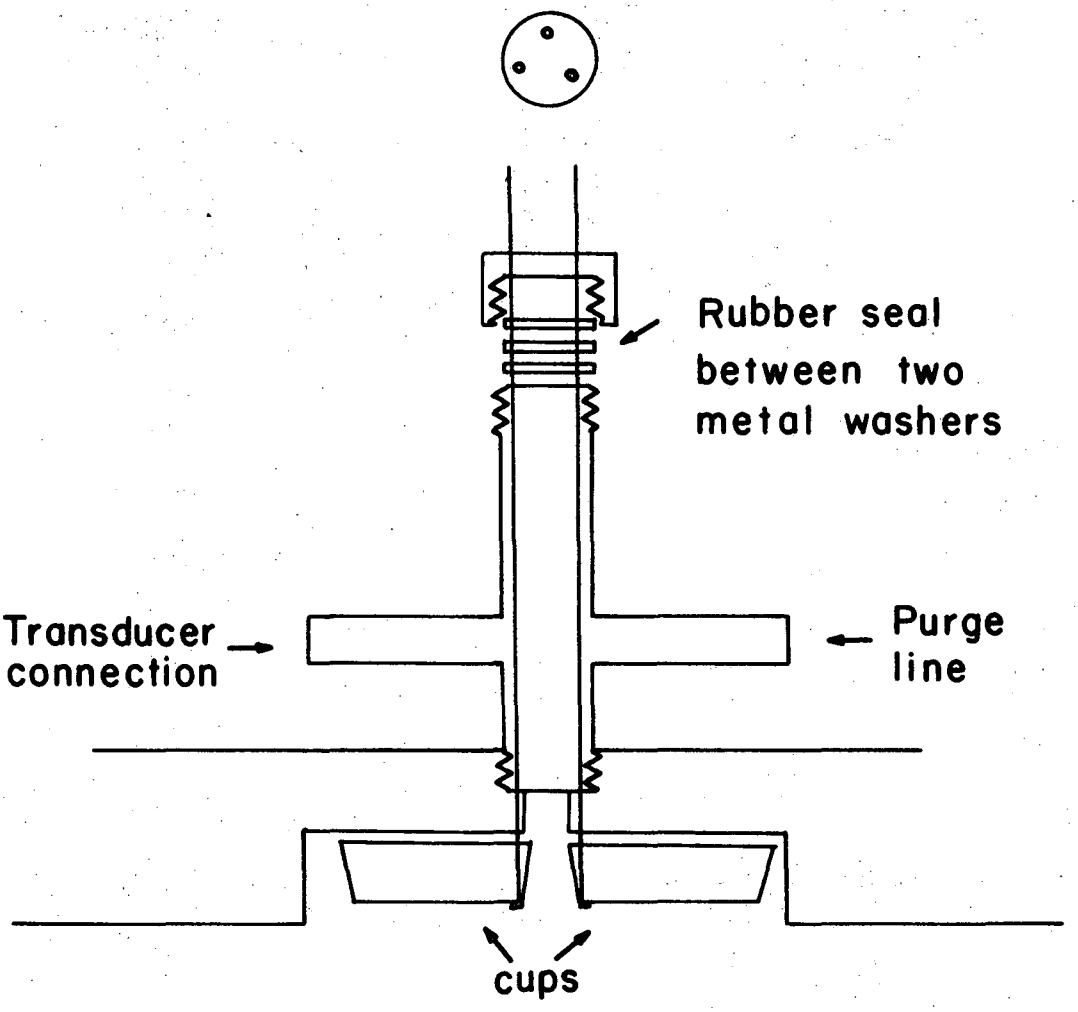

XBL 6910-5767

Fig. A-2. Drawing of center inlet to chamber lid, showing movable cups and gas line connections.

THE BALLOONS

The Neoprene balloons, connected to their respective glass chambers through a manifold and four lengths of 1/2 inch i.d. butyl rubber vacuum tubing, were placed inside sheet metal boxes. The insides of the boxes were contoured to an elliptical shape by insertion of pieces of hardwood (see Fig. A-3) so that a good sine wave response in gas pressure of the chambers could be obtained when the hinged covers of the boxes were moved to compress and expand the balloons. The balloons (3 liter, Neoprene, No. 20795), obtained from Monoghan Co., 500 Alcott Ave., Denver, Colorado, 80204, had to be modified slightly before use. Since the balloons were intended for hospital use the ends were not rounded, (see Fig. A-4). This meant that the balloons did not fit comfortably in the boxes; the ends had to be folded over. The pressure response of the two separate chambers reacted more nearly identically after the ends of the balloons were tucked inside the balloons and the ends plugged with either Duco cement or silicone rubber sealant.

Interconnecting lines containing metering valves allowed one to purge both chambers either through the lid or through the manifolds. Purge was possible with sulfur dioxide or air through an exhaust line leading to a hood.

THE DRIVE SYSTEM

The mechanical linkage and drive system used to compress and expand the balloons is shown in Fig. 3 of Chapter I. The components are described below.

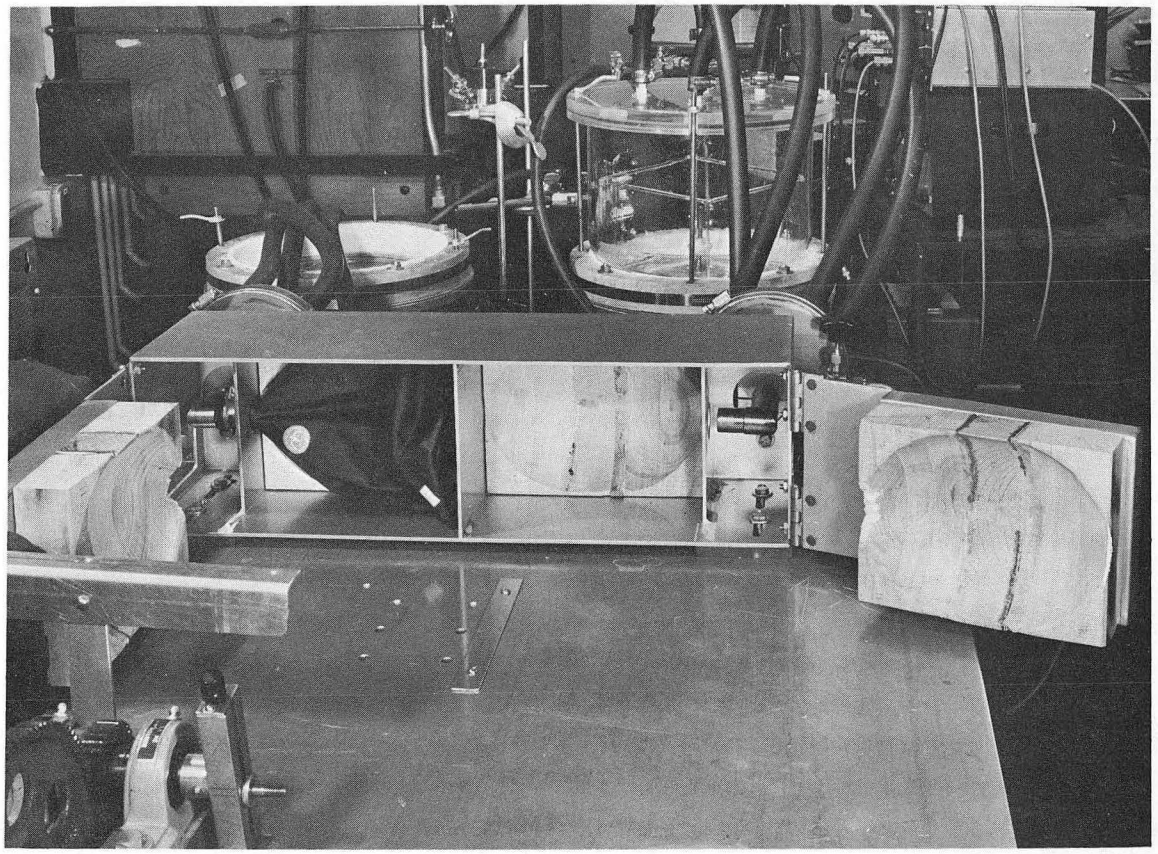

XBB 693-1583

Fig. A-3. Photograph of insides of sheet metal boxes.

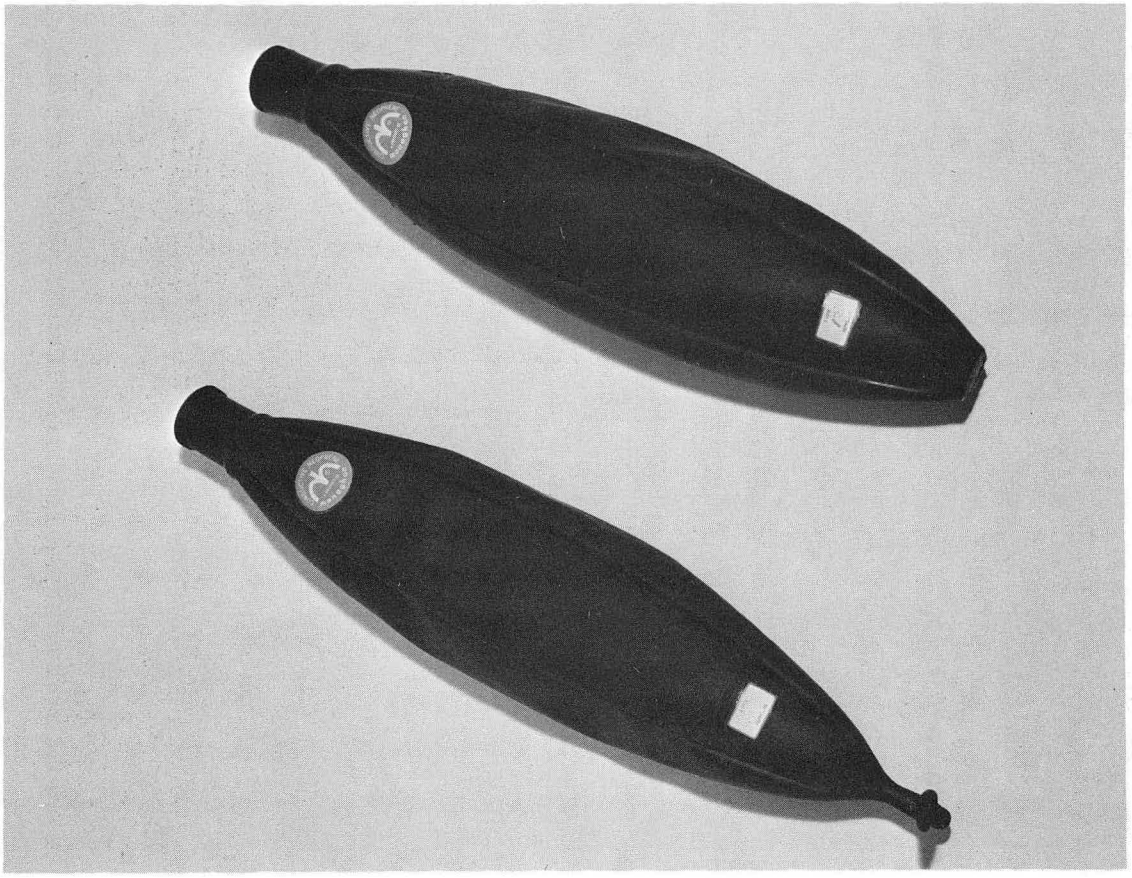

XBB 693-1585

Fig. A-4. Photograph of Neoprene balloons before and after modification.

A d.c. shunt-wound motor (2500 rpm, 1/3 hp, No. G56-25) and a SCR controller (No. SH-73) were obtained from Minarik Electric Co., 224 East 3rd Street, Los Angeles, California, 90013. The motor was attached to a Zero-Max Drive (model Q1) obtained from Zero-Max Co., 2845 Harriet Ave., South, Minneapolis, Minnesota. The Zero-Max Drive is a mechanical speed reducer that gives stepless variable speed from zero to maximum by changing the distance that four or more one-way ratchets rotate the output shaft when they move back and forth successively. From the input shaft an eccentric motion causes linear motion to be applied to the one-way ratchets. By varying the degree of eccentricity on the input shaft, the output speed may be continuously varied from nearly zero to maximum. By using four or more overrunning clutches and driving them from the eccentrics successively, the output rotation is continuous.

One drawback to this unit is that the output shaft is not self-locking. The Zero-Max unit was connected to a worm gear reducer (Winsmith, 1-LR, Series No. 1 CB, 15:1 and 40:1) obtained from the Otrich Co., 3654 Grand Ave., Oakland, California. The worm gear served two purposes: it served as a self locking mechanism between the Zero-Max unit and the shaft driving the balloons, and the use of reducers of two different reductions expanded the range of variable speed for the drive system. The worm grear reducer rotated an arm which was attached to a variable length shaft. The degree of eccentricity of the shaft on this arm could be varied to allow amplitude variation in the gas pressure waves. The linear motion of the shaft was directed through porous bronze sleeves housed in a metal casing and bathed in oil.

The single shaft drove two separate arms attached to each of the hinged doorways. It was hoped that this mechanical linkage would produce nearly identical volume changes in the two chambers. Through the combination of the SCR controlled motor, mechanical speed reducer, and use of two different-ratio worm gear reducers, it was possible to vary the output speed of the mechanical drive continuously from 0.03 to 9 cycles/sec. Some typical pressure waves generated by this system are shown in Fig. A-5, for which the frequency of oscillation was 0.5 cycles/sec.

ELECTRICAL EQUIPMENT

Since the difference of nearly identical signals was needed, differential pressure transducers capable of measuring signals less than one inch of water were purchased from Hewlett Packard, Sandborn Division, 1101 Embarcadero Rd., Palo Alto, California. A single ended transducer (model 268A, range ± 20 inches of water) was purchased to measure the pressure of one of the chambers relative to atmospheric pressure. These signals were on the order of ± 16.6 inches of water. A differential transducer (model 270, range ± 15 inches of water) was purchased to measure the pressure difference between chambers. By experiment, this transducer was capable of detecting changes in pressure as small as 0.001 inch of water. The signals to be measured were on the order of 0.025 inch of water. The differential transducer was approximately three times as sensitive as the single ended transducer and was reported to produce a differential error less than 0.01% of the applied pressure. The transducers were connected to a Sanborn Transducer-Amplifier-Indicator (model 311A) and then to a Sanborn two-channel inking recorder.

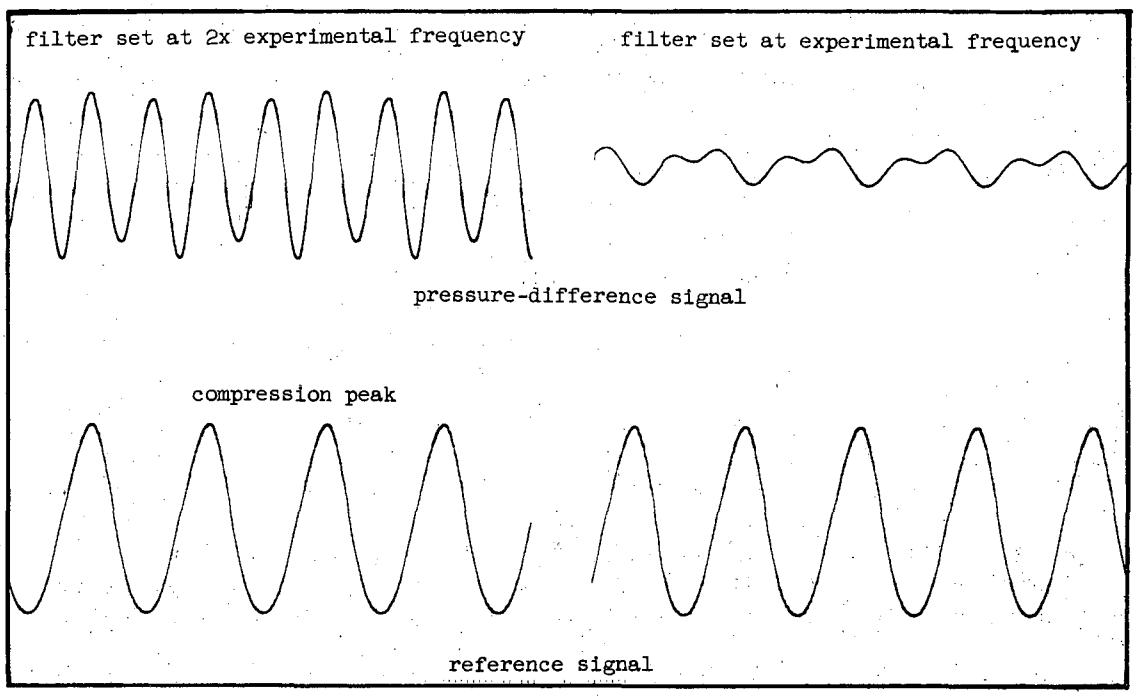

XBL 6910-5704

Fig. A-5. Typical generated pressure waves at 0.5 cycles/sec. The upper waves represent a balance signal at two different filter settings (note second harmonic content), attenuation ×20. Lower waves represent input signal to a single chamber, attenuation ×2000.

Because of the signal noise and introduction of harmonics due to an imperfectly generated sine wave input, it was necessary to filter the difference signal. For this purpose, a variable band-pass filter (model 330B(R), range 0.02 to 20.0 cycles/sec) was purchased from Krohn-Hite Corporation, 580 Massachusetts Ave., Cambridge, Mass., 02139. The upper and lower cutoff frequencies could be selected independently. For our purposes, setting both cutoff frequencies to the desired experimental frequency gave best results.

Although the phase relationship between the measured difference signal and the pressure response of one of the chambers could be determined from the recorder output, a much more accurate and convenient result could be obtained by direct analysis of the electric signal. The electronics department of the College of Chemistry built a quadrature demodulator that could handle the signals directly. The apparatus, like a lock-in-amplifier, is basically a phase-sensitive detector which can be considered simply as a double-pole, double-throw reversing switch. The position of the switch is determined by the polarity of the reference input. If the input signal is a noise-free sinusoid and is in phase with the reference signal, the output of the switch will be a full wave rectified sinusoidal waveform. When filtered by an RC integrator the output will be proportional to the rms value of the input signal. However, if the input signal and the reference signal are shifted in phase by 90°, the integrated output of the switch will be zero. Thus, the output of the integrator is proportional to the rms value of the input signal and to the cosine of the phase angle between the input signal and the reference.

The demodulator consists of two circuits as described above, but with the reference signal shifted 90° in phase in the second circuit. The output of the second circuit is proportional to the rms value of the input signal and to the sine of the phase angle between the input signal and the reference. A somewhat analogous detector may be constructed using an analog computer. Figure A-6 shows a block diagram of the apparatus and also the equivalent analog computer circuits. A complete circuit diagram of the Quadrature Demodulator may be found in record book 58-400 D-R on file in the Department of Chemical Engineering, University of California, Berkeley.

Since the input-output phase relationship of the band-pass filter is frequency dependent, a small device named the Harmonic Analyzer was built to aid in adjustment of the frequency relationship between the filter and the experimental apparatus. The principle of operation relies on the fact that the generated sine wave has considerable second harmonic content. Figure A-7 shows a block diagram of the apparatus and a circuit diagram. Notice that the difference of the pressure signal of one of the chambers and this signal filtered, when the frequency is properly adjusted, will contain the harmonic and noise content of the original signal. Adjustment of the filter setting while observing this difference reduced the fundamental content until at the proper frequency no fundamental was left. Balancing was not difficult.

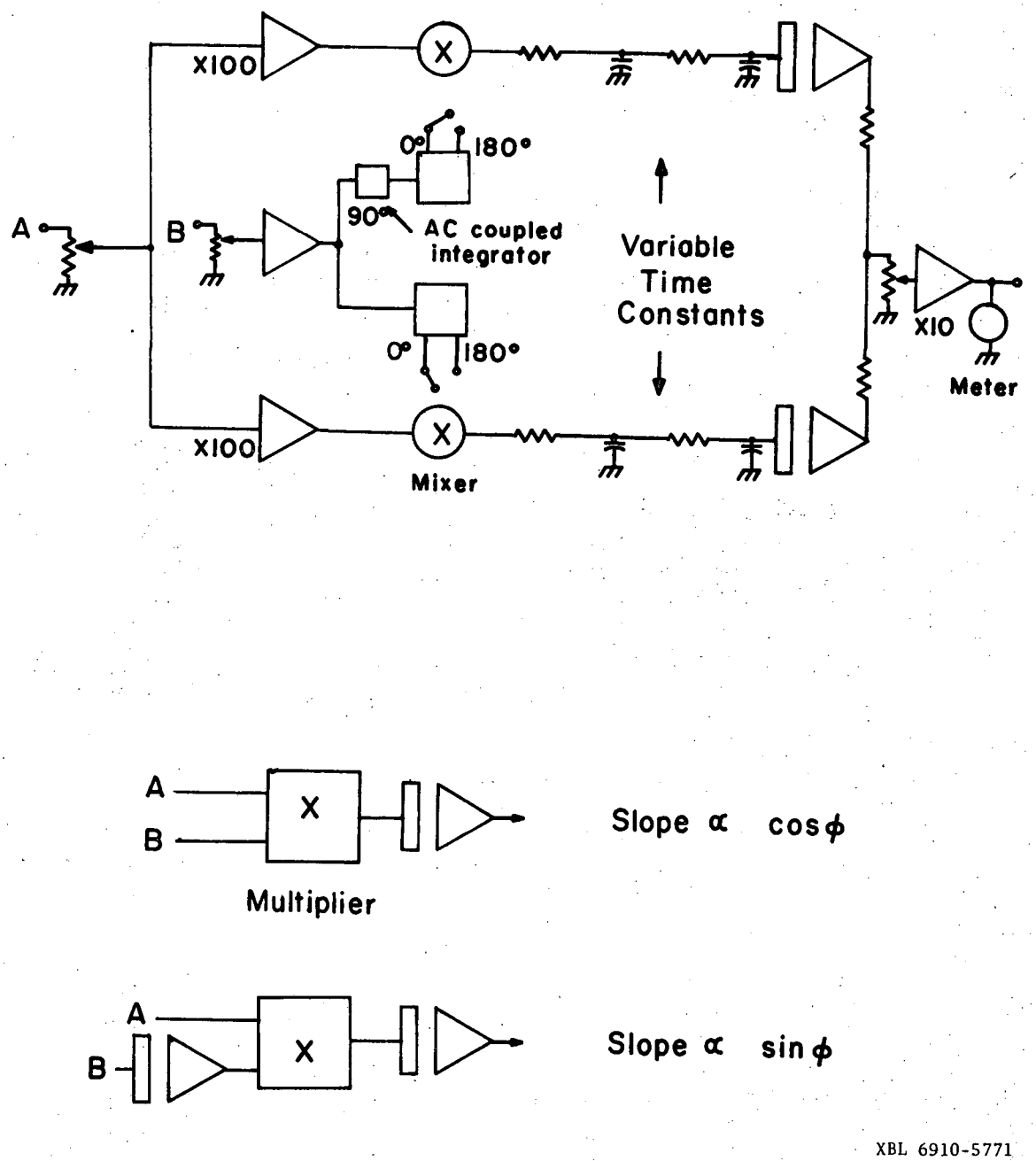

Fig. A-6. Block diagram of the quadrature demodulator and the equivalent analog of circuits.

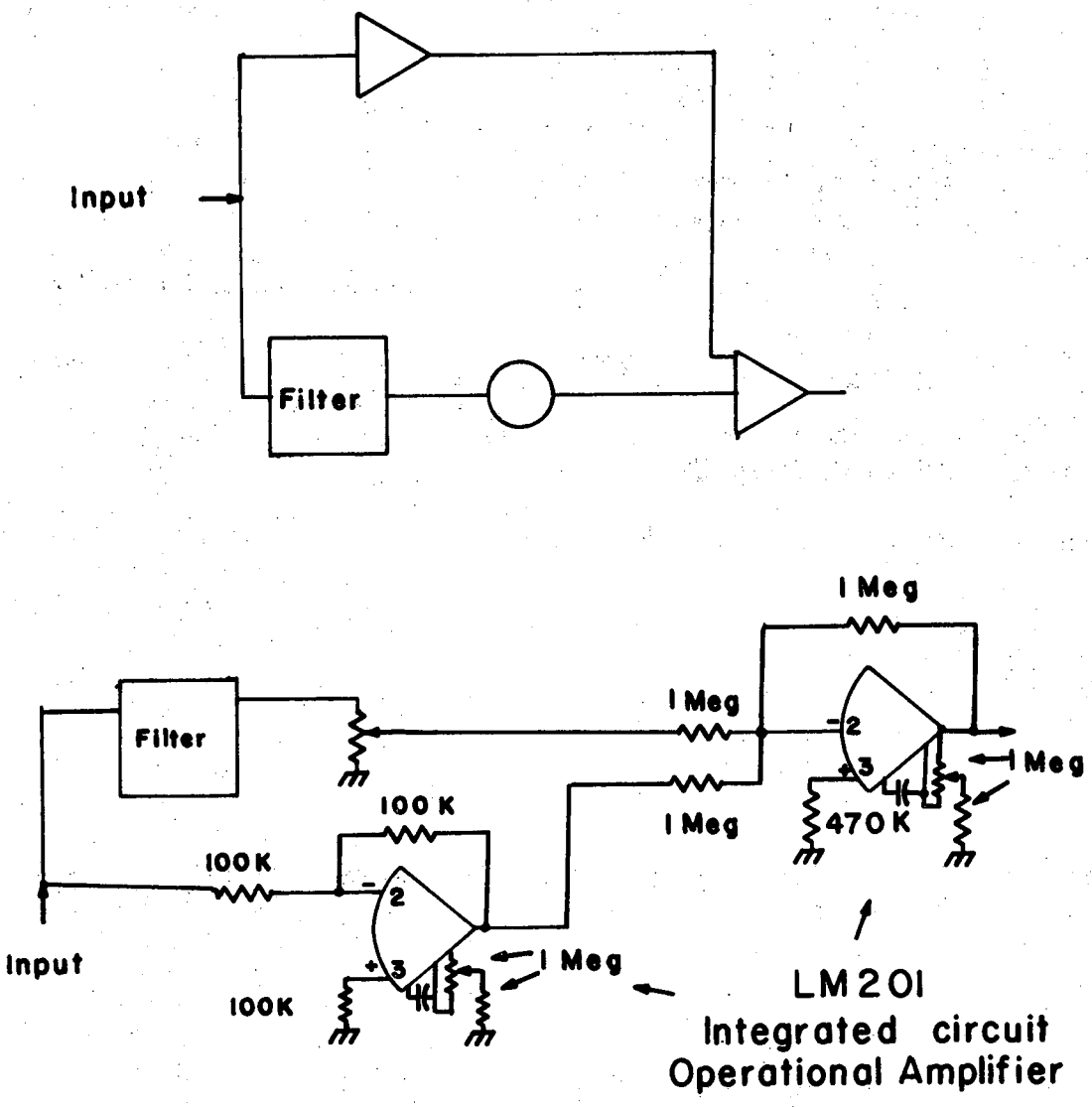

Fig. A-7. Block diagram and circuit diagram of the harmonic analyzer.

STIRRER SYSTEM

The stirring shaft entered through the bottom of the test chamber so that the interface would not be disturbed. A machined Teflon ball was press-fitted onto the shaft and pinned there. The ball mated with the 28/12 Pyrex ball joint that had been fused into the bottom of the chamber. Teflon dry spray lubricant (no. 516945, Chemical Rubber Co., 2310 Superior Ave., Cleveland, Ohio) was used on the ball joint and no leakage of solution was detected at any time.

The only stirring paddle used in this work was three-bladed with allowance for adjustment of the angle of inclination of each blade. The blades, constructed of 1/16-inch stainless steel, were 2.5 inches long and 3/4 inch wide. The outside edge of the blade was located three inches from the centerline of the stirrer. The angle of inclination (25° from the horizontal) was selected by visual examination of the character of turbulence produced at the interface until the most random interface was produced. The stirrer was located approximately 2.5 inches from the bottom of the container and was approximately 4 inches from the liquid surface. The stirrer was rotated in such a way as to force liquid toward the liquid surface. Figure A-8 shows the stirring paddle, shaft and type of ball joint used. The six-bladed impeller shown in this figure was not used because even in the baffled tank a significant vortex was formed.

The stirrer was driven by a Bodine shunt wound d.c. motor (1725 rpm, 1/15 Hp, no. SH33) purchased from the Minarik Electric Co. Speeds as low as approximately 100 rpm could be obtained. A piece of

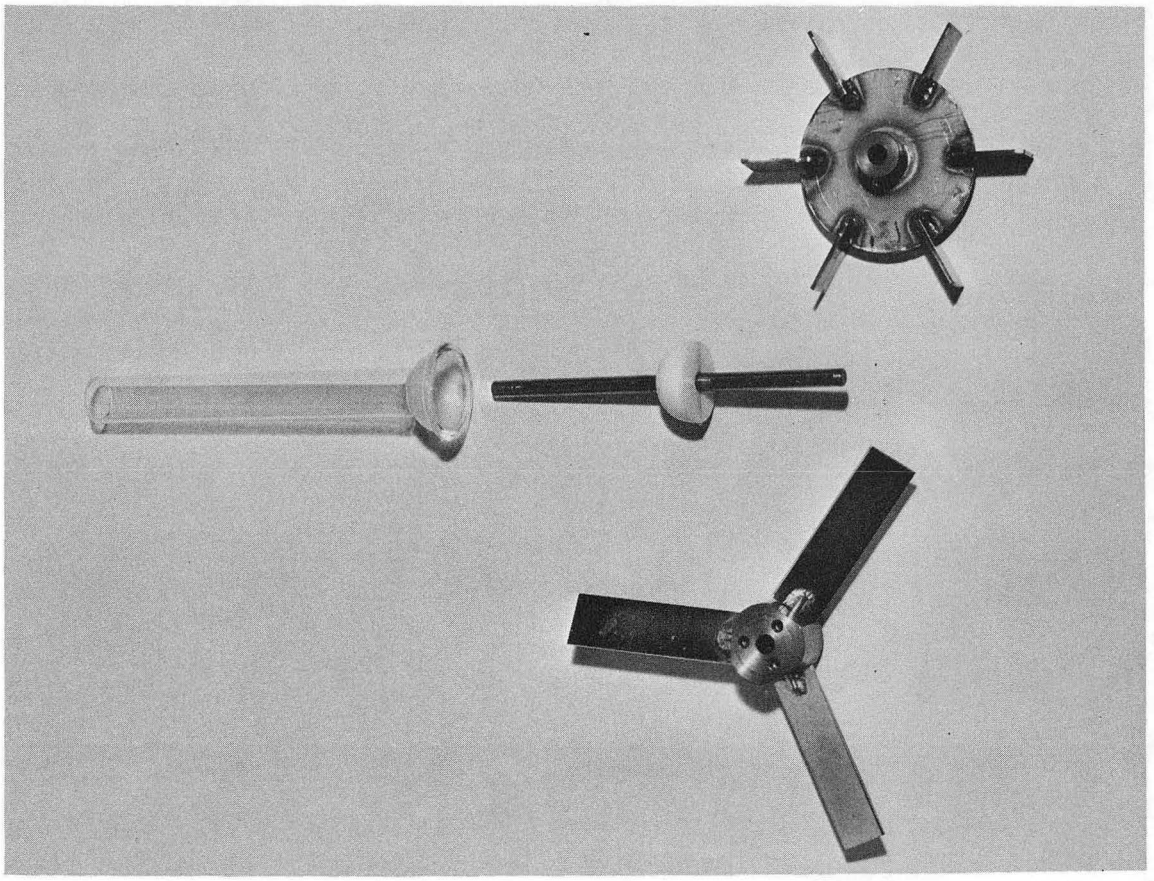

XBB 693-1586

Fig. A-8. Photograph of stirrer and shaft.

butyl rubber tubing was used to connect the stirrer shaft and motor. Turbulence tests were made at two stirring speeds, 150 and 230 rpm. Figures A-9 and A-10 show the type of interface formed for a clean water solution at the indicated stirring speeds.

Photographs of turbulent interfaces with surfactants added were also taken. The effect of the presence of 2 monolayers of 1-hexadecanol on surfaces at 150 and 230 stirring speeds showed no noticable change in the appearance of the turbulent interface. Stirring of 0.001-M solution of sodium lauryl sulfonate at the two speeds also produced an interface indistinquishable from the clean interfaces. The photographs may be found in record book 58-400 D-R on file in the Department of Chemical Engineering at the University of California, Berkeley.

MATERIALS

The Lawrence Radiation Laboratory distilled water system was used as a water supply. Surface tension measurements indicated that the water was relatively free from impurities. The water was degassed by passing it through a packed column filled with glass rings. Distilled water entered at the top of the column and was withdrawn from a boiling flask at the bottom. The liquid was then saturated with sulfur dioxide gas and stored under a sulfur dioxide atmosphere.

Anhydrous grade (99.90% pure by weight) sulfur dioxide gas was obtained from the Matheson Company, Inc.

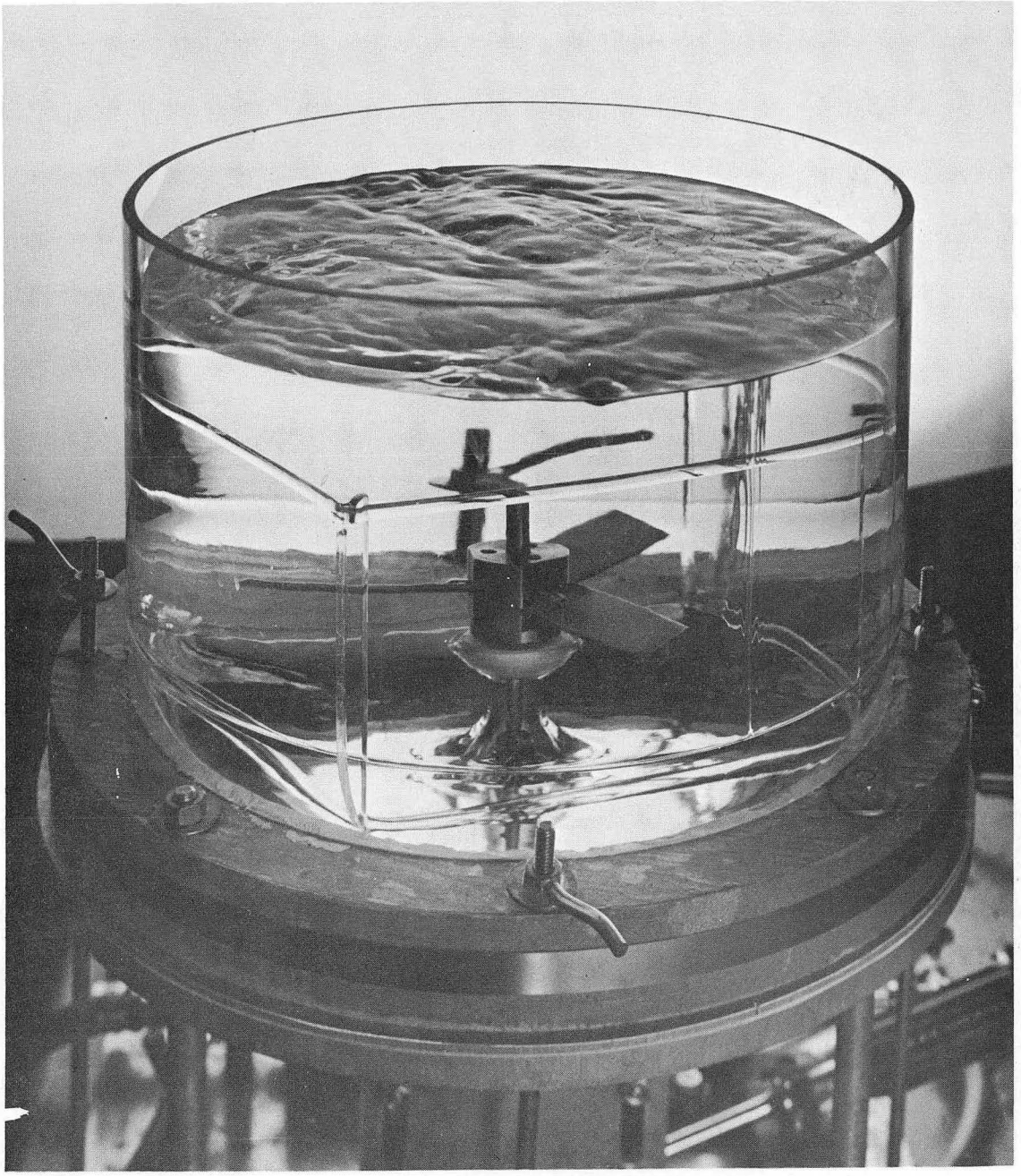

XBB 699-6006

Fig. A-9. Photograph oc a clean turbulent water interface stirred at a rate of 150 rpm.

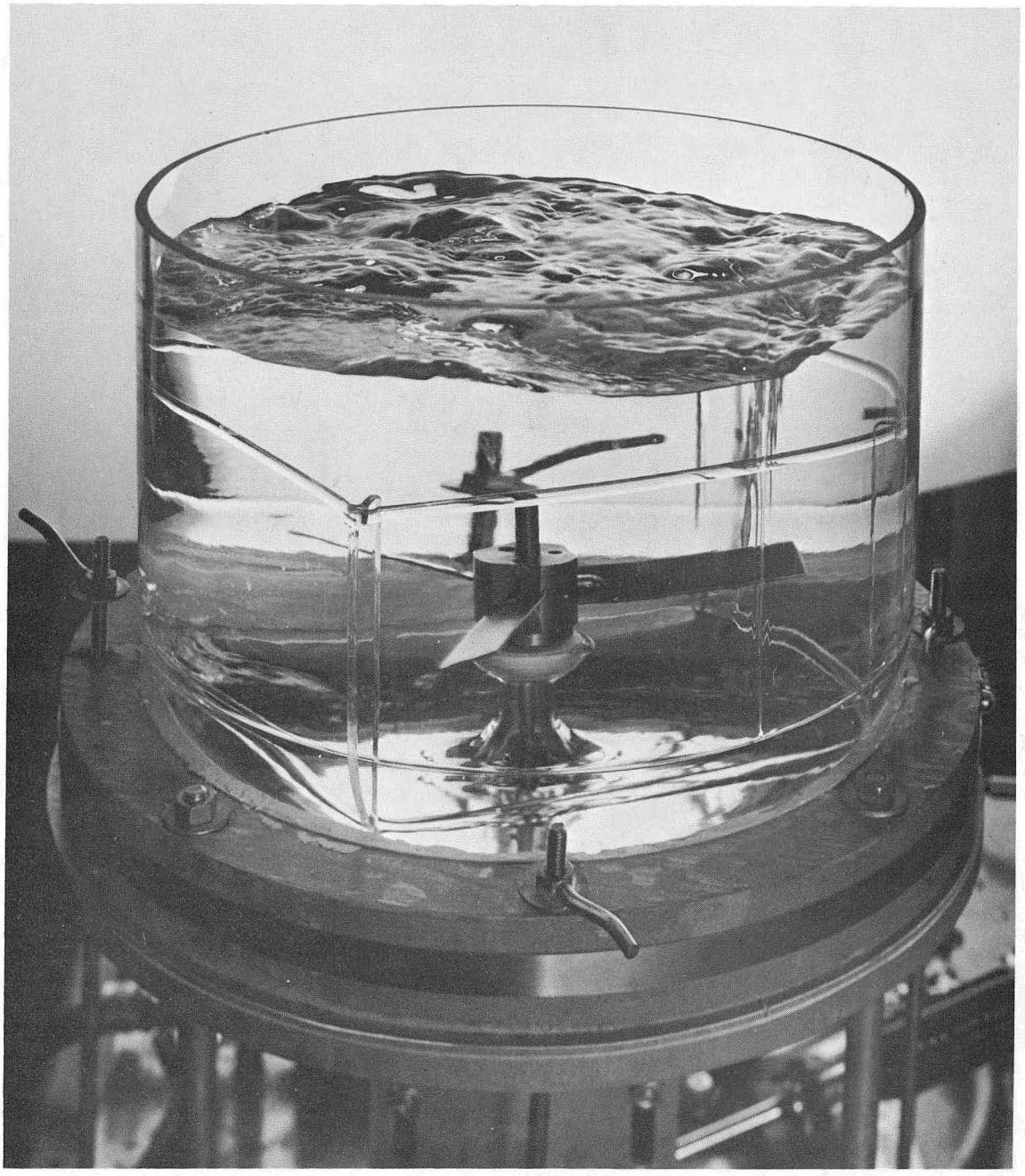

XBB 699-6009

Fig. A-10. Photograph of a clean turbulent water interface stirred at a rate of 230 rpm.

Two surfactants were tested, sodium lauryl sulfonate (water soluble) and 1-hexadecanol (water insoluble). 99% pure sodium lauryl sulfonate was obtained from Procter and Gamble, Cincinnati, Ohio. A second sample of unknown purity was obtained from E. I. du Pont de Nemours Co., Wilmington, Delaware. The chemical formula of this compound is $NaC_{12}H_{25}SO_3$ and its molecular weight is 272.39. 1-hexadecanol was obtained from Eastman Chemicals Co. The chemical was classified as "Eastman Grade", which was reported as being "similar to reagent grade." The melting point range was reported as being 48-49 °C. The chemical formula of this compound is $C_{16}H_{33}OH$ and its molecular weight is 242.44. No attempt was made to purify any of the chemicals.

In some experimental tests, a thin film was laid on the water surfaces to make them impermeable to mass transfer. The film chosen was Du Pont's polyvinyl fluoride, Tedlar, of 1 mil thickness.

APPENDIX B

EXPERIMENTAL PROCEDURES

SURFACE CLEANING

Before each group of experiments was begun an attempt was made to clean the liquid interfaces. Solid particles, such as dust, and any insoluble surfactants could be removed this way, but soluble contaminants would remain. Pieces of shark skin analytical filter paper (Schleicher and Schuell) were cut to just fit on the liquid surfaces in the chambers. The filter paper was placed on the surface and used as a blotter in an attempt to remove a layer of liquid from the interface along with contaminants. This method of cleaning did remove visible dust particles from distilled water samples and slightly increased the measured surface tension. As a further test of the cleaning method, a single monolayer of 1-hexadecanol was placed on a surface of distilled water just before blotting was attempted. The resulting observed surface tension was nearly that of pure water. Each time water was transferred into the test chambers, the liquid surfaces were cleaned in this manner several times before experimental measurements were begun.

ADDITION OF SURFACTANT

The movable cup arrangement allowed addition of surfactant to the liquid interface in the test chamber without interruption of the balance adjustment of the bridge. Attempts to add surfactant by using a solvent and then evaporating the solvant by sulfur dioxide purge for several minutes revealed that the bridge balance was affected enough to prohibit accurate measurement of the impedance change of the interface due to addition of the surfactant.

Sodium lauryl sulfonate was placed in the cups in solid form. After balancing of the bridge, one of the cups was immersed into the liquid and the effect of the surfactant on the bridge impedance was examined. For stagnant liquid measurements the cup could be left under the surface without interferring with the interface or measurements in any way. But, the presence of the cup between the interface and stirrer in the turbulent experiments could interfere with mixing in the liquid. After it was determined that the soluble surfactant did not add any measurable surface resistance to mass transfer, the test chamber was opened and the cup removed from the chamber, since rebalancing of the bridge could be accomplished as if no surfactant were present. The other cups remained in the test chamber with solid surfactant in them for later measurements at higher concentrations.

Since such small quantities of insoluble surfactant needed to be added, it was not practical to attempt to weigh this material into the cups in solid form. Solutions of 1-hexadecanol ethyl ether were prepared and the proper amount pipetted (0.2 ml) into the cups. It was found that proper spreading of the film could only be obtained if a small amount of water was first added to the cups before the solution was placed on the liquid. The cups were prepared prior to filling the chambers with the saturated sulfur dioxide solution; purge of the chambers ensured that all solvent was certainly evaporated before balancing of the bridge was begun. In the stagnant liquid experiments, the cups were immersed in the liquid but were not left there. After spreading of the surfactnat had occured, the cup was removed through the interface and secured tightly against the lower surface of the lid. To be sure that the above

procedure worked effectively, many preliminary tests were made by placement of films on distilled water in this manner followed by measurement of the resulting surface tension.

PHASE MEASUREMENT

The quadrature demodulator, built for phase measurement, was ineffective for signal frequencies below 0.3 cycles/second. For experimental measurements below this frequency, the phase was measured directly from the strip chart outputs. Signals at 0.3 cycles/second were measured in both ways for comparison of results. It was found that the results agreed within approximately 2-3 degrees of phase angle.

For frequencies below 0.3 cycles/second, the following procedure was followed. The band-pass filter was set at the desired experimental frequency and through use of the harmonic analyzer the motor speed was adjusted until the experimental frequency and the filter setting were nearly equal. Since phase adjustment could not be made exactly, the input-output phase relationship of the filter had to be measured by using the pressure signal of one of the chambers as an input signal. By knowing the phase characteristics of the filter, it was possible to find the true phase difference between the filtered pressure-difference signal and a reference pressure signal by measurement of the recorder outputs.

When the frequency of gas pressure oscillations was greater than 0.3 cycles/second, the demodulator was used. Before measurement the demodulator had to be calibrated at each new frequency to be tested, since the reference signal input contained a variable phase adjust control that

allowed variation of the phase relationship between the reference input and the signal input. For calibration we used one of the chamber pressure signals as input and as reference signal to the demodulator. By observation of the output of one of the channels of the demodulator, the phase difference between the two input signals could be adjusted to zero.

After calibration one could adjust the filter frequency and the experimental frequency to be nearly equal by observation of the phase difference between the input and output of the filter. One of the chamber pressure signals was used as filter input and reference input to the demodulator while the filter output was used as the input signal to the demodulator. Observation of a single channel of the demodulator indicated when the phase relationship of the input-output of the filter was zero within the accuracy of the instrument. The demodulator could now be used for measurement of the phase difference of the desired experimental signals.

The output of the demodulator consisted of two electrical signals, one proportional to the sine of the phase difference between the input signal and the reference and the other proportional to the cosine of the phase difference. The arctangent of their ratio gave the desired phase difference.

The accuracy of the demodulator was examined by generating sine waves in an analog computer of known phase differences and measuring the phase differences using the demodulator. The results are shown in Fig. B-1. These curves were used to make slight corrections in the demodulator measurements of experimental signals.

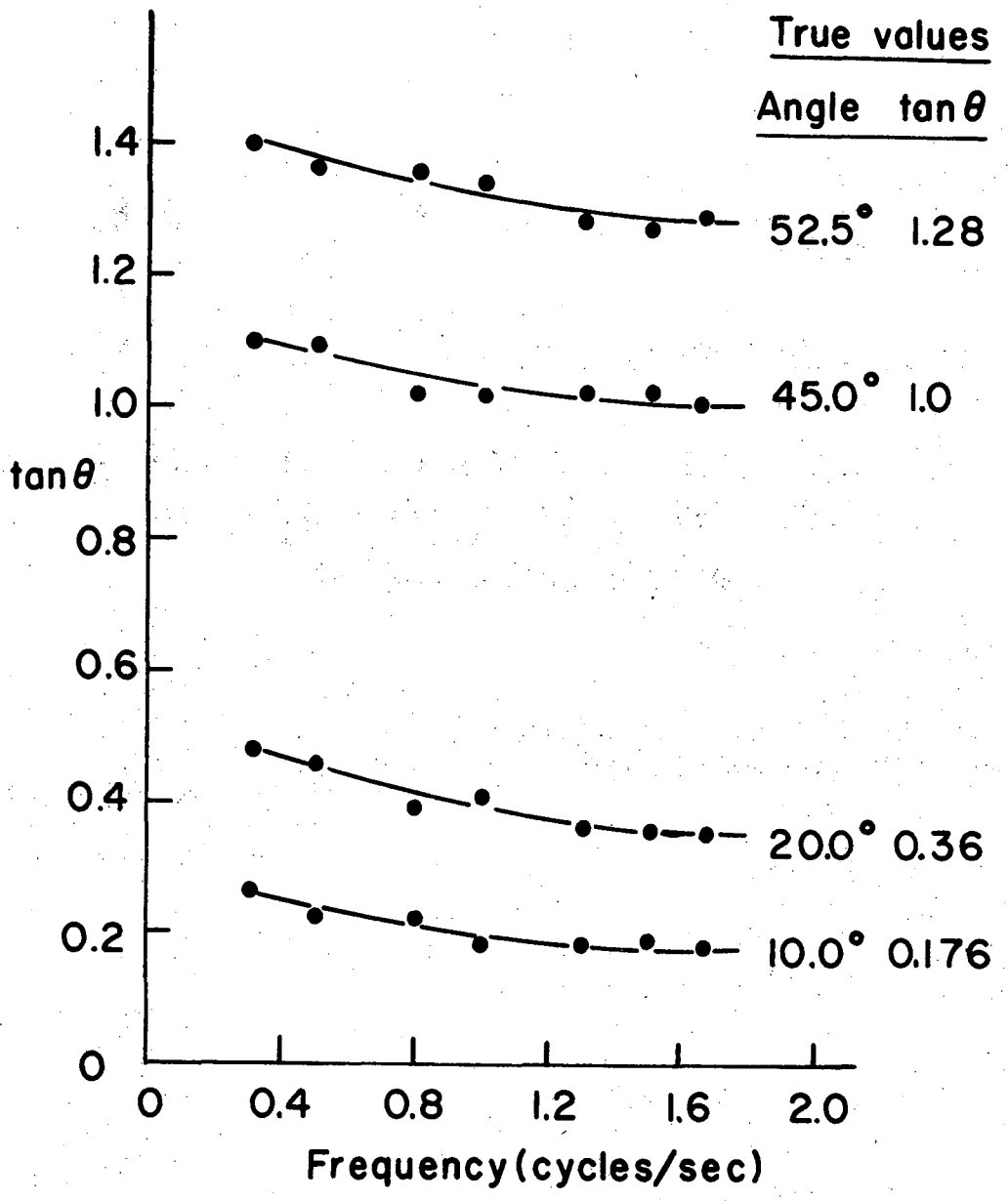

XBL 6910-5769

Fig. B-1. The phase response characteristics of the demodulator as a function of signal frequency. (Test signals supplied at analog computer.)

AMPLITUDE MEASUREMENT

It was found that the generated sine waves contained on the order of 10% harmonics (mostly second harmonic) and random noise. The difference of two such impure signals that are nearly identical must contain large amounts of noise and harmonics in comparison to the small fundamental difference. The band-pass filter eliminated the noise but was not able to reject all of the second harmonic content. To avoid doing a complete Fourier analysis of the output signals, the following method was devised.

The amplitude of the pressure-difference signal was measured at two different settings of the filter frequency. First, the amplitude was measured with the frequency of the experiment and the filter equal. The filter was then set at twice the experimental frequency and the amplitude measured a second time. The first measurement emphasized the fundamental content of the pressure-difference signal while the second measurement emphasized the second harmonic content. By knowing the attenuation characteristics of the filter one could calculate the fundamental content of the signal assuming it was composed of only first and second harmonics. The attenuation characteristics of the filter were measured by the use of the analog computer. The results are shown in Fig. B-2.

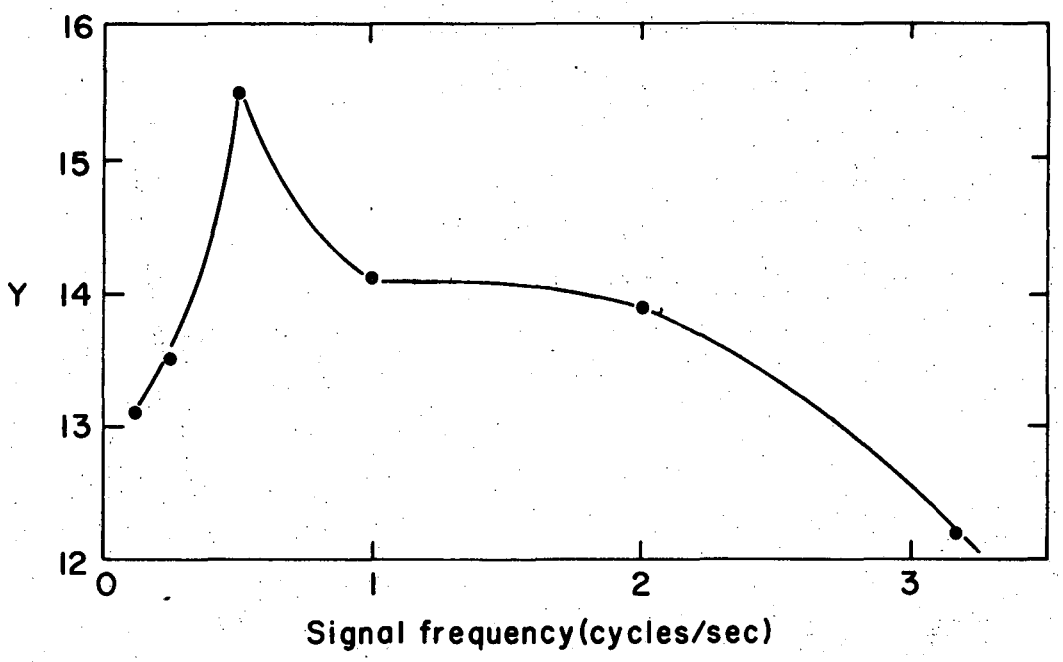

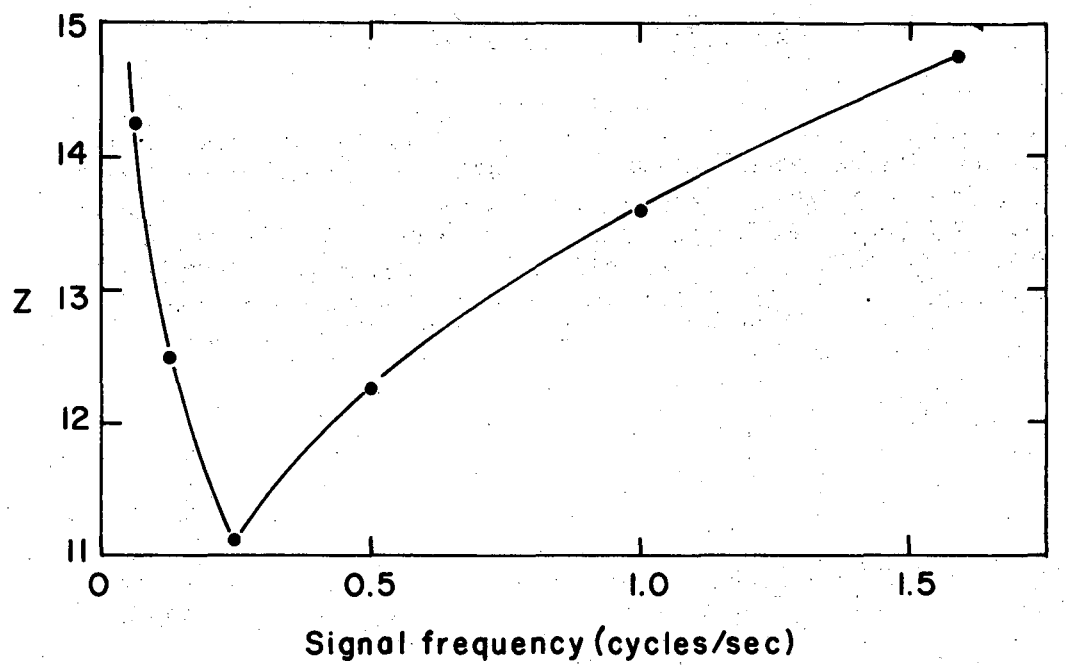

XBL 6910-5770

Fig. B-2. Attenuation characteristics of the band-pass filter as a function of frequency where Y = the amplitude ratio when the filter frequency is set at 1/2 the signal frequency and Z = the amplitude ratio when the filter frequency is set at twice the signal frequency. X, the amplitude ratio when the filter frequency and signal frequency are identical, is a constant 1.89. (Test signals supplied by analog computer.)

BRIDGE OPERATION

Both Pyrex chambers and all parts that could come into contact with the liquid solutions were cleaned using hexane followed by rinsing with distilled water, warm chromic acid solution, and distilled water once more. After cleaning, the chambers were placed on their bases and all parts assembled. This included positioning of the stirrer, securing of the lids and connection of input-output lines to the chambers. The liquid solutions were forced from storage chambers to the test chambers by increasing the sulfur dioxide gas pressure above the liquids in the storage chambers. At the same time, the whole apparatus was flushed with sulfur dioxide to remove traces of air. After the chambers were filled to the desired level, purging with sulfur dioxide was continued and the balloons were oscillated. After several minutes the oscillations were stopped and the gas pressure set at the average operating value. It was discovered that an initial average pressure of 21.8 inch of water above atmospheric pressure was needed to produce reasonably good sine waves by compression and expansion of the balloons. This average pressure was maintained by bleeding sulfur dioxide into the gas space until equilibrium between gas and liquid was obtained. Stirring of the liquid helped to reduce the time required for saturation. In some cases gas was also bubbled through the liquids to speed up saturation.

After saturation of the liquid in both chambers, the liquid interfaces were cleaned as explained previously. Many times it was also necessary to wipe the chamber lids dry since splashing of liquid onto them during saturation often occured.

The bridge was now ready for experimental measurements to be made. Since many different experiments were run, slightly different operating procedures were used, but always the above preparation was necessary.

During bridge operation several parameters must be measured for proper analysis of the data. The liquid level in each chamber must be measured so that one may calculate the volume of the gas space. The level in the test chamber was kept at nearly the same value for all experiments. The liquid temperature in each chamber was measured during every run. For experiments with turbulent surfaces, the stirring speed was measured and adjusted by a Strobo-Tac. All of the above information was recorded along with the pressure measurements and is shown with the tabulated data in Appendix C.

For measurement of mass transfer through a clean stagnant interface, the following procedure was followed. After preparation of the bridge as explained above, a Tedlar film was placed on the surface of the liquid in each chamber. The lids were secured and the gas space purged with sulfur dioxide to remove all traces of air. After gas-liquid equilibrium had been reached at the average operating pressure, the filter and the experimental frequencies were adjusted as described earlier. Since response of the two chambers should be identical, the pressure-difference signal between them was adjusted to its smallest possible value by removal of liquid from one of the chambers. When reduction of the signal was no longer possible, the bridge was considered balanced. The balance signal was recorded and then the Tedlar film on the test

surface was immersed in the liquid. Because the density of the film was nearly that of the liquid, immersion was not difficult.

After immersion of the film the response of the clean, stagnant surface was measured at one frequency. Similar experiments were carried out at several frequencies. Each time the frequency was changed, the balance of the bridge was disrupted. Therefore, one must begin the procedure by replacing the submerged film and rebalancing the bridge again at each new frequency.

If one wishes to compare any interface, except a clean, stagnant surface, with an impermeable surface, the following procedure may be followed. After preparation of the bridge apparatus as described earlier, a Tedlar film is placed on the liquid surface of the reference chamber. The chambers are purged with sulfur dioxide to remove air and the gas and liquid allowed to come to equilibrium at the average operating pressure. Experiment has shown that mass transfer through a clean, stagnant interface is reproducible and agrees well with theory (see Fig. 5 of Chapter I). One may take advantage of this result by using the known response of a stagnant water interface as a reference surface for the bridge. The phase response of such an interface was not shown earlier but was also quite reproducible as mentioned in Chapter I. It was found that the bridge could most easily be balanced by comparison of its phase response to the theoretical value of -45 degrees, since the phase is much more sensitive than the amplitude response.

After the experimental frequency and the filter setting were adjusted, the bridge was balanced by comparing a stagnant, clean interface with an impermeable one through phase readings. The conditions

in the test chamber were then fixed depending upon what measurements were to be made. The response of the bridge at the indicated frequency was recorded. For example, if one wished to measure the response of a turbulent interface, the stirring speed was adjusted and the stirrer turned on. The response was then measured. If one wished to measure the response of a stagnant, film-covered surface, the cups, containing surfactant, were immersed into the liquid and a short time allowed to ensure spreading of the film or solution of the soluble surfactant.

Since the liquid and gas are not exactly in equilibrium, stirring of the liquid in one of the chambers causes a slight drift in the pressure-difference signal. During response measurements, the drift is compensated by addition of sulfur dioxide to the gas space through a metering valve. The optimum conditions for operation was obtained when the liquid in the test chamber is just slightly undersaturated. Compensation for gas lost owing to solution is a simple matter. On the other hand, if the liquid is slightly oversaturated, stirring of the liquid causes the average pressure in the chamber to increase and compensation is difficult.

After one has made measurements at one frequency, a new operating frequency is picked and the bridge balance is compared with the theoretical response. Only minor adjustments are usually needed when using the clean, stagnant interface in the bridge reference chamber. For tests on a clean turbulent liquid rebalancing is a simple matter since one need only turn off the stirrer and change the frequency. But, when measuring the surface resistance of a film layer, the test chamber must be emptied, cleaned and reassembled before balance can be achieved again. The new liquid surface in the test chamber must be cleaned and

the bridge balanced before measurements at the new frequency can be made.

If one wishes to measure interfacial responses compared to a clean, stagnant liquid as a standard reference, the following procedure could be followed. After preparation of the bridge apparatus as described earlier, the experimental frequency was adjusted to the value of the filter setting. Since the response of two clean, stagnant liquid surfaces should be identical, the difference signal between two such surfaces is used as the bridge balance point. The pressure-difference signal of the two chambers is made as small as possible by removing liquid from one of the chambers. When the signal cannot be reduced further, the bridge is considered balanced and the small residual balance signal is measured. The surface conditions in the test chamber may be altered as desired and the response measured. When one wishes to change to a new operating frequency, rebalancing is necessary as described in the preceeding paragraph.

Since it was determined that sodium lauryl sulfonate exhibited no measurable surface resistance to mass transfer, turbulent experiments with this surfactant could be carried out using the same balancing procedures mentioned for measurement of clean interface responses.

The procedure for measurement of the response of turbulent interfaces was slightly modified when 1-hexadecanol films were initially spread on the stagnant surface. Data on such surfaces were only taken relative to a clean, stagnant liquid surface as a standard reference. After preparation of the bridge apparatus, the experimental frequency

was adjusted to match that of the filter. The bridge was balanced by minimizing the pressure difference between two clean, stagnant surfaces. The balance point was recorded and surfactant added to the surface of the test chamber. To ensure that the film had spread, the film resistance was measured and compared to earlier tests. The stirrer was turned on and the response of the film-covered, turbulent surface measured.

Analysis showed that when a film of 1-hexadecanol was spread on a distilled water interface, the surface tension reduction could be reproducibly measured in the test chamber. If such a film-covered surface was made turbulent and then the turbulence removed, the originally measured surface tension reduction could be measured after allowing a few minutes for the film to reorient itself at the liquid surface. Since the turbulent action of the liquid was found not permanently to affect the film's properties, several surface resistance measurements could be made in succession at one frequency without having to rebalance the bridge. After examining the turbulent response of a film-covered surface, the stirrer was turned off and, after a few minutes, the films surface resistance on a stagnant liquid was remeasured. Since it was found that the film resistance had not changed, measurements at a different stirring rate could be carried out without rebalancing of the bridge. Indeed, the surface resistances of 1-hexadecanol films of three different concentrations with each film subjected to two different turbulence levels were measured at each experimental frequency without rebalancing of the bridge. After each turbulent measurement, the return of the film's surface resistance was measured.

Of course, when measurements at a different frequency and desired, the test chamber must be drained, cleaned, reassembled and the proper balancing procedures begun again.

EXPERIMENTAL ERRORS AND DIFFICULTIES

Air in the gas space of either chamber created errors in the measured absorption signals. Two steps were taken to minimize the amount of air in the chambers. The water was initially degassed and stored under a sulfur dioxide atmosphere, and particular care was taken to ensure that the entire bridge apparatus was purged with sulfur dioxide sufficiently to remove nearly all traces of air contamination.

Slight mechanical or physical differences in the two sides of the impedance bridge were unavoidable. These minor differences produced a certain irremovable error signal when the bridge apparatus was balanced.

Condensation of water vapor onto the chamber lids could change the observed response of the bridge by changing the exposed liquid surface area of either chamber in an unknown amount. Splashing of liquid onto the lids during turbulent runs might also occur. Particular care was taken to dry the lids before operation and to be certain that they remained dry during measurements.

There was a slight random drift of the pressure-difference signals due to irregularities of turbulence levels and slight under-saturation of the liquid solutions. The responses were calculated from the chart recordings that showed the least drift and several cycles were averaged to ensure that error owing to the drift was minimized.

The input pressure signal to each of the chambers contained approximately 10% second harmonic. Assuming the bridge apparatus behaves linearly, the response of the bridge must be the superposition of the separate responses when a pure sine wave and a pure second harmonic are supplied to the bridge. The amplitude of the fundamental response was extracted from the combined signal by assuming that only fundamental and second harmonic were present. Analysis showed that this was a good approximation.

Analysis of the combined response to obtain the phase characteristics of the fundamental response was carried out as if the second harmonic had no effect. A small amount of error must have been introduced in the phase results from this assumption. It was reasoned that the error should be small for the following reasons. At all frequencies above 0.3 cycles/sec the signals were filtered twice before measurement of phase occured, once by the band-pass filter and again by the built in filters of the quadrature demodulator. The amount of second harmonic remaining in the response should have been a small fraction of the initial content. Also, the phase response of the bridge approached a limiting value as frequency got large, where second harmonic content was largest, and the phase response of the fundamental and second harmonic signals approached each other. As frequency became small, the pressure-difference signal became large and the second harmonic content decreased. The error in the phase measurement in this manner would be largest for intermediate values of frequency. Rough calculation shows that a maximum error of less than two degrees would be expected.

The major experimental difficulty encountered in this work was owing to the nonreproducible performance of the Neoprene balloons. Many new balloons performed unacceptably in that balance of the bridge without the presence of a large error signal was impossible. Even the balloons that were acceptable initially often changed their behavior with time. The balloons were also quite susceptible to puncture, requiring frequent repair and termination of experimental tests being made at the time. After balancing of the bridge the balance point could not be relied on for very long periods of time, necessitating frequent balancing during measurements.

It is desirable to improve this part of the apparatus if additional work is to be carried out using this equipment. One needs a reproducible way of varying the gas volume of each chamber. Stainless steel expansion bellows might be successfully used but their cost is high. Another alternative is to use two machined pistons, but possible gas leakage might prove to be too big of a problem. Lamb (1965) used machined Teflon bellows. Reinvestigation of these bellows might be fruitful.

REPRODUCIBILITY OF DATA

The linearity of the bridge response was verified by measuring the response at different gas pressure amplitudes. The reproducibility of data was tested by measuring the same response in several different runs. The reproducibility of the data was also supported by measuring responses of interfaces compared to two different standard references. Conversion of data from one standard reference to the other showed quite good agreement between the results.

APPENDIX C

Tabulation of Individual Runs

Run Number	Signal Measured	Interface Conditions
1-8	$(p_s - p_t)/p_t$	Clean, Turbulent-230 rpm
9	$(p_f - p_s)/p_f$	Stagnant, 0.000327-M sodium lauryl sulfonate
10	$(p_s - p_t)/p_t$	Turbulent-230 rpm, 0.000327-M sodium lauryl sulfonate
11	$(p_I - p_t)/p_t$	Turbulent-230 rpm, 0.000327-M sodium lauryl sulfonate
12	$(p_s - p_t)/p_t$	Turbulent-150 rpm, 0.000327-M sodium lauryl sulfonate
13	$(p_f - p_s)/p_f$	Stagnant, 0.00106-M sodium lauryl sulfonate
14	$(p_I - p_t)/p_t$	Turbulent-230 rpm, 0.00106-M sodium lauryl sulfonate
15	$(p_s - p_t)/p_t$	Turbulent-230 rpm, 0.00106-M sodium lauryl sulfonate
16	$(p_I - p_t)/p_t$	Clean, Turbulent-150 rpm
17	$(p_s - p_t)/p_t$	Clean, Turbulent-150 rpm
18-20	$(p_I - p_f)/p_t$	Stagnant, 1 monolayer 1-hexadecanol
21-26	$(p_f - p_s)/p_f$	Stagnant, 1/2, 1 & 2 monolayer 1-hexadecanol
27-30	$(p_s - p_t)/p_t$	Turbulent-150 & 230 rpm 1/2, 1 & 2 monolayer 1-hexadecanol
31-32	$(p_I - p_s)/p_s$	Clean, Stagnant
33-34	$(p_s - p_t)/p_t$	Turbulent-150 & 230 rpm 0.0001635-M sodium lauryl sulfonate

(continued)

Tabulation of Individual Runs Continued

Run Number	Signal Measured	Interface Conditions
36	$(p_s - p_t)/p_t$	Turbulent-150 rpm, 0.00106-M sodium lauryl sulfonate

Run # 1-8

Type of Reference Chamber (Chamber 1)	Clean, Stagnant Surface
Surface Conditions of Test Chamber (Chamber 2)	Turbulent, 230 rpm stirring speed
Surfactant	None

	Reference Chamber	Test Chamber
Liquid Temp. (°C)	25.5-26.0	25.5-26.0
Gas Space Height (cm)	3.175-3.227	2.859-2.870

Frequency cycles/sec	Comparison of Stagnant and Turbulent Surface (Measured Signal) $(\hat{p}_1 - \hat{p}_2)/\hat{p}_2$		Comparison of Impermeable and Turbulent Interface (Calculated Signal) $(\hat{p}_I - \hat{p}_t)/\hat{p}_t$	
0.03	0.212	∠ -95.6	0.255	∠ -88.6
0.055	0.104	∠ -99.1	0.132	∠ -87.0
0.083	0.0635	∠ -101.9	0.0855	∠ -85.4
0.090	0.0609	∠ -101.9	0.0820	∠ -85.3
0.167	0.0286	∠ -104.6	0.0442	∠ -80.1
0.20	0.0247	∠ -104.7	0.0390	∠ -79.1
0.30	0.0146	∠ -105.7	0.0268	∠ -74.2
0.48	0.00858	∠ -102.3	0.0190	∠ -67.8
0.50	0.00712	∠ -103.5	0.0175	∠ -65.8
0.51	0.00693	∠ -102.9	0.0173	∠ -65.3
0.80	0.00418	∠ -96.7	0.0130	∠ -59.9
1.15	0.00277	∠ -90.0	0.0105	∠ -55.9
1.50	0.00202	∠ -83.5	0.00900	∠ -53.2
2.00	0.00162	∠ -77.7	0.00777	∠ -51.6

Run # 9

Type of Reference Chamber (Chamber 1)	Clean, Stagnant Surface
Surface Conditions of Test Chamber (Chamber 2)	Stagnant
Surfactant	0.000327-M sodium lauryl sulfonate

	Reference Chamber	Test Chamber
Liquid Temp. (°C)	25.9	26.5
Gas Space Height (cm)	3.37	2.82

Frequency cycles/sec	Comparison of Two Stagnant Surfaces (Balance Signal) $\lvert(p_1 - p_2)/p_2\rvert$	Comparison of a Stagnant and Film-Covered Stagnant Surface (Measured Signal) $\lvert(p_s - p_f)/p_f\rvert$
0.07	0.00033	0.00064
0.10	0.0005	0.00073
0.30	0.00087	0.00073
0.50	0.00118	0.0011
1.00	0.00105	0.0012

Run # 10

Type of Reference Chamber (Chamber 1)	Clean, Stagnant Surface
Surface Conditions of Test Chamber (Chamber 2)	Turbulent-230 rpm stirring speed
Surfactant	0.000327-M sodium lauryl sulfonate

	Reference Chamber	Test Chamber
Liquid Temp. (°C)	25.9	26.5
Gas Space Height (cm)	3.212	2.820

Frequency cycles/sec	Comparison of Stagnant and Turbulent Surface (Measured Signal) $(\hat{p}_1 - \hat{p}_2)/\hat{p}_2$		Comparison of Impermeable and Turbulent Interface (Calculated Signal) $(\hat{p}_I - \hat{p}_t)/\hat{p}_t$	
0.064	0.0381	$\angle$ -102.8	0.0648	$\angle$ -76.4
0.30	0.00561	$\angle$ -85.0	0.021	$\angle$ -55.2
0.70	0.00232	$\angle$ -74.9	0.0128	$\angle$ -50.4
1.00	0.00191	$\angle$ -64.9	0.0108	$\angle$ -48.6

Run # 11

Type of Reference Chamber (Chamber 1)	Impermeable Surface
Surface Conditions of Test Chamber (Chamber 2)	Turbulent, 230 rpm stirring speed
Surfactant	0.000327-M sodium lauryl sulfonate

	Reference Chamber	Test Chamber
Liquid Temp. (°C)	25.9	26.5
Gas Space Height (cm)	3.212	2.82

Frequency cycles/sec	Comparison of Impermeable and Turbulent Interface (Measured Signal) $(\hat{p}_1 - \hat{p}_2)/\hat{p}_2$		Comparison of Stagnant and Turbulent Interface (Calculated Signal) $(\hat{p}_s - \hat{p}_t)/\hat{p}_t$	
0.048	0.0830	∠ -80.0	0.0531	∠ -103.5
0.10	0.0459	∠ -72.0	0.0238	∠ -102.6
0.20	0.0266	∠ -60.0	0.00873	∠ -94.6
0.50	0.016	∠ -53.1	0.00382	∠ -79.9
1.00	0.0112	∠ -48.8	0.00230	∠ -63.0

Run # 12

Type of Reference Chamber (Chamber 1)	Clean, Stagnant Surface
Surface Conditions of Test Chamber (Chamber 2)	Turbulent, 150 rpm stirring speed
Surfactant	0.000327-M sodium lauryl sulfonate

	Reference Chamber	Test Chamber
Liquid Temp. (°C)	25.8	26.2
Gas Space Height (cm)	3.175	2.86

Frequency cycles/sec	Comparison of Stagnant and Turbulent Surface (Measured Signal) $(\hat{p}_1 - \hat{p}_2)/\hat{p}_2$		Comparison of Impermeable and Turbulent Interface Calculated Signal) $(\hat{p}_I - \hat{p}_t)/\hat{p}_t$	
0.05	0.0336	∠ -112.0	0.0618	∠ -76.6
0.07	0.0242	∠ -114.3	0.0482	∠ -74.2
0.10	0.0144	∠ -116.6	0.0356	∠ -68.4
0.20	0.00491	∠ -120.3	0.0218	∠ -57.9
0.30	0.00304	∠ -118.3	0.0175	∠ -54.9
0.50	0.00153	∠ -110.6	0.0134	∠ -51.2

Run # 13

Type of Reference Chamber (Chamber 1)		Clean, Stagnant Surface
Surface Conditions of Test Chamber (Chamber 2)		Stagnant
Surfactant		0.00106-M sodium lauryl sulfonate
	Reference Chamber	Test Chamber
Liquid Temp. (°C)	26.0	26.3
Gas Space Height (cm)	3.175	2.86

Frequency cycles/sec	Comparison of two Stagnant Surfaces (Balance Signal) $\lvert(p_1 - p_2)/p_2\rvert$	Comparison of Stagnant and Film-Covered Stagnant Surface (Measured Signal) $\lvert(p_s - p_f)/p_f\rvert$
0.10	0.00005	0.00018
0.30	0.00073	0.00046
0.50	0.00185	0.0017
1.00	0.00087	0.00087

Run # 14

Type of Reference Chamber (Chamber 1)	Impermeable Surface
Surface Conditions of Test Chamber (Chamber 2)	Turbulent, 230 rpm stirring speed
Surfactant	0.00106-M sodium lauryl sulfonate

	Reference Chamber	Test Chamber
Liquid Temp. (°C)	26.2	26.5
Gas Space Height (cm)	2.937	2.86

Frequency cycles/sec	Comparison of Impermeable and Turbulent Interface (Measured Signal) $(\hat{p}_1 - \hat{p}_2)/\hat{p}_2$		Comparison of Stagnant and Turbulent Interface (Calculated Signal) $(\hat{p}_s - \hat{p}_t)/\hat{p}_t$	
0.05	0.113	∠ -77.5	0.0797	∠ -90.2
0.10	0.063	∠ -71.0	0.0387	∠ -88.2
0.20	0.0324	∠ -60.0	0.0138	∠ -80.9
0.50	0.0166	∠ -51.5	0.00419	∠ -70.6

Run # 15

Type of Reference Chamber (Chamber 1)	Clean, Stagnant Surface
Surface Conditions of Test Chamber (Chamber 2)	Turbulent, 230 rpm stirring speed
Surfactant	0.00106-M sodium lauryl sulfonate

	Reference Chamber	Test Chamber
Liquid Temp. (°C)	26.1	26.4
Gas Space Height (cm)	3.21	2.86

Frequency cycles/sec	Comparison of Stagnant and Turbulent Surface (Measured Signal) $(\hat{p}_1 - \hat{p}_2)/\hat{p}_2$		Comparison of Impermeable and Turbulent Interface (Calculated Signal) $(\hat{p}_I - \hat{p}_t)/\hat{p}_t$	
0.30	0.0100	$\angle$ -71.4	0.0258	$\angle$ -55.3
0.50	0.00468	$\angle$ -67.0	0.0172	$\angle$ -51.1
1.00	0.00179	$\angle$ -63.6	0.0107	$\angle$ -48.2

Run # 16

Type of Reference Chamber (Chamber 1)	Impermeable Surface
Surface Conditions of Test Chamber (Chamber 2)	Turbulent, 150 rpm stirring speed
Surfactant	None

	Reference Chamber	Test Chamber
Liquid Temp. (°C)	25.9	26.2
Gas Space Height (cm)	3.33	2.86

Frequency cycles/sec	Comparison of Impermeable and Turbulent Interface (Measured Signal) $(\hat{p}_1 - \hat{p}_2)/\hat{p}_2$		Comparison of Stagnant and Turbulent Interface (Calculated Signal) $(\hat{p}_s - \hat{p}_t)/\hat{p}_t$	
0.05	0.0785	∠ -81.50	0.0505	∠ -107.0
0.07	0.0548	∠ -79.4	0.0321	∠ -113.3
0.10	0.0414	∠ -75.0	0.0215	∠ -113.7
0.20	0.0240	∠ -64.6	0.00828	∠ -116.4
0.30	0.0185	∠ -59.6	0.00482	∠ -116.0

Run # 17

Type of Reference Chamber (Chamber 1)	Clean, Stagnant Surface
Surface Conditions of Test Chamber (Chamber 2)	Turbulent, 150 rpm stirring speed
Surfactant	None

	Reference Chamber	Test Chamber
Liquid Temp. (°C)	25.9	26.2
Gas Space Height (cm)	3.33	2.86

Frequency cycles/sec	Comparison of Stagnant and Turbulent Surface (Measured Signal) $(\hat{p}_1 - \hat{p}_2)/\hat{p}_2$		Comparison of Impermeable and Turbulent Interface (Calculated Signal) $(\hat{p}_I - \hat{p}_t)/\hat{p}_t$	
0.10	0.0211	∠ -113.4	0.0412	∠ -74.5
0.50	0.00234	∠ -116.6	0.0136	∠ -54.6
1.00	0.00083	∠ -108.4	0.00937	∠ -49.7

Run # 18-20

Type of Reference Chamber (Chamber 1)	Impermeable Surface
Surface Conditions of Test Chamber (Chamber 2)	Stagnant
Surfactant	1-monolayer of 1-hexadecanol

	Reference Chamber	Test Chamber
Liquid Temp. (°C)	25.9	26.0
Gas Space Height (cm)	3.175	2.86

Frequency cycles/sec	Comparison of Impermeable and Film-Covered Stagnant Surface (Measured Signal) $(\hat{p}_1 - \hat{p}_2)/\hat{p}_2$		Comparison of a Stagnant and Film-Covered Stagnant Surface (Calculated Signal) $(\hat{p}_f - \hat{p}_s)/\hat{p}_f$	
0.05	0.0300	∠ -58.0	0.0124	∠ -11.9
0.10	0.0167	∠ -62.3	0.0131	∠ -22.3
0.20	0.0110	∠ -67.3	0.0106	∠ -21.5
0.50	0.00560	∠ -73.0	0.00810	∠ -25.9
1.00	0.00286	∠ -76.7	0.00667	∠ -31.8
2.00	0.00180	∠ -75.7	0.00486	∠ -34.0

Run # 21-26

Type of Reference Chamber (Chamber 1)	Clean, Stagnant Surface
Surface Conditions of Test Chamber (Chamber 2)	Stagnant
Surfactant	1/2-monolayer of 1-hexadecanol

	Reference Chamber	Test Chamber
Liquid Temp. (°C)	23.4	23.8
Gas Space Height (cm)	3.175	2.86

Frequency cycles/sec	Comparison of a Stagnant and Film-Covered Stagnant Surface (Measured Signal) $(\hat{p}_2 - \hat{p}_1)/\hat{p}_1$		Comparison of Impermeable and Film-Covered Stagnant Surface (Calculated Signal) $(\hat{p}_I - \hat{p}_f)/\hat{p}_f$	
0.05	0.0100	∠ -7.0	0.0324	∠ -56.0
0.10	0.00850	∠ -11.7	0.0216	∠ -57.5
0.20	0.00784	∠ -14.8	0.0137	∠ -61.7
0.50	0.00648	∠ -20.2	0.00726	∠ -67.0
1.00	0.00431	∠ -23.9	0.00516	∠ -62.5
2.00	0.00383	∠ -29.1	0.00284	∠ -66.6

Run # 21-26

Type of Reference Chamber (Chamber 1)	Clean, Stagnant Surface
Surface Conditions of Test Chamber (Chamber 2)	Stagnant
Surfactant	1 monolayer of 1-hexadecanol

	Reference Chamber	Test Chamber
Liquid Temp. (°C)	23.4	23.8
Gas Space Height (cm)	3.175	2.86

Frequency cycles/sec	Comparison of a Stagnant and Film-Covered Stagnant Surface (Measured Signal) $(\hat{p}_2 - \hat{p}_1)/\hat{p}_1$		Comparison of Impermeable and Film-Covered Stagnant Surface (Calculated Signal) $(\hat{p}_I - \hat{p}_f)/\hat{p}_f$	
0.05	0.0142	∠ -11.0	0.0289	∠ -60.8
0.10	0.0124	∠ -17.9	0.0179	∠ -63.2
0.20	0.0112	∠ -23.5	0.0103	∠ -68.1
0.50	0.00925	∠ -28.1	0.00458	∠ -80.3
1.00	0.00643	∠ -30.9	0.00310	∠ -75.0
2.00	0.00490	∠ -35.5	0.00169	∠ -73.3

Run # 21-26

Type of Reference Chamber (Chamber 1)	Clean, Stagnant Surface
Surface Conditions of Test Chamber (Chamber 2)	Stagnant
Surfactant	2 monolayers of 1-hexadecanol

	Reference Chamber	Test Chamber
Liquid Temp. (°C)	23.4	23.8
Gas Space Height (cm)	3.175	2.86

Frequency cycles/sec	Comparison of a Stagnant and Film-Covered Surface (Measured Signal) $(\hat{p}_2 - \hat{p}_1)/\hat{p}_1$		Comparison of Impermeable and Film-Covered Stagnant Surface (Calculated Signal) $(\hat{p}_I - \hat{p}_f)/\hat{p}_f$	
0.05	0.0160	∠ -14.2	0.0270	∠ -62.5
0.10	0.0135	∠ -18.3	0.0170	∠ -65.5
0.20	0.0122	∠ -24.0	0.00949	∠ -71.9
0.50	0.00942	∠ -27.6	0.00454	∠ -82.8
1.00	0.00731	∠ -32.9	0.00233	∠ -85.5
2.00	0.00591	∠ -35.7	0.00106	∠ -107.7

Run # 27

Frequency = 1.00 cycles/sec for all data shown below

Type of Reference Chamber (Chamber 1)	Clean, Stagnant Surface
Surfactant	1-hexadecanol

	Reference Chamber	Test Chamber
Liquid Temp. (°C)	23.5	24.0
Gas Space Height (cm)	3.175	2.86

Surface Conditions	Comparison of Stagnant and Indicated Surface (Measured Signal) $(\hat{p}_1 - \hat{p}_2)/\hat{p}_2$		Comparison of Impermeable and Indicated Surface (Calculated Signal) $(\hat{p}_I - \hat{p})/\hat{p}$	
stagnant,0.5[a]	0.00565	∠ -25.6	0.00406	∠ -72.4
turbulent-150[b],0.5	0.00090	∠-110.8	0.00938	∠ -50.2
stagnant,0.5	0.00511	∠ -25.5	0.00445	∠ -67.4
turbulent-230,0.5	0.00344	∠ -92.3	0.0116	∠ -58.0
stagnant,0.5	0.00432	∠ -25.7	0.00506	∠ -61.3
stagnant,1.0	0.00696	∠ -32.9	0.00256	∠ -79.1
turbulent-150,1.0	0.00068	∠-110.1	0.00928	∠ -49.0
stagnant,1.0	0.00698	∠ -31.5	0.00273	∠ -80.1
turbulent-230,1.0	0.00438	∠ -86.7	0.0126	∠ -58.6
stagnant,1.0	0.00671	∠ -32.8	0.00275	∠ -75.7
stagnant,2.0	0.00783	∠ -32.9	0.00205	∠ -96.8
turbulent-150,2.0	0.00072	∠-109.6	0.00930	∠ -49.1
stagnant,2.0	0.00675	∠ -31.7	0.00281	∠ -78.1
turbulent-230,2.0	0.00440	∠ -85.5	0.0127	∠ -58.3

[a]Surface concentration of 1-hexadecanol in equivalent monolayers.

[b]Stirring speed producing the turbulence in rev/min.

Run # 28

Frequency = 0.50 cycles/sec for all data shown below

Type of Reference Chamber (Chamber 1)	Clean, Stagnant Surface
Surfactant	1-hexadecanol

	Reference Chamber	Test Chamber
Liquid Temp. (°C)	23.5	24.0
Gas Space Height (cm)	3.21	2.86

Surface Conditions	Comparison of Stagnant and Indicated Surface (Measured Signal) $(\hat{p}_1 - \hat{p}_2)\hat{p}_2$		Comparison of Impermeable and Indicated Surface (Calculated Signal) $(\hat{p}_I - \hat{p})/\hat{p}$	
stagnant, 0.5[a]	0.00689	∠ -20.7	0.00693	∠ -69.0
turbulent-150[b],0.5	0.00208	∠ -118.4	0.0134	∠ -53.8
stagnant,0.5	0.00649	∠ -19.6	0.00730	∠ -67.4
turbulent-230,0.5	0.00644	∠ -102.6	0.0170	∠ -64.0
stagnant,0.5	0.00570	∠ -18.4	0.00795	∠ -63.7
stagnant,1.0	0.00817	∠ -28.9	0.00525	∠ -70.1
turbulent-150,1.0	0.00210	∠ -120.6	0.0134	∠ -53.9
stagnant,1.0	0.00787	∠ -27.9	0.00557	∠ -69.2
turbulent-230,1.0	0.00704	∠ -102.6	0.0175	∠ -65.3
stagnant,1.0	0.00657	∠ -27.6	0.00664	∠ -62.0
stagnant,2.0	0.00917	∠ -30.0	0.00440	∠ -76.9
turbulent-150,2.0	0.00218	∠ -120.5	0.0134	∠ -54.2
stagnant,2.0	0.00817	∠ -28.9	0.00525	∠ -70.1
turbulent-230,2.0	0.00654	∠ -102.6	0.0171	∠ -64.2

[a]Surface concentration of 1-hexadecanol in equivalent monolayers.

[b]Stirring speed producing the turbulence in rev/min.

Run # 29

Frequency = 0.10 cycles/sec for all data shown below

Type of Reference Chamber (Chamber 1): Clean, Stagnant Surface

Surfactant: 1-hexadecanol

	Reference Chamber	Test Chamber
Liquid Temp. (°C)	23.5	24.0
Gas Space Height (cm)	3.135	2.86

Surface Conditions	Comparison of Stagnant and Indicated Surface (Measured Signal) $(\hat{p}_1 - \hat{p}_2)/\hat{p}_2$		Comparison of Impermeable and Indicated Surface (Calculated Signal) $(\hat{p}_I - \hat{p})/\hat{p}$	
stagnant,0.5[a]	0.00804	∠ -12.6	0.0218	∠ -56.4
turbulent-150[b],0.5	0.0203	∠ -114.3	0.0403	∠ -74.1
stagnant,0.5	0.00734	∠ -13.3	0.0223	∠ -55.0
turbulent-230,0.5	0.0543	∠ -100.6	0.0748	∠ -83.5
stagnant,0.5	0.00710	∠ -16.2	0.0222	∠ -53.8
stagnant,1.0	0.0132	∠ -21.4	0.0168	∠ -63.0
turbulent-150,1.0	0.0188	∠ -116.4	0.0387	∠ -73.4
stagnant,1.0	0.0113	∠ -22.3	0.0182	∠ -58.6
turbulent-230,1.0	0.0544	∠ -104.1	0.0738	∠ -85.9
stagnant,1.0	0.0113	∠ -22.4	0.0182	∠ -58.6
stagnant,2.0	0.0143	∠ -20.9	0.0160	∠ -65.9
turbulent-150,2.0	0.0189	∠ -116.4	0.0388	∠ -73.5
stagnant,2.0	0.0140	∠ -21.0	0.0162	∠ -65.1
turbulent-230,2.0	0.0523	∠ -100.7	0.0730	∠ -83.0

[a] Surface concentration of 1-hexadecanol in equivalent monolayers.

[b] Stirring speed producing the turbulence in rev/min.

Run # 30

Frequency = 0.05 cycles/sec for all data shown below

Type of Reference Chamber (Chamber 1) — Clean, Stagnant Surface

Surfactant — 1-hexadecanol

	Reference Chamber	Test Chamber
Liquid Temp. (°C)	23.5	24.1
Gas Space Height (cm)	3.175	2.86

Surface Conditions	Comparison of Stagnant and Indicated Surface (Measured Signal) $(\hat{p}_1 - \hat{p}_2)/\hat{p}_2$		Comparison of Impermeable and Indicated Surface (Calculated Signal) $(\hat{p}_I - \hat{p})/\hat{p}$	
stagnant,0.5[a]	0.00939	∠ -5.4	0.0331	∠ -55.5
turbulent-150[b],0.5	0.0480	∠ -104.7	0.0772	∠ -79.3
stagnant,0.5	0.00926	∠ -5.5	0.0332	∠ -55.3
turbulent-230,0.5	0.101	∠ -99.5	0.131	∠ -86.5
stagnant,0.5	0.00870	∠ -5.9	0.0335	∠ -54.5
stagnant,1.0	0.0144	∠ -13.4	0.0283	∠ -60.4
turbulent-150,1.0	0.0500	∠ -105.1	0.0788	∠ -80.3
stagnant,1.0	0.0142	∠ -13.5	0.0284	∠ -60.0
turbulent-230,1.0	0.102	∠ -99.5	0.132	∠ -86.6
stagnant,1.0	0.0138	∠ -13.6	0.0287	∠ -59.4
stagnant,2.0	0.0155	∠ -11.2	0.0280	∠ -62.8
turbulent-150,2.0	0.0505	∠ -105.1	0.0792	∠ -80.5
stagnant,2.0	0.0147	∠ -11.4	0.0285	∠ -61.5
turbulent-230,2.0	0.0995	∠ -99.5	0.129	∠ -86.4

[a]Surface concentration of 1-hexadecanol in equivalent monolayers.

[b]Stirring speed producing the turbulence in rev/min.

Run # 31-32

Type of Reference Chamber (Chamber 1)	Impermeable Surface
Surface Conditions of Test Chamber (Chamber 2)	Clean, Stagnant Surface
Surfactant	None

	Reference Chamber	Test Chamber
Liquid Temp. (°C)	25.9	26.1
Gas Space Height (cm)	3.175	2.86

Frequency cycles/sec	Comparison of an Impermeable and Clean, Stagnant Surface (Measured Signal) $(\hat{p}_I - \hat{p}_s)/\hat{p}_s$	
0.03	0.05249	$\angle$ -49.98
0.06	0.03594	$\angle$ -48.58
0.10	0.02731	$\angle$ -46.21
0.20	0.02124	$\angle$ -43.86
0.50	0.01349	$\angle$ -45.62
1.00	0.00929	$\angle$ -44.53
2.00	0.00669	$\angle$ -44.61
3.00	0.00520	$\angle$ -47.41

Run # 33-34

Type of Reference Chamber (Chamber 1)	Clean, Stagnant Surface
Surface Conditions of Test Chamber (Chamber 2)	Turbulent, 150 rpm stirring speed
Surfactant	0.0001635-M sodium lauryl sulfonate

	Reference Chamber	Test Chamber
Liquid Temp. (°C)	25.8	26.1
Gas Space Height (cm)	3.175	2.86

Frequency cycles/sec	Comparison of Stagnant and Turbulent Surface (Measured Signal) $(\hat{p}_1 - \hat{p}_2)/\hat{p}_2$		Comparison of Impermeable and Turbulent Interface (Calculated Signal) $(\hat{p}_I - \hat{p}_t)/\hat{p}_t$	
0.05	0.0416	∠ -105.0	0.0712	∠ -77.0
0.07	0.0280	∠ -114.6	0.0511	∠ -77.3
0.10	0.0174	∠ -113.8	0.0383	∠ -71.0
0.20	0.00639	∠ -117.3	0.0228	∠ -60.9
0.50	0.00151	∠ -120.2	0.0132	∠ -51.5
1.00	0.00067	∠-113.7	0.00924	∠ -49.0

Run # 33-34

Type of Reference Chamber (Chamber 1)	Clean, Stagnant Surface
Surface Conditions of Test Chamber (Chamber 2)	Turbulent, 230 rpm stirring speed
Surfactant	0.0001635-M sodium lauryl sulfonate

	Reference Chamber	Test Chamber
Liquid Temp. (°C)	25.8	26.1
Gas Space Height (cm)	3.175	2.86

Frequency cycles/sec	Comparison of Stagnant and Turbulent Surface (Measured Signal) $(\hat{p}_1 - \hat{p}_2)/\hat{p}_2$		Comparison of Impermeable and Turbulent Interface (Calculated Signal) $(\hat{p}_I - \hat{p}_t)/\hat{p}_t$	
0.05	0.0723	∠ -105.4	0.0997	∠ -86.4
0.07	0.0463	∠ -104.0	0.0706	∠ -80.9
0.10	0.0311	∠ -103.4	0.0522	∠ -76.8
0.20	0.0132	∠ -102.1	0.0294	∠ -67.8
0.50	0.00388	∠ -91.5	0.0156	∠ -55.7
1.00	0.0223	∠ -74.4	0.0110	∠ -50.9

Run # 36

Type of Reference Chamber (Chamber 1)	Clean, Stagnant Surface
Surface Conditions of Test Chamber (Chamber 2)	Turbulent, 150 rpm stirring speed
Surfactant	0.00106-M sodium lauryl sulfonate

	Reference Chamber	Test Chamber
Liquid Temp. (°C)	25.9	26.2
Gas Space Height (cm)	3.21	2.86

Frequency cycles/sec	Comparison of Stagnant and Turbulent Surface (Measured Signal) $(\hat{p}_1 - \hat{p}_2)/\hat{p}_2$		Comparison of Impermeable and Turbulent Interface (Calculated Signal) $(\hat{p}_I - \hat{p}_t)/\hat{p}_t$	
0.05	0.0279	∠ -116.4	0.0557	∠ -74.6
0.10	0.0111	∠ -119.6	0.0331	∠ -64.6
0.20	0.00411	∠ -120.5	0.0214	∠ -56.0
0.30	0.00235	∠ -120.7	0.0171	∠ -52.9
0.50	0.0012	∠ -117.5	0.0131	∠ -50.2

APPENDIX D

NUMERICAL EVALUATION OF A FOURIER INTEGRAL

It was shown in Chapter II that one must evaluate

$$f(\theta) = (\theta/\pi\mathcal{D})^{1/2}\int_0^\infty \{(3R - 2\omega\theta I)\cos(\omega\theta) - (3I + 2\omega\theta R)\sin(\omega\theta)\}d\omega \qquad (D\text{-}1)$$

where $G(\omega) = R(\omega) + iI(\omega)$, to determine $f(\theta)$ from experimental measurements of $G(\omega)$. Numerical evaluation of this type of integral from discrete values of $G(\omega)$ is not simple owing to the severe oscillation of trigonometric functions as their argument becomes large. An approximating method, first introduced by Filon (1928) and more recently discussed by Luyben et al. (1969), was employed with success.

Consider the integral

$$F(x) = \int_0^T f(y)\ \exp(ixy)\ dy$$

without loss of rigor we can divide the interval 0-T into a number of subintervals (N) for the purpose of integration.

$$F(x) = \sum_{j=0}^{N}\int_{\beta_j}^{\beta_{j+1}} f(y)\ \exp(ixy)\ dy$$

where $\beta_j = \sum_{k=1}^{j} \Delta T_k$, $\beta_o = 0$ and ΔT_k = sampling interval.

If one assumes that the function $f(y)$ may be represented by a parabola in each interval, one may analytically integrate the above equation for each interval. Obviously the error depends on how well one can approximate $f(y)$ by a parabola in each interval. If the function is fairly smooth, one should be able to pick a ΔT_k small enough to reduce the error to a reasonable value.

A general formula for integration of Eq. (D-1) in a single interval may be derived. Let

$$f(\theta) = \int_{\alpha}^{\beta} [A \cos(\omega\theta) - B \sin(\omega\theta)]d\omega \qquad \text{(D-2)}$$

and assume in each interval

$$A = a_0 + a_1\omega + a_2\omega^2 \qquad \text{(D-3)}$$

$$B = b_0 + b_1\omega + b_2\omega^2 \quad . \qquad \text{(D-4)}$$

Substitution of Eqs. (D-3) and (D-4) into (D-2) and integration yields

$$\begin{aligned} f(\theta) = (1/\theta)\{&[a_0 + a_1\beta + a_2\beta^2 - 2a_2/\theta^2 - b_1/\theta - 2b_2\beta/\theta] \sin(\beta\theta) \\ &- [a_0 + a_1\alpha + a_2\alpha^2 - 2a_2/\theta^2 - b_1/\theta - 2b_2\alpha/\theta] \sin(\alpha\theta) \\ &+ [a_1/\theta + 2a_2\beta/\theta + b_0 + b_1\beta + b_2\beta^2 - 2b_2/\theta^2] \cos(\beta\theta) \\ &- [a_1/\theta + 2a_2\alpha/\theta + b_0 + b_1\alpha + b_2\alpha^2 - 2b_2/\theta^2] \cos(\alpha\theta)\} \quad . \end{aligned} \qquad \text{(D-5)}$$

a_0, a_1, a_2 and b_0, b_1, b_2 are found by fitting a parabola to three points in the interval of interest. α and β are the endpoints of the interval over which integration is being performed.

Since one is limited to a rather small range of frequency over which one may take data experimentally, two major problems in evaluating Eq. (D-1) still exist: the upper integration limit is infinite and the integral kernel increases as frequency increases, at least over part of the range. To circumvent these problems, one needs an integral kernal whose value approaches zero rapidly as frequency gets large.

Since preliminary results of the frequency response of turbulent interfaces indicate that the Danckwerts distribution is a good approximation, it may be best to subtract the Danckwerts distribution from both sides of Eq. (D-1).

$$f(\theta) = s \exp(-s\theta)$$

and

$$\mathcal{D}^{-1/2} G(\omega) = (s + i\omega)^{1/2} \quad .$$

Since

$$(s + i\omega)^{1/2} = \left[\frac{(s^2 + \omega^2)^{1/2} + s}{2} \right]^{1/2} + i \left[\frac{(s^2 + \omega^2)^{1/2} - s}{2} \right]^{1/2}$$

and remembering that in Eq. (D-1) that $G(\omega) = R(\omega) + i\, I(\omega)$.

Let

$$R^*(\omega) = \mathcal{D}^{-1/2} R(\omega) - \left[\frac{(s^2 + \omega^2)^{1/2} + s}{2}\right]^{1/2}$$

$$I^*(\omega) = \mathcal{D}^{-1/2} I(\omega) - \left[\frac{(s^2 + \omega^2)^{1/2} - s}{2}\right]^{1/2} .$$

Equation (D-1) becomes

$$f(\theta) - s \exp(-s\theta) = (\theta/\pi)^{1/2} \int_0^\infty [(3R^* - 2\omega\theta I^*)\cos(\omega\theta) - (3I^* + 2\omega\theta R^*)\sin(\omega\theta)]d\omega \qquad (D\text{-}6)$$

If one assumes that outside the experimental range of frequencies the Danckwerts distribution applies, the integral in Eq. (D-6) is zero everywhere except in the region where the response is measured. The limits of integration become the limits of the range over which the frequency response measurements were made. The infinite upper limit is replaced by the maximum observed frequency. The results obtained by this method are deviations from the Danckwerts model.

Examination of the experimental data shows that the above assumption is reasonable. The slope of the frequency response data at both low and high frequency approaches the limiting value predicted by a Danckwerts model.

Since the increment size over which numerical integration is to be carried out may be smaller than the spacing of experimental data points, interpolation between points may be necessary. A six point Lagrangian interpolation scheme for non-equidistant data points was utilized.

Prior to interpolation, the data were smoothed by using a least squares criterion. The center point of each group of five data points was smoothed by fitting a second order polynomial through the points. All data points were smoothed in this way except the two points at each end of the range of data. These points were smoothed by first calculating data points outside the range of measured points using the Danckwerts solution. The s value used in the Danckwerts solution was found from a best fit to the measured data. By using two calculated data points outside each end of the range of measured data, the end experimental points were smoothed using the same technique as was used on the rest of the data.

A computer program was developed to carry out the numerical evaluation of $f(\theta)$ from Eq. (D-6) with the integration limits being the range of the measured experimental frequency response. The following sequence of operations were carried out.

1. The input data consisted of the pressure signal $\hat{\Delta p}/\hat{p}_t$.
2. The data were smoothed and the integral kernel calculated.
3. Interpolation of the calculated data was carried out.
4. Parabolic numerical integration of Eq. (D-6) was carried out.

A copy of the program and results may be found in record book 58-400 D-R on file in the Department of Chemical Engineering, University of California, Berkeley. Typical graphical results were shown in Figs. 4 and 5 in Chapter II.

One major problem was encountered in the above numerical procedure. It was found that there was a discontinuity in the integral

kernel at the end of the range of integration since the kernel changed abruptly from some finite value to zero. This discontinuity caused oscillations to appear in the solution. The problem was solved by smoothing the last point of the interval of integration to a zero value to remove the discontinuity.

APPENDIX E

DATA REDUCTION

CALCULATION OF Q^*

$$Q^* = Q\mathscr{D}^{1/2} = HART_o\mathscr{D}^{1/2}/V_o \quad .$$

The dimensionless quantity $HART_o$ was taken to be 42.25, from Washburn (1928) A = surface area of stagnant liquid = 625 cm^2 (chamber diameter, 11.1 inch) $\mathscr{D} = 1.46 \times 10^{-5}$ cm^2/sec, taken from Lynn et al. (1955).

The gas space volume V_o, was measured by adding 50 cc of liquid to one of the chambers and observing the resulting pressure change. The result was $V_o = 4500$ cc when the gas space height in the test chamber was 1.125 inches. When the bridge was balanced, the gas space height in the reference chamber was 0.125 inch larger than that of the test chamber.

By combining these values, $Q^* = 0.0225$. This value agreed very well with experimental data comparing a stagnant clean surface with an impermeable one, as evidenced by Fig. 5 of Chapter I.

CALCULATION OF THE TRUE PRESSURE SIGNAL FROM THE MEASURED RESPONSE

The experimental frequency response data, tabulated in Appendix C, were computed from an abbreviated Fourier analysis of the strip chart recordings. The raw data are on file with the Chemical Engineering Department of the University of California, Berkeley in laboratory notebook number S98-Q-300. Procedures for data reduction are shown below.

The first step in the analysis was to determine the amplitude of the pressure-difference signal and the reference signal. The height of several of the sinusoidal waves were measured from the chart recordings and averaged. The amplitude ratio of the difference and

reference signal was determined taking into account the sensitivities of the transducers. The differential transducer was determined to be 2.901 times as sensitive as the reference transducer. Measurement of the amplitude ratio at two different filter settings was necessary so that a modified Fourier analysis method could be utilized. Since it has been assumed that only fundamental and second harmonic are present in the response signal, the following equations had to be solved to extract the fundamental content of the response.

$$\frac{H_1}{X} + \frac{H_2}{Y} = A$$

$$\frac{H_2}{X} + \frac{H_1}{Z} = B$$

where H_1 and H_2 are the first and second harmonic content, respectively, A and B are the measured amplitudes, and X, Y, and Z are the attenuation constants for the filter as shown in Fig. B-2. Solution of these equations for the fundamental gives

$$H_1 = (XYZ/(YZ - X^2))(A - BX/Y) \quad .$$

One now may calculate the fundamental content of the amplitude signal.

If the phase difference between the signal was measured from the strip charts, several peaks of the reference wave were transferred to the pressure-difference signal recording and the distance between peak values measured and averaged. By knowing the phase characteristics of the band-pass filter one could determine the actual phase difference

between the pressure-difference and reference signal. Measurement of the phase by use of the demodulator was even simpler since one needed only to record the demodulator outputs and correct their ratio by using Fig. B-1.

One now had the amplitude and phase characteristics of the fundamental content of the measured response. The same procedure was carried out on the bridge null-balance signal to obtain its fundamental content also. The true pressure-difference response could be obtained by subtraction of the two complex quantities since the true signal and balance signal are superimposed to form the measured response.

INTERCHANGE OF THE STANDARD REFERENCE OF MEASURED RESPONSES

From Eq. (5) of Chapter I, it can be shown that

$$A = \frac{(\hat{p}_t - \hat{p}_s)}{\hat{p}_t} = \frac{Q_t k_{Lt} - Q_s k_{Ls}}{i\omega + Q_s k_{Ls}}$$

$$B = \frac{(\hat{p}_s - \hat{p}_I)}{\hat{p}_s} = \frac{Q_s k_{Ls}}{i\omega}$$

and

$$C = \frac{(\hat{p}_t - \hat{p}_I)}{\hat{p}_t} = \frac{Q_t k_{Lt}}{i\omega} \quad .$$

If signal A has been measured and C is desired, it is simple to see that

$$C = (1 + B)\,A + B \quad .$$

Conversely, if signal C has been measured and A is desired, it is easy to see that

$$A = (C - B)/(1 + B) \quad .$$

In these equations signal B may be calculated from theory since it has been shown in Chapter I measured values of signal B agree quite well with theory.

LEAST SQUARES ANALYSIS

Computer programs were written using linear least squares analysis for treatment of the data. The programs and output results may be found in record book 58-400 D-R on file in the Chemical Engineering Department of the University of California, Berkeley. All results were shown in Tables I-IV of Chapter II. Turbulent results were treated to determine the best values of the constants s and Q^* according to the Danckwerts model. Stagnant data were treated to find the best fit of the mass transfer coefficient of the film layer.

APPENDIX F

SURFACE CONCENTRATION OF THE SOLUBLE SURFACTANT

Using the Gibbs adsorption equation, Lamb (1965) calculated that the surface concentration of sodium lauryl sulfate was on the order of 1.36×10^{-10} g-moles/sq cm for a bulk liquid composition of 0.000327-M.

It was assumed that this was a reasonable value for sodium lauryl sulfonate also. This surface concentration corresponds to approximately 7.8×10^{13} moles/cm^2. Davies and Rideal (1961) reported that a surface monolayer contains approximately 10^{14} moles/cm^2. We have assumed here that the above bulk composition produces a surface concentration approximately equivalent to a monolayer of sodium lauryl sulfonate.

APPENDIX G

POWER INPUT

The Reynolds Number for a stirred tank is defined by

$$N_{Re} = D^2 N \rho/\mu$$

where D = diameter of impeller, ft

N = impeller revolutions/second

ρ = density of liquid, lb/ft^3

μ = dynamic viscosity, lb/(ft)(sec).

For a stirring speed of 230 rpm, the Reynolds Number becomes

$$N_{Re} = (0.5)^2(3.8)(62.5)/(0.000675) = 87,500 \quad .$$

From Perry (1963), the power input to a baffled tank may be calculated from

$$P = K N^3 D^5 \quad .$$

For a three-bladed impeller with a blade angle of 30° from the horizontal, K = 1.

$$P = 1\ (3.8)^3(0.5)^5 = 1.72\ (ft)(lb)/sec = 1.42\ Hp/1000\ gal.$$

A similar analysis for a stirring speed of 150 rpm gives

$$P = 1\ (2.5)^3(0.50)^5 = 0.98\ (ft)(lb)/sec = 0.81\ Hp/1000\ gal.$$

ACKNOWLEDGMENTS

I would especially like to thank Dr. Robert L. Pigford for his many suggestions and comments during the course of this research and the preparation of this thesis. His willingness to help me in many other ways has also been deeply appreciated.

The many suggestions and excellent work of G. G. Young and especially Fred Wiltens of the Lawrence Radiation Laboratory machine shop during construction of the experimental apparatus was appreciated.

I would like to thank the Proctor and Gamble Company, Cincinnati, Ohio, and E. I. du Pont de Nemours Company, Wilmington, Delaware, for donation of one of the surfactants used in this work.

Finally, I wish to thank my wife, Kay, for her understanding and patience during the long working hours in the final months of this work.

This work was performed under the auspices of the U. S. Atomic Energy Commission Contract W-7405-eng-48.

LEGAL NOTICE

TECHNICAL INFORMATION DIVISION
LAWRENCE RADIATION LABORATORY
UNIVERSITY OF CALIFORNIA
BERKELEY, CALIFORNIA 94720